UNIVERSITAT POLITÈCNICA DE CATALUNYA BARCELONATECH

Multi-objective optimization of an energy hub using artificial intelligence

by

Konstantinos Kampouropoulos

MULTI-OBJECTIVE OPTIMIZATION OF AN ENERGY HUB USING ARTIFICIAL INTELLIGENCE

by

Konstantinos Kampouropoulos

A thesis submitted in partial fulfillment
of the requirements for the degree of
Doctor of Philosophy in Electrical Engineering

School of Doctoral and Postdoctoral Studies
Universitat Politècnica de Catalunya
Barcelona, Catalonia, Spain
February, 2018

Supervisors:
Dr. Jose Luis ROMERAL MARTINEZ
Dr. Antonio GARCIA ESPINOSA

To my lovely sisters,
Helen and Sotiria

To my precious parents

Στις λατρεμένες μου αδερφές,
Λένα και Σωτηρία

Στους πολυαγαπημένους
μου γονείς

“ἀρχὰς εἶναι τῶν ὅλων ἀτόμους καὶ κενόν,
τὰ δ'ἄλλα πάντα νενομίσθαι”

Δημόκριτος, 470-370 π.Χ.,
Αρχαίος Έλληνας φιλόσοφος

Acknowledgments

Τί νόημα έχει τούτη η ζωή αν δεν έχεις δίπλα σου αγαπητούς ανθρώπους να σου την συντροφεύουν;

Όπως είπε μιά φορά ο καλός μου φίλος Στέφανος "το πιό σημαντικό πράγμα σε αυτόν τον κόσμο είναι οι ανθρώπινες σχέσεις. Ποτέ μην ξεχάσεις τους ανθρώπους που σε βοήθησαν".

Αυτό το μικρό κεφάλαιο είναι αφιερωμένο σε όλους εκείνους που ο καθένας με τον δικό του διαφορετικό τρόπο συμμετείχε στην επίτευξη αυτού του σημαντικού στόχου της ζωής μου, να ολοκληρώσω την διατριβή μου.

Θα ήθελα να ευχαριστήσω τους επιβλέποντες καθηγητές μου Jose Luis Romeral και Antonio Garcia για την εμπιστοσύνη και υποστήριξη που μου έδειξαν όλα αυτά τα χρόνια. Ένα θερμό ευχαριστώ στον Luis για τις πολύτιμες συμβουλές του, την καθοδήγηση που μου προσέφερέ και την υπομονή του.

Ένα τεράστιο ευχαριστώ στους γονείς μου. Που με μεγάλωσαν με αξίες, με συμβούλεψαν, με υποστήριξαν πάντα σε όλες μου τις αποφάσεις και με βοήθησαν να ανοίξω τα φτερά μου και να ακολουθήσω τον δρόμο που διάλεξα. Στις γλυκές μου αδερφές Λένα και Σωτηρία, που αν και από μακριά, ήταν πάντα δίπλα μου και με βοηθούσαν να συνεχίσω μέχρι τέλους.

Στην Ισπανίδα γιαγιά μου Μαρία, που άνοιξε τις πόρτες του σπιτιού της και με έκανε να αισθανθώ μέλος της οικογενείας της.

Στον αγαπητό μου φίλο Fabio και την υπέροχη γυναίκα του Jenny, τους οποίους θεωρώ μέλη της οικογένειας μου, για τις πολύτιμες συμβουλές τους, την υποστήριξη τους και τις ουσιώδης συζητήσεις μας όλα αυτά τα χρόνια.

Στην γλυκιά μου Lidia, για τις όμορφες στιγμές και συντροφιά της.

Τους καθηγητές και συναδέλφους μου στην Terrassa, σε όλα αυτά τα χρόνια, Juan Antonio, Jordi R., Juan Manuel, Vicenç, Miguel, Tomasz, Carlos A., Carles, Tomás, Jordi A., Maria, Jose, Jesús, Daniel, Eva, Jordi G., Efrén, Carlos L., Alejandro, Ricardo, Fernando, Tecilli, Joan, Juan José, Julio, Harold, Petya και Alessandra, οι οποίοι με συντροφεύουν σαν ισπανική οικογένεια.

Τους συναδέλφους μου στην CTM, αλλά ιδιαίτερα τον Mario, Jordi, Marc Garcia, Didac, Joan, Eva και Laia, για τον επαγγελματισμός τους αλλά και τις όμορφες καθημερινές στιγμές που περνάμε παρέα στο γραφείο.

Ένα ξεχωριστό ευχαριστώ στους φίλους μου Marc Castellà και Enric Sala, για την βοήθεια τους, τις συμβουλές τους, τις εξαιρετικές συζητήσεις μας και για την υπομονή τους που με άντεξαν και με αντέχουν τόσες ώρες στο ίδιο γραφείο.

Στους αγαπημένους μου φίλους Carolina και Etienne, Στέφανο και Σοφία, Χριστίνα και Simon, όπως επίσης στον Βασίλη και στον Γιώργο, για τις υπέροχες καθημερινές στιγμές που περάσαμε και περνάμε παρέα, την συμπαράσταση τους και την ενέργεια που μου δίνουν.

Στην γλυκιά μου Μαργαρίτα, που φέρει ένα σημαντικό μέρος της ευθύνης για το ότι βρίσκομαι εδώ. Για την συντροφιά της τόσα χρόνια, για τις συμβουλές τις και την βοήθειά της.

Τέλος, ένα θερμό ευχαριστώ στους καθηγητές μου Βαφειαδάκη Δαμιανό και Προβόπουλο Λάμπρο, οι οποίοι με το πάθος και την αγάπη τους για την ηλεκτρολογία, με την διδασκαλία τους και τις συμβουλές τους με βοήθησαν και με ενέπνευσαν να ακολουθήσω αυτόν τον δρόμο.

Σας ευχαριστώ όλους θερμά.

Agradecimientos

¿Cuál es la gracia de esta vida si no estás rodeado de gente querida para que te acompañen en tu camino?

Como dijo una vez mi buen amigo Stefanos, "Lo más importante en este mundo son las relaciones con la gente. Nunca olvides las personas que te han ayudado".

Esta pequeña sección está dedicada a todos aquellos que con una u otra forma me han ayudado a conseguir este objetivo de mi vida, a realizar mi tesis doctoral.

Me gustaría agradecer a mis supervisores Jose Luis Romeral y Antonio Garcia para su confianza y el soporte que me han dado durante todos estos años. Un especial agradecimiento a Luis, para sus valiosos consejos, su guía y su paciencia.

Un gran agradecimiento a mis padres, quienes me criaron con valores, me aconsejaron y me apoyaron siempre en todas mis decisiones y me ayudaron a seguir el camino que elegí. A mis hermosas hermanas Lena y Sotiria, que, aunque desde lejos, siempre estuvieron a mi lado y me ayudaron a continuar hasta el final.

A mi abuela española María, quien abrió las puertas de su casa y me hizo sentir como un miembro de su familia.

A mí querido amigo Fabio y su maravillosa esposa Jenny, a quienes considero como miembros de mi familia, por sus valiosos consejos, su apoyo y amistad a lo largo de todos estos años.

A mi dulce Lidia, por los hermosos momentos que pasamos juntos, su paciencia y compañía.

A los profesores y compañeros de Terrassa, en todos estos años, Juan Antonio, Jordi R., Juan Manuel, Vicenç, Miguel, Tomasz, Carlos A., Carles, Tomás, Jordi A., María, José, Jesús, Daniel, Eva, Jordi G., Efrén, Carlos L., Alejandro, Ricardo, Fernando, Tecilli, Joan, Juan José, Julio, Harold, Petya y Alessandra, con los cuales hemos pasado muchos años trabajando juntos y se han convertido a mi familia española.

A mis compañeros de CTM, y especialmente a Mario, Jordi, Marc García, Didac, Joan, Eva y Laia, por su profesionalismo y por todos los momentos que pasamos en el trabajo.

Un agradecimiento especial a mis amigos, Marc Castellà y Enric Sala, por su ayuda, sus consejos, nuestras excelentes conversaciones y charlas, y por su paciencia por soportándome tanto tiempo en la oficina.

A mis queridos amigos Carolina y Etienne, Stefano y Sofia, Christina y Simon, como también a Vasilis y Giorgos, por los momentos maravillosos que hemos pasamos, su apoyo y energía que me han trasmitido.

A mi hermosa Margarita, que tiene una parte significativa de responsabilidad por estar yo aquí hoy. Gracias por su amistad y ayuda en todos estos años.

Finalmente, doy las más sinceras gracias a mis maestros Vafeiadaki Damiano y Provopoulo Lambro, quienes con su pasión y amor por la ingeniería eléctrica, con su enseñanza y sus consejos me ayudaron y me inspiraron a seguir este camino.

Gracias a todos.

Abstract

The present dissertation is focused on the energy optimization of systems which contain multiple energy carriers. The objective of the research is the development of a methodology and the corresponding software tools, which permit to calculate the optimal energy flow of a multi-carrier system in order to satisfy its energy demands and minimize a set of established optimization criteria. The topics that are covered in this research include the description of the mathematical formulation of a multi-carrier energy system based on the energy hub concept, the modelling and prediction algorithms that are used to forecast the energetic needs of the plant, as well as the proposed optimization methodology to obtain the system's optimal operating strategy and its complete state, including transmission and conversion of multiple energy carriers within defined security constraints.

Digital models and software-based simulations demonstrate the feasibility of the proposed solution. The testing and validation of the proposal was made under real operating conditions of a car manufacturing plant in the framework of the FP7 European research project *EuroEnergest*. The findings provided valuable output conclusions of the suitability and usefulness of this methodology to calculate the optimal control of a multi-carrier energy system, as well as the potential energetic, environmental and economic benefits that could be resulted from its application.

Περίληψη

Η παρούσα Διδακτορική Διατριβή πραγματεύεται την βελτιστοποίηση ενέργειας συστημάτων που περιέχουν ή αποτελούνται από πολλαπλές πηγές ενέργειας και καταναλώσεις. Αντικείμενό αυτής, είναι η μελέτη και ο σχεδιασμός μιας μεθοδολογίας, καθώς επίσης και ο προγραμματισμός των ανάλογων προγραμμάτων, για τον υπολογισμό της βέλτιστης λειτουργίας ενός ενεργειακού συστήματος με τελικό σκοπό την ικανοποίηση του ενεργειακού του φορτίου και την ελαχιστοποίηση πολλαπλών αντικειμενικών κριτηρίων. Τα θέματα που καλύπτονται στην παρούσα έρευνα περιλαμβάνουν την μαθηματική περιγραφή των ενεργειακών συστημάτων πολλών πηγών και καταναλώσεων, την επεξήγηση και παρουσίαση των αλγόριθμων για την μοντελοποίηση και πρόγνωση των ενεργειακών απαιτήσεων του συστήματος, καθώς επίσης και την προτείνουσα μεθοδολογία για την βελτιστοποίηση της ροής ενέργειας στο σύστημα.

Η μελέτη και επικύρωση της πρότασης πραγματοποιήθηκε υπό πραγματικές συνθήκες σε ένα εργοστάσιο κατασκευής αυτοκινήτων της Ισπανίας, στο πλαίσιο του Ευρωπαϊκού ερευνητικού προγράμματος FP7 *EuroEnergest*. Τα αποτελέσματα της μελέτης παρείχαν πολύτιμα συμπεράσματα σχετικά με την καταλληλότητα και αποτελεσματικότητα της μεθοδολογίας για τον υπολογισμό της βέλτιστης λειτουργίας ενός ενεργειακού συστήματος πολλαπλών πηγών και καταναλώσεων. Κατά την διάρκεια της μελέτης κατέστη δυνατόν να υπολογιστούν τα οικονομικά, περιβαλλοντικά και ενεργειακά οφέλη της προτείνουσας μεθοδολογίας, σε σύγκριση με την συμβατική λειτουργία του συστήματος δοκιμής.

Resumen

En la presente Tesis doctoral se estudia la optimización energética en sistemas que contienen múltiples fuentes y demandas energéticas. El objetivo de la investigación es desarrollar una metodología y los correspondientes algoritmos de control, que permitan controlar la operación de sistemas con múltiples portadores energéticos de forma óptima, con fin de satisfacer sus demandas energéticas y minimizar una serie de criterios establecidos. Los temas que se tratan en esta investigación consisten en la descripción, formulación matemática y análisis de sistemas multiportadoras de energía, basándose en el concepto del Hub Energético y en algoritmos adaptativos para el modelado y predicción de las demandas energéticas de estos sistemas. Además, se desarrolla una metodología de optimización para calcular la óptima estrategia de operación de los equipos y el uso de sus energías.

Los modelos digitales y las simulaciones realizadas demuestran la viabilidad de la solución. La evaluación y validación de la metodología se ha realizado bajo condiciones de operación reales en una planta de fabricación de automóviles, en el marco del proyecto de investigación Europeo FP7 *EuroEnergest*. Los resultados de validación presentan un gran potencial de ahorro cuando se aplica la estrategia de operación calculada por el algoritmo, mostrando beneficios energéticos, económicos y medioambientales.

Index

List of figures

Nomenclature

List of abbreviations

ANFIS	Adaptive neuro fuzzy inference system
ANN	Artificial Neural Network
CHP	Cogeneration equipment (combined heat and power)
CO_2	Carbon Dioxide
COP	Coefficient of Performance
DB	Database
DEA	Differential Evolution Algorithms
DSM	Demand Side Management
EH	Energy Hub
EMS	Energy Management System
FIS	Fuzzy Inference System
GA	Genetic Algorithms
GSA	Gravitational Search Algorithms
MF	Membership Function
MIMO	Multi-Input-Multi-Output
NN	Neural Network
PSO	Particle Swarm Optimization
RLSE	Recursive Least Square Estimator
SA	Simulated Annealing
SEH	Smart Energy Hub
SISO	Single-Input-Single-Output
SVR	Support Vector Regression

Indices

α	Index of hub's input energy carriers $[1 : A]$.
β	Index for hub's output energy carriers $[1 : B]$.
t	Index for optimization time instances $[1 : T]$.
i	Index for energy converter types $[1 : I]$.
j	Index for optimization criteria $[1 : O]$.
k	Index for the number of installed components within the hub $[1 : K]$.

x	Set of continuous optimization variables.
y	Set of discrete optimization variables.

Functions

g	Equality constraint functions.
h	Inequality constraint functions.
f	Multiobjective optimization function.
$f_j^{\max}$	Maximum objective function value of criterion j.
f_j^{trans}	Transformed objective function value of criterion j.
f_j^{o}	Utopia point of objective function j.

Parameters

T	Number of time instances of the optimization horizon.
$C_i^{\beta\alpha}$	Efficiency of the hub's energy converter of type i, for converting energy carrier α to energy carrier β.
$\underline{P}_i^{in}$	Minimum input power for the energy converter of type i.
$\overline{P}_i^{in}$	Maximum input power for the energy converter of type i.
$\underline{P}_{Tot}^{in,\alpha}$	Minimum supply limit of energy carrier α.
$\overline{P}_{Tot}^{in,\alpha}$	Maximum supply limit of energy carrier α.
lb_i	Minimum operating bound of energy converter of type i.
ub_i	Maximum operating bound of energy converter of type i.
L_β	Total output load of the hub of energy carrier β.
λ_t^α	Energy price of energy carrier α at the time instance t.

Variables

P_{Tot}^{in}	Total input power of the hub.
P_{Tot}^{out}	Total output power of the hub.
P_{ik}^{in}	Input power of the k^{th} energy converter of type i.
P_{ik}^{out}	Output power of the k^{th} energy converter of type i.
e^α	Emission factor of the input energy carrier α.

Definitions

Short-term demand forecasting. Demand prediction of an energy consumption for a period of 24 hours ahead.

Dynamic Optimization. Determination of a sequence of decisions for a time horizon to maximize (or minimize) an objective function, where each period's decision can affect the future possibilities of the optimizing agent.

Energy carrier. Energetic infrastructure that forms a connection between an energy supplier and a demand.

Ampacity. The maximum current that a conductor can carry continuously under the conditions of use without exceeding its temperature rating.

Utopia Point. The utopia point of an optimization criterion describes the global optimal point (ideal point), either for cases of maximization or of minimization.

1. Introduction

In order to settle the scope of this research, Chapter 1 presents the framework and outline of this dissertation, as well as it describes the research objectives and the starting hypotheses.

1.1 Thesis Framework and Outline

In recent years, the production and usage of energy has become a hot topic over the word. Due to the climate change and the decrease in fossil fuel reserves, society has been significantly focused on the development of more efficient systems. Reforms such as the restructuring of monopolistic frameworks toward liberalized markets have provided an open access to various new energy participants. Furthermore, new established legislations now permit the use of small distributed energy resources for power generation, opening the way for the implementation of self-supporting independent energy systems. However, there still a major problem in the treatment of energy sources in today's research due to its specific focus on the electric power management but the reduced attention to other kinds of energy systems. Even though promising development have been observed in the area of energy technologies, the overall energy efficiency can be greatly improved if multi-energy sources are analyzed and be utilized in a more unified way. This will allow to face critical issues which

concern the energy utilities and the community such as the global political target of reducing the greenhouse gas emissions. Important examples of this aim are the established EU 20/20/2020 climate and energy package and 2030 climate and energy framework which intend to convert Europe to highly energy-efficient and low carbon economy [1]. Furthermore, another demanding subject that has to be handled is the minimization of use of fossil fuel energy sources that are inherently being limited. Fossil fuels today account for 65% of electricity production and over 80% of the world's energy consumption [2]. This situation cannot continue, as reserves of fossil fuels are not infinite and even worse, they are the main cause of the environmental contamination. Furthermore, the promotion of the use of renewable energies and self-consumption systems are strategic plan for the European industry. Renewable energies have experienced a notable increase in Europe in the last decade, presenting a great technological progress in the fields of photovoltaics, wind energy and biomass. During 2015, three relevant events occurred in the international sphere, concerning the energy sector: oil price developments, European climate and energy framework 2030 and Paris COP 21. The sharp fluctuations in the price of oil over the last decade, which have ranged the oil price from $130 to $30 for a barrel, highlight more than ever the economic, geopolitical and stability benefits that can be obtained by the renewable energies. The mirage of the transient drop in oil prices may induce to exhaust the option of fossil fuels or, on the contrary, take advantage of the savings of resources that the low price entails to reinforce and relaunch the renewable option.

Focused on these targets, the energy hub concept has been recently introduced by Geidl and Anderson as a new paradigm for future multicarrier energy systems [3]. Its key idea is to link different energy sources using current energy infrastructures and a variety of energy converter and storage elements in an optimal manner. It is considered as a unit where multiple energy carriers can be converted, conditioned and stored, representing an interface between different energy infrastructures and/or loads. It is a concept that can be applied to industrial plants, buildings of the tertiary sector, as well as urban and rural districts, as they contain multi-source and multi-production structures. One of its main advantages is that it increases the operational flexibility of a multi-carrier energy system due to the redundancy in connections between the system´s inputs and outputs. This flexibility, apart from improving the reliability of supply, also permits to optimize the energy flow of the system, focusing on different objectives that can have an energetic, economic or environmental aspect. On the other hand, the multi hub systems permit an easier local management of the energies and thus are a great paradigm for the promotion of the use of renewable sources. These benefits

are as the main factors incentivizing the extension of energy hubs' utilization, being the main topic of this dissertation which is focused on the development of a methodology for energy portfolio optimization applied to multi-carrier systems. Along these lines, this dissertation tries to deal with the improvement of energy efficiency and energy reliability, as they have emerged as the greatest societal challenges of our age.

Settled the framework, it is the objective of this thesis to provide methods that allow to adequate optimize the energy use in multi-carrier energy systems, especially focused on real time operations of industrial environments, where a high accuracy of the results and a low computation effort are required. The optimization methodology, proposed in this dissertation, combines different approaches that are executed systematically. Initially, **a modelling process of the energetic behavior of the plant** (energy consumptions) is made by use of a hybrid algorithm, consisting of genetic algorithms (GA) and adaptive neuro-inference systems (ANFIS). This algorithm permits to accurately characterize the different types of energy demands in the system, correlated with parameters that potentially affect their consumption behavior. This is especially important for the proposed methodology, as it permits to calculate short-term demand forecasts that are later be used during the dynamic optimization of the system. Then, the **system's structure is formulated mathematically by using the energy hub concept**, in order to obtain the relations between the primary energy sources and the demands (energy carriers), and to identify possible restrictions on its operating. Finally, a mixed-integer **multi-objective optimization algorithm is applied in order to calculate the optimal operation of the system** for the whole prediction horizon, focusing on the satisfaction of the energy demands and the minimization of the established criteria. During the calculation, the algorithm takes into consideration the dynamic system response to guarantee that the calculated operation strategy is feasible and it does not provoke any anomalies to the system's operating.

On this line of topics, the dissertation is structured as follows. Chapter 1 presents the Thesis framework, its objectives and its main hypothesis. In chapter 2, the energy hub concept is presented in detail, describing the state of the art, the benefits that it provides as well as the methodology for its mathematical formulation, including a detailed analysis of the system of the car manufacturing plant that has been used for the validation of the proposal. Chapter 3 describes the methodology for energy load modelling and prediction, showing several validation results of its implementation in the validation plant. Chapter 4 presents the optimization methodology and formulation, as well as several validation results and

comparisons that were obtained by its testing through simulations, compared with real-site data. In both of the above chapters, the state of the art for load modelling and prediction as well as for optimization methodologies applied to energy management are presented respectively. Finally, chapter 5 states the general conclusions of the dissertation, it proposes future researching work activities and presents a list with the published articles of this work.

The following figure summarizes the thesis structure in chapters and partial contents.

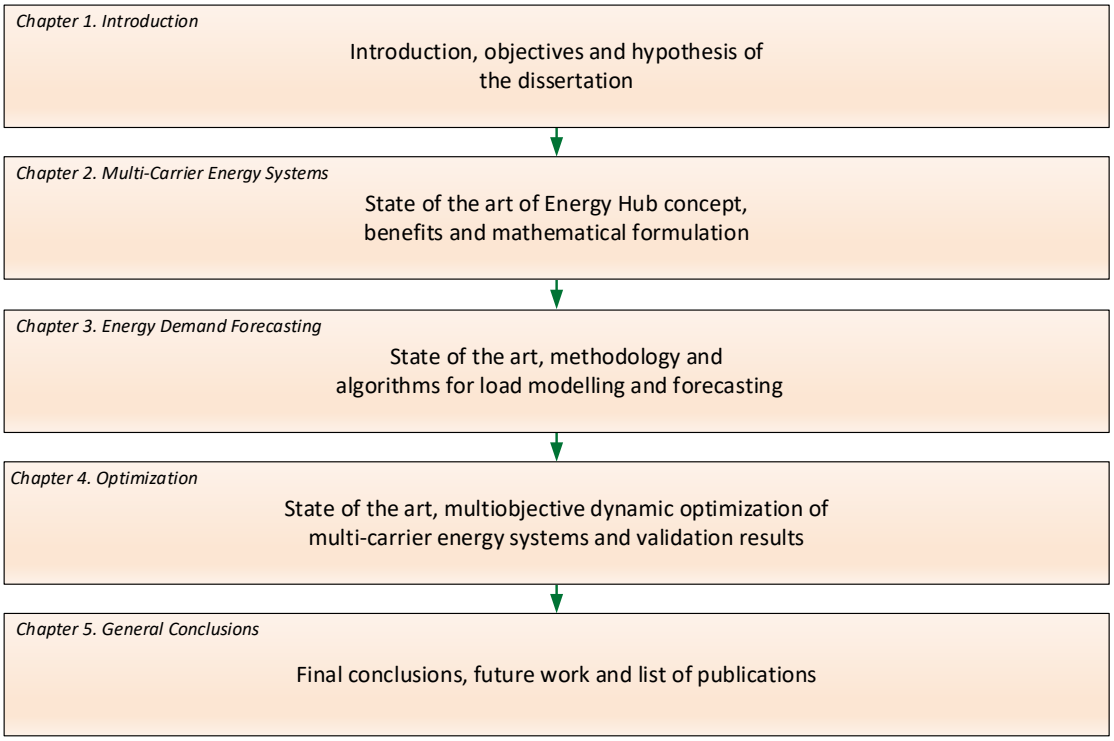

Figure 1.1: Block diagram of the Thesis overview.

1.2 Objective

The main objective of this thesis is to determine an optimization methodology and tools that permit to obtain the optimal operating strategy of an energy plant and its complete state for a specified future horizon, including transmission and conversion of multiple energy carriers within defined security constraints. This is managed by the implementation of a hybrid multi-objective optimization methodology based on artificial intelligence methods and energy prediction, applied to multi-carrier energy systems. The proposed methodology has as objective to improve the energy use efficiency of the multi-carrier energy systems, as well as to reduce their energy consumptions, their associated costs and the system's overall CO_2 emissions.

1.3 Hypotheses

In order to achieve the thesis objective, the following hypotheses were performed.

- Artificial intelligent algorithms can be used to accurately characterize the operation of the energy consumptions of a multi-carrier energy system, based on their historical data, as well as to precisely predict their future behavior under given conditions.
- By using a hybrid algorithm, which combines energy predictions and optimization algorithms, it is possible to calculate the optimal operations of a multi-carrier energy system that maximizes the overall energy efficiency of the system and minimizes a set of established criteria, taking into account the future demand profiles and considering influence parameters that can affect to the system´s operating.
- The use of a mixed-integer optimization algorithm will permit to resolve problems of energy systems which can contain production equipment with a non-linear operation behavior.

The exposed hypotheses are investigated by means of the research work that is reflected in the core of this dissertation document and presented in the subsequent chapters.

2. Multi-Carrier Energy Systems

2.1 Overview

Residential, commercial and industrial consumers require various types of energy services that are provided by different energetic infrastructures. The coal, the biomass as well as grid-bound energy carriers such as electricity, natural gas, district heating and district cooling are the most commonly used [4]. However, standard planning tools for the design of the energy networks do not generally provide an integrated view of the different infrastructures. In these cases the production, transmission and distribution of various energy carriers are treated as a set of independent problems, where each system is optimized individually without taking into account the possible existing interactions between the available energy carriers [5].

In some cases, it may be better to produce and supply the energy locally instead of consuming it from higher network levels. Subsequently, the characteristics of the infrastructure nodes change from passive points of distribution to entities, giving the flexibility to not only transmit but also convert and store the energy. These flexible systems can be represented as energy hubs [6] and are considered as an interface between different energy infrastructures and power loads. The core idea of the energy hub concept is the definition of a conversion matrix, which is able to describe the energy interactions of production, transmission and consumption in multi-carrier energy systems.

The energy hubs consume power at their inputs (e.g. electricity, natural gas, district heat, etc.) and provide certain energy services at their outputs. It should be noted that input power can

be generated locally or be supplied by external grids. The possibility of local generation encourages the concept of self-consumption energies, mainly provided by renewable energies. Within the hub, the energy can be converted and be stored to different forms by the use of energy equipment, such as transformers, heat exchangers and compressors among others. An example of an energy hub structure of a system with multiple energy carriers is presented in Figure 2.1, consisting of four inputs (i.e. electricity, natural gas, district heat and biomass source), several energy conversion equipment (i.e. transformer, CHP, heat exchanger, biomass boiler and chiller), an energy storage system (i.e. electric batteries) and three outputs (i.e. electricity, heat and cool).

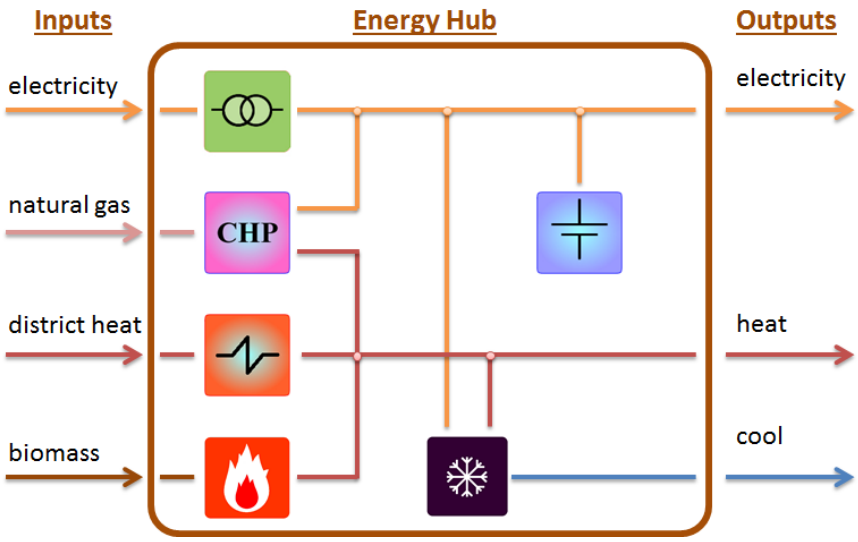

Figure 2.1: Example of an energy hub structure.

The concept of the multicarrier energy systems, formulated as an energy hub structure was initially presented in [7]-[8]. Before that, several conceptual approaches for an integrated view of transmission and distribution systems with dispersed generation and storage have been published, such as “energy-services supply systems” [9], “basic units” [10] and “micro grids” [11]. There are few studies that discuss the hub design issue, while the majority are focused on the different operational concerns in the multi-carrier energy systems, such as the economic dispatch [12]-[13], the optimal power flow [14]-[15], the unit commitment [16]-[17], and the optimal coupling of the energy carriers [18]. An approach in [19] considers the optimization of couplings among multiple energy networks consisting of electricity, natural gas and district-heating loads, while [20] presents a financial investment valuation method for energy hubs which includes conversion, storage and demand side management capabilities. An integrated planning approach based on portfolio theory is discussed in [21], which calculates the optimal portfolio of energy supplies. In [22], a mixed-integer nonlinear

programming problem is discussed, focused on the optimal coupling of the energy hub. This method is then extended in [23], evaluating the potential of connecting renewable energies into the system.

On the other hand, recent studies have focused on the integration of the EH in the framework of the Smart Grid, characterizing the concept of the smart energy hubs [24]. In this topic, a cloud-computing framework is presented in [25] that aims to resolve the problem of coordinating several SEH, in order to optimize the performance of the network. Furthermore, an integrated DSM technique is shown in [26], which models the interactions between different SEH as a non-cooperative game. Other studies of this topic propose and integrate a demand response program for SEH in order to modify the consumption patterns on the customer side [27]-[28], a MINLP probabilistic scheduling model for demand response programs integrated into Energy Hubs [29] and scheduling strategies for the integration of renewable energy sources and how to tackle the volatility and randomness of their production [30]-[31].

Nevertheless, the usage of the EH concept is mainly applied in real-time control applications that take decisions depending on data that are being received from the plant at the moment, or in some cases, the state of the network. Therefore there is great potential for improvement in this regard, when taking into consideration the future status of the plant in two aspects: upcoming changes in power demand and the system's dynamics in terms of the equipment's operation inertias. Together these aspects may cause inefficiencies and instabilities to the system because of the EH's inability to entirely satisfy the energy demands, or due to operating decisions that result to unstable operation for the equipment.

2.2 Potential Benefits

Due to the existence of different energy forms, as well as multiple energy carriers inside of an energy hub, it presents several advantages over the conventional or traditional energetic infrastructures. The increased reliability of the system, the flexibility of the energy supply, as well as the improvement of the system's overall performance are some of the key advantages of this concept [32].

Reliability is the ability of a power system to maintain a continuous service even with large changes in the supply or the demand side. The fact that energy hubs contain several ways of producing and transmitting the energy to the system's output ports gives the advantage of a flexible distribution. In this case, the system can fulfill the demand by using several energy carriers, involving simultaneously different production or conversion technologies. Furthermore, the existence of alternative ways of the energy supplying enables the system to continue operating properly in the face of the failure of some of its components.

Based on the above characteristics, the energy flow of the system can be optimized by selecting the proper energy carriers that can satisfy the demands at every instant of time. That means that the energy flow of the system can be controlled in such a way that fulfills a set of specific conditions or criteria, such as the minimization of energy use and costs, the prioritization of energy sources or production technologies, or the reduction of the system's emissions. To improve such optimization, demand forecasts and dynamics of the system must be considered, which define the control problem of the system in real time.

Finally, the overall performance of the system can be improved by taking into advantage the characteristics of the different energy forms that are available into the hub, such as the energy storage in thermal or compressed air form, the energy transmission in electric form, etc.

2.3 Mathematical Formulation

A multi-carrier energy system can be formulated as a set of vectors and matrices that describe the transmission and conversions of power from the inputs to the outputs of the system, indicating the available energy carriers. The generic modeling concept is presented in (2.1), whereas $P \in \mathbb{R}^{\psi}$ is defined as the energy source vector (input ports), as $\eta \in \mathbb{R}^{\psi \cdot \omega}$ the coupling matrix that contains the energy efficiencies of the equipment and by the vector $L \in \mathbb{R}^{\omega}$ are represented the energy demands of the system (output ports).

$$\begin{bmatrix} L_\alpha \\ L_\beta \\ \vdots \\ L_\psi \end{bmatrix} = \begin{bmatrix} \eta_{\alpha\alpha} & \eta_{\alpha\beta} & \cdots & \eta_{\alpha\omega} \\ \eta_{\beta\alpha} & \eta_{\beta\beta} & \cdots & \eta_{\beta\alpha} \\ \vdots & \vdots & \vdots & \ddots \\ \eta_{\psi\alpha} & \eta_{\psi\beta} & \cdots & \eta_{\psi\omega} \end{bmatrix} * \begin{bmatrix} P_\alpha \\ P_\beta \\ \vdots \\ P_\omega \end{bmatrix} \tag{2.1}$$

where

$$L = \left(L_\alpha, \dots, L_\psi\right), P = (P_\alpha, \dots, L_\omega) \; and \; \eta = \left(\eta_{\alpha\alpha}, \dots, \eta_{\psi\omega}\right) \tag{2.2}$$

2.3.1 Energy conversion

Four basic conversion systems can be considered for a multicarrier system, which can be classified by the number of their energy inputs and outputs (energy sources and productions, respectively).

- Single input and single output conversion systems, which are able to convert a determined energy form to another (e.g. gas boilers, electric chillers, etc.) or transmit and modify the characteristics of a same energy form (e.g. power electronics, transformers, etc.);
- Single input and multiple outputs conversion systems, which transform a single energy form to multiple energy types (e.g. cogeneration and tri-generation equipment, etc.);
- Multiple input and single output conversion systems, which require more than a single energy sources and produce one output (e.g. absorption machines, heat pumps, etc.);

- Multiple input and multiple output conversions systems, which consumes several energy types and produce numerous outputs of different energy forms (e.g. gasification processes).

An energy production equipment can be considered as an energy converter that produces a specific energy form at its input (*P*) and converts it to a different one at its output (*L*). The conversion factor depends on the coefficient of performance of the equipment (COP) and can be constant or variable depending on the equipment, the technology and the environmental conditions.

An example of a single input and output converter with constant conversion efficiency is presented in Figure 2.2.

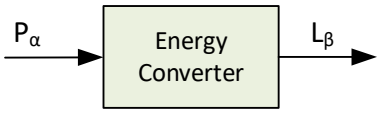

Figure 2.2: Converter with single input and single output, with constant COP.

The relationship between input and output of the equipment can be formulated as presented in (2.3), whereas $\eta_{\beta\alpha}$ is described the coefficient of performance of the equipment in order to produce energy of *γ* form by consuming energy of *α* form.

$$L_\beta = P_\alpha \cdot \eta_{\beta a} \tag{2.3}$$

Due to the conservation of power, the produced energy must be equal or lower than the input, considering the same power units, resulting to a coupling factor limitation, as described in (2.4). In cases of an energy conventions to different forms, the coupling factor can be higher than 1 (e.g. heat pump equipment).

$$L_\beta \le P_\alpha \quad \Rightarrow \quad 0 \le \eta_{\beta a} \le 1 \tag{2.4}$$

Thus the energy converters can be classified to 5 types (Table I) depending on their coupling factor and energy carriers [33].

Table I. Conversion Types

TYPE OF COUPLING	COUPLING FACTOR	ENERGY CARRIERS
Lossless transmission	$\eta_{\beta\alpha} = 0$	$\alpha = \beta$
Lossy transmission	$0 < \eta_{\beta\alpha} \le 1$	$\alpha = \beta$

Lossless conversion	$\eta_{\beta\alpha} = 1$	$\alpha \neq \beta$
Lossy conversion	$0 < \eta_{\beta\alpha} \leq 1$	$\alpha \neq \beta$
No coupling	$\eta_{\beta\alpha} = 0$	

As mentioned previously, there are energy converters with a variable COP values. In such cases, the performance of the converter can be found influenced by different external or internal factors (e.g. operating temperature, state of maintenance, operation point, etc.), varying the energy amount that is consumed by the converter, and thus its efficiency, in order to achieve its established setpoint. In this respect, the COP can be formulated as a transfer function with dependence on the influence factors, as described in (2.5).

$$\eta_{\beta\alpha} = f(x_1, x_2, \dots, x_n) \tag{2.5}$$

Whereas x_1, x_2,…, x_n are defined the influence factors of the converter´s performance and as $\eta_{\beta\alpha}$ its COP value, as depicted in Figure 2.3.

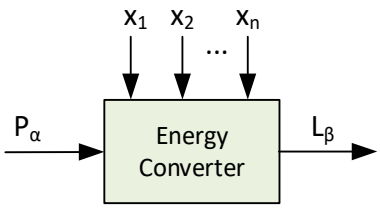

Figure 2.3: Converter with single input and single output, with variable COP.

2.3.2 Multi-stage energy conversion

A multi-carrier energy system can contain numerous stages of energy conversion to transmit the input energy source to the required output energy form. The multi-carrier energy system topologies are very common in industrial installations. For instance, in processes of cool production, where there is an initial stage of water heating through cogeneration or boiler technologies (consumption of gas) and a second stage of water cooling through absorption chillers (consumption of heat). Figure 2.6 presents an example of multi-stage energy conversion for a case of a double conversion, while (2.6) describes the mathematical relationship between the energy source (P_α) and the output (L_ϑ).

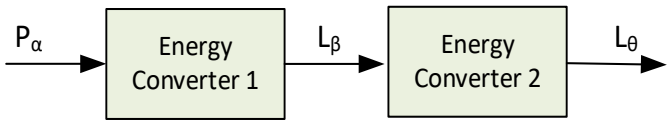

Figure 2.4: Example of a double-stage energy conversion.

$$L_\theta = L_\beta \cdot \eta_{\theta\beta} = P_\alpha \cdot \eta_{\beta\alpha} \cdot \eta_{\theta\beta} \qquad \forall \alpha \in \mathrm{A}, \quad \forall\ \beta, \theta \in \mathrm{B} \tag{2.6}$$

Whereas L_γ and L_ϑ are defined the energies that are produced by converter 1 and 2 respectively, as P_α is defined the energy source of the system and $\eta_{\gamma\alpha}$ and $\eta_{\vartheta\gamma}$ represent the COP values of the converters. It has to be mentioned, that the simple states of the equipment can be influenced by external factors, as mentioned previously.

2.3.3 System restrictions

The operation restrictions of an Energy Hub can be classified in to two main categories:

- Restrictions related to the dispatch of converted energy inside the hub;
- Restrictions related to the dispatch of input energy of the hub.

In the first case, the total energy amount that is produced by a single converter (or group of converters) and is distributed to the energy carriers cannot exceed the nominal power of the converter (or group of converters). Taking as an example the system of Figure 2.5, the aggregation of the dispatched energy $L_{\beta 1}$ and $L_{\beta 2}$ cannot surpass the total production of Converter 1 (COP = $\eta_{\beta\alpha}$).

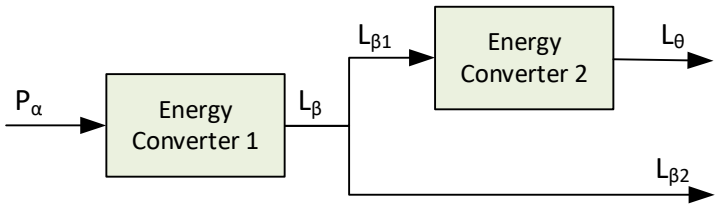

Figure 2.5: Dispatch of converted energy.

Mathematically, the system´s dispatch restriction can be described in a form of inequality as presented in (2.7).

$$0 \le \sum_{i=1}^{2} L_{\beta i} \le P_{\alpha} \cdot \eta_{\beta a} \quad \forall \alpha \in \mathrm{A}, \quad \forall \beta \in \mathrm{B} \tag{2.7}$$

where

$$L_{\beta i} = L_{\beta} \cdot v_i \text{ and } 0 \le v_i \le 1, \quad i = (1, 2), \tag{2.8}$$

whereas *v* is defined the dispatch factor of the total energy input L_{γ} to the different carriers.

In the case of a restriction related to the dispatch of the input energy, the total energy amount that is distributed to the energy carriers cannot exceed the total energy supply of the input. Taking as an example the system of Figure 2.6, the aggregation of the dispatched energy $P_{\alpha 1}$, $P_{\alpha 2}$,…, $P_{\alpha n}$, cannot exceed the total energy supply of P_{α}.

$$0 \le \sum_{i=1}^{n} P_{\alpha i} \le P_{\alpha} \tag{2.9}$$

where

$$P_{\alpha i} = P_{\alpha} * v_i, \quad i = (1,2, \dots, n) \tag{2.10}$$

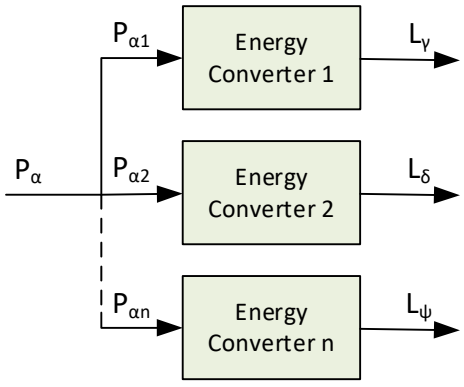

Figure 2.6: Dispatch of input energy.

2.3.4 Operating bounds

The operating bounds describe the lower and upper energy production limits of a converter. Mathematically, the bounds can be formulated as an inequality relationship, as presented in

(2.12), where the lb_γ and ub_γ describe the lower and upper bounds of the converter of Figure 2.3. P_α describes the energy consumption of the equipment, L_γ^{min} the minimum possible operation value of the converter and the $\eta_{\gamma\alpha}$ the converter´s COP.

$$lb_\gamma \le P_\alpha \cdot \eta_{\gamma\alpha} \le ub_\gamma \tag{2.11}$$

where

$$lb_\gamma = \begin{Bmatrix} 0 & , & L_\gamma^{min} = 0 \\ (0 | L_\gamma^{min}) & , & L_\gamma^{min} > 0 \end{Bmatrix} \tag{2.12}$$

2.4 Procedure for calculating the mathematical formulation of an energy hub system

For a given hub configuration, the mathematical equations that describe the energy flow between the input and output ports, the system's restrictions as well as the converters' operation bounds can be obtained according to the following procedure.

(1) **Determination of the different output port groups:** To analyze the hub's structure and determine which loads are being supplied from the same energy sources. The number of the load groups defines the size of the coupling matrix of the system (rows of the matrix).

(2) **Determination of the different energy converts:** To analyze the hub's structure and determine the different energy converts as well as the interconnections between them (e.g., gas to electricity, gas to heating water, electricity to cooling water, etc.). The total number of energy transmissions and conversions defines the column number of the coupling matrix.

(3) **Determination of the energy flow inside the hub:** In this step, the formulation of the coupling matrix of the hub is made, which describes the energy flow from the system's input ports to the outputs, towards the energy converts.

(4) **Determination of the system´s restrictions:** To formulate the necessary matrices that describe the energy dispatch restrictions (related to the converted energy and input energy respectively) in a set of inequalities relationships.

(5) **Calculation of the converter´s operation bounds:** The last step of the formulation is the calculation of the upper and lower bounds of the converters, in relation to their energy inputs.

2.5 Application Example

This section contains a short example, demonstrating the use of the suggested procedure for formulating the mathematical equations and constraints that describe a stable operation of an energy hub system. The example considers an actual case of an automotive industrial manufacturing system, depicted in Figure 2.7. The system is supplied from the electrical grid and the natural gas network and it contains a total of 4 loads with 3 types of energy demands for each one: electrical, heating and cooling demand. The total heating demand is fulfilled by a cogeneration equipment and three gas boilers with identical characteristics. The cooling supply is provided by two absorption machines and six electric chillers, connected in pairs.

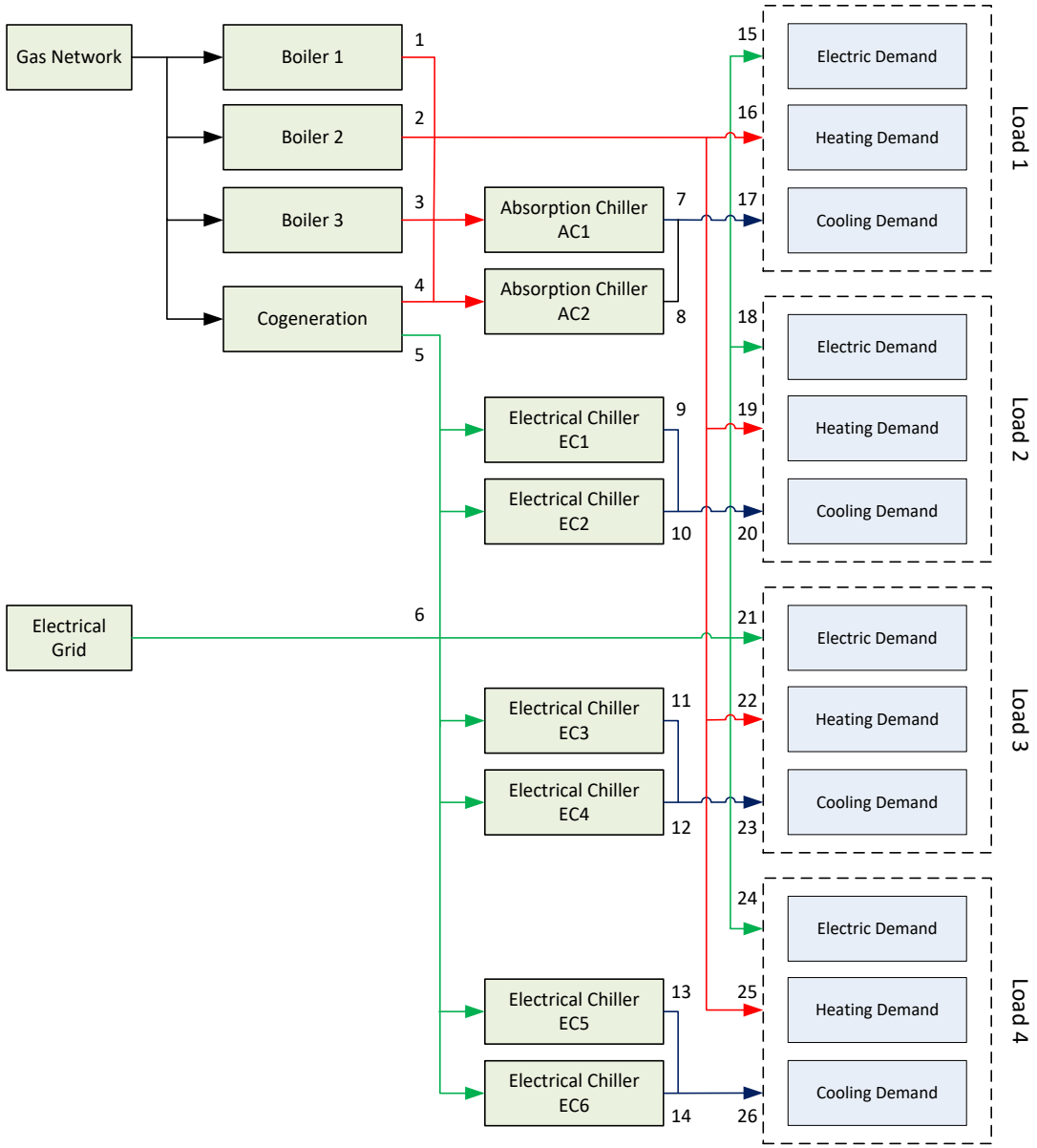

Figure 2.7: Block diagram of the energy hub system of an automotive manufacturing system.

The system of Figure 2.7 has been used as an experimental plant for the testing and validation of the different hypotheses of this dissertation, as presented in the following chapters.

Determination of the different output port groups:

Based on Figure 2.7, it can be observed that the electric demands of the four loads are all connected to the same input port and converter (i.e. electric grid and cogeneration equipment). Thus, they can be grouped and considered as a unique demand, formed by their sum. Similarly, the same action and can be made for the heating demands, due to they are all supplied by the same converters (i.e. three boiler equipment and cogeneration).

Moreover, the energy hub supplies four cooling demands that are independent of each other as they are connected to different group of converters. Thus, by the number of demand groups, it can be concluded that the coupling matrix has a row size of six.

Determination of the different energy converts:

By analyzing the energy transmission and conversion possibilities of the energy hub system, result a total of fourteen cases, as detailed in Table II.

Table II. Energy transmission and conversion cases of the energy hub of Figure 2.7.

#	DESCRIPTION
1	*A direct transmission of electricity to electricity (from the grid to the demand)*
2	*A gas to heat conversion through the gas boiler 1 equipment*
3	*A gas to heat conversion through the gas boiler 2 equipment*
4	*A gas to heat conversion through the gas boiler 3 equipment*
5	*A gas to heat conversion through the cogeneration equipment*
6	*A gas to electricity conversion through the cogeneration equipment*
7	*A heat to cool conversion through the AC1 absorption equipment*
8	*A heat to cool conversion through the AC2 absorption equipment*
9	*An electricity to cool conversion through the EC1 electric chiller*
10	*An electricity to cool conversion through the EC2 electric chiller*
11	*An electricity to cool conversion through the EC3 electric chiller*
12	*An electricity to cool conversion through the EC4 electric chiller*
13	*An electricity to cool conversion through the EC5 electric chiller*
14	*An electricity to cool conversion through the EC6 electric chiller*

Nevertheless, as the electric and heating production by the cogeneration are not autonomous but linked, the total conversion cases result to thirteen. Thus it can be concluded that the coupling matrix of the energy hub has a size of six by thirteen (6×13).

Determination of the energy flow inside the hub:

The following equations describe the energy flow of each point inside the hub of Figure 2.7. Q_x define the electric or the thermal power of a numeric point *x*, as numerated in the scheme.

The heat production from the cogeneration equipment and the gas boilers can be formulated as the product of the amount of natural gas consumed by each equipment and its thermal coefficients, as described by the following equations, where *g2h* represents an energy conversion from natural gas to heat and $P_{gas}^{in_{\max}}$ defines the maximum amount of natural gas that is supplied by the network.

$$Q_1 = \eta_{boiler1}^{\text{g2h}} \cdot P_{gas}^{in_{\max}} \cdot v_1 \quad , \quad 0 \le v_1 \le 1 \tag{2.13}$$

$$Q_2 = \eta_{boiler2}^{\text{g2h}} \cdot P_{gas}^{in_{\max}} \cdot v_2 \quad , \quad 0 \le v_2 \le 1 \tag{2.14}$$

$$Q_3 = \eta_{boiler3}^{\text{g2h}} \cdot P_{gas}^{in_{\max}} \cdot v_3 \quad , \quad 0 \le v_3 \le 1 \tag{2.15}$$

$$Q_4 = \eta_{CHP}^{\text{g2h}} \cdot P_{gas}^{in_{\max}} \cdot v_4 \quad , \quad 0 \le v_4 \le 1 \tag{2.16}$$

The electric power that is generated by the cogeneration depends on its thermal production as well as on the amount of its primary energy consumption. It can be formulated as presented in (2.17), where *g2e* represent an energy conversion from natural gas to electricity.

$$Q_5 = \eta_{CHP}^{\text{g2e}} \cdot P_{gn}^{in_{\max}} \cdot v_4 \tag{2.17}$$

The electric power that is supplied by the grid can be varied from 0 to the maximum value of the contracted power (or the power that the infrastructure supports), represented as $P_{grid}^{in_{\max}}$.

$$0 \le Q_6 \cdot v_5 \le P_{grid}^{in_{\max}} \quad , \quad 0 \le v_5 \le 1 \tag{2.18}$$

The supplying of cold water for load 1 is provided by the two absorption machines, which consume a part of the heat produced by the cogeneration and the three boilers. The cooling production can be formulated as the product of the quantity of the absorption machines' input source (heat) and their thermal coefficients. Whereas *h2c* and *e2c* are described an energy conversion from heat to cool and an energy conversion from electricity to cool, respectively.

$$Q_7 = (Q_1 + Q_2 + Q_3 + Q_4) \cdot v_6 \cdot \eta_{AC1}^{\text{h2c}} \quad , \quad 0 \le v_6 \le 1 \tag{2.19}$$

$$Q_8 = (Q_1 + Q_2 + Q_3 + Q_4) \cdot v_7 \cdot \eta_{AC2}^{\text{h2c}} \quad , \quad 0 \le v_7 \le 1 \tag{2.20}$$

Similarly, in the case of the electric chillers, the cooling production can be formulated taking into account the electric consumption of each equipment and their thermal coefficients.

$$Q_9 = (Q_5 + \mathrm{Q}_6) \cdot v_8 \cdot \eta_{EC1}^{\text{e2c}} \quad , \quad 0 \le v_8 \le 1 \tag{2.21}$$

$$Q_{10} = (Q_5 + \mathrm{Q}_6) \cdot v_9 \cdot \eta_{EC2}^{\text{e2c}} \quad , \quad 0 \le v_9 \le 1 \tag{2.22}$$

$$Q_{11} = (Q_5 + \mathrm{Q}_6) \cdot v_{10} \cdot \eta_{EC3}^{\text{e2c}} \quad , \quad 0 \le v_{10} \le 1 \tag{2.23}$$

$$Q_{12} = (Q_5 + \mathrm{Q}_6) \cdot v_{11} \cdot \eta_{EC4}^{\text{e2c}} \quad , \quad 0 \le v_{11} \le 1 \tag{2.24}$$

$$Q_{13} = (Q_5 + \mathrm{Q}_6) \cdot v_{12} \cdot \eta_{EC5}^{\text{e2c}} \quad , \quad 0 \le v_{12} \le 1 \tag{2.25}$$

$$Q_{14} = (Q_5 + \mathrm{Q}_6) \cdot v_{13} \cdot \eta_{EC6}^{\text{e2c}} \quad , \quad 0 \le v_{13} \le 1 \tag{2.26}$$

The points Q_{15} *to* Q_{26} represent the energy demands of the system, whose values are considered as known.

Table III. Description of node points of Figure 2.7.

POINT IN HUB	DESCRIPTION
P_{15}	*Electric demand of Load 1*
Q_{16}	*Heating demand of Load 1*
Q_{17}	*Cooling demand of Load 1*
P_{18}	*Electric demand of Load 2*
Q_{19}	*Heating demand of Load 2*
Q_{20}	*Cooling demand of Load 2*
P_{21}	*Electric demand of Load 3*
Q_{22}	*Heating demand of Load 3*
Q_{23}	*Cooling demand of Load 3*
P_{24}	*Electric demand of Load 4*
Q_{25}	*Heating demand of Load 4*
Q_{26}	*Cooling demand of Load 4*

Combining the above equations, the total heating demand can be expressed in terms of energy input as described in (2.27).

$$L_{total}^{heat} = Q_{16} + Q_{19} + Q_{22} + Q_{25} = P_{gas}^{in_{\max}} \cdot (\eta_{boiler1}^{\mathrm{g2t}} \cdot v_1 + \eta_{boiler2}^{\mathrm{g2t}} \cdot v_2 + \eta_{boiler3}^{\mathrm{g2t}} \cdot v_3 + \eta_{CHP}^{\mathrm{g2t}} \cdot v_4) \quad (2.27)$$

Likewise, the electric power flow from the source to the demand can be described as:

$$L_{total}^{electric} = Q_{15} + Q_{18} + Q_{21} + Q_{24} = Q_6 + \eta_{CHP}^{\mathrm{g2e}} \cdot P_{gas}^{in_{\max}} \cdot v_4 \quad (2.28)$$

Equations (2.29), (2.30), (2.31) and (2.32) refer to the energy flow from the energy sources to the cooling demand for Loads 1 to 4 respectively.

$$Q_{17} = \left(\sum_{i=1}^{4} Q_i \right) \cdot (\eta_{AC1}^{\mathrm{h2c}} \cdot v_6 + \eta_{AC2}^{\mathrm{h2c}} \cdot v_7) \quad (2.29)$$

$$Q_{20} = (\eta_{CHP}^{\mathrm{g2e}} \cdot P_{gas}^{in_{\max}} \cdot v_4 + \mathrm{Q}_6) \cdot (\eta_{EC1}^{\mathrm{e2c}} \cdot v_8 + \eta_{EC2}^{\mathrm{e2c}} \cdot v_9) \quad (2.30)$$

$$Q_{23} = (\eta_{CHP}^{\mathrm{g2e}} \cdot P_{gas}^{in_{\max}} \cdot v_4 + \mathrm{Q}_6) \cdot (\eta_{EC3}^{\mathrm{e2c}} \cdot v_{10} + \eta_{EC4}^{\mathrm{e2c}} \cdot v_{11}) \quad (2.31)$$

$$Q_{26} = (\eta_{CHP}^{\mathrm{g2e}} \cdot P_{gas}^{in_{\max}} \cdot v_4 + \mathrm{Q}_6) \cdot (\eta_{EC5}^{\mathrm{e2c}} \cdot v_{12} + \eta_{EC6}^{\mathrm{e2c}} \cdot v_{13}) \quad (2.32)$$

Finally, by combining the above equations, the expression (2.1) can be rewritten as follows, describing the case of the system of Figure 2.7.

$$L = \eta \cdot P \quad (2.33)$$

where

$$L = \underset{6\times 1}{\begin{bmatrix} L_{total}^{electric} \\ L_{total}^{heat} \\ Q_{17} \\ Q_{20} \\ Q_{23} \\ Q_{26} \end{bmatrix}} \quad , \quad P = \underset{13\times 1}{\begin{bmatrix} P_{grid}^{in_{\max}} \cdot v_5 \\ P_{gas}^{in_{\max}} \cdot v_1 \\ P_{gas}^{in_{\max}} \cdot v_2 \\ P_{gas}^{in_{\max}} \cdot v_3 \\ P_{gas}^{in_{\max}} \cdot v_4 \\ P_{heat1} \\ P_{heat2} \\ P_{grid}^{in_{\max}} \cdot v_8 \\ P_{grid}^{in_{\max}} \cdot v_9 \\ P_{grid}^{in_{\max}} \cdot v_{10} \\ P_{grid}^{in_{\max}} \cdot v_{11} \\ P_{grid}^{in_{\max}} \cdot v_{12} \\ P_{grid}^{in_{\max}} \cdot v_{13} \end{bmatrix}} \tag{2.34}$$

Whereas P_{heat1} and P_{heat2} are defined the amount of heating energy that is consumed by the absorption machine 1 and absorption machine 2, respectively.

$$\eta = \underset{6\times 13}{\begin{bmatrix} 1 & 0 & 0 & 0 & \eta_{CHP}^{g2e} & 0 & 0 & 0 & 0 & 0 & 0 & 0 & 0 \\ 0 & \eta_{boiler1}^{g2t} & \eta_{boiler2}^{g2t} & \eta_{boiler3}^{g2t} & \eta_{CHP}^{g2h} & 0 & 0 & 0 & 0 & 0 & 0 & 0 & 0 \\ 0 & 0 & 0 & 0 & 0 & \eta_{AC1}^{h2c} & \eta_{AC2}^{h2c} & 0 & 0 & 0 & 0 & 0 & 0 \\ 0 & 0 & 0 & 0 & 0 & 0 & 0 & \eta_{EC1}^{e2c} & \eta_{EC2}^{e2c} & 0 & 0 & 0 & 0 \\ 0 & 0 & 0 & 0 & 0 & 0 & 0 & 0 & 0 & \eta_{EC3}^{e2c} & \eta_{EC4}^{e2c} & 0 & 0 \\ 0 & 0 & 0 & 0 & 0 & 0 & 0 & 0 & 0 & 0 & 0 & \eta_{EC5}^{e2c} & \eta_{EC6}^{e2c} \end{bmatrix}} \tag{2.35}$$

Determination of the system´s restrictions:

The total of electric power that is used to fulfill the electric demand together with the power that is consumed by the electric chillers cannot exceed the maximum limit of power that is available in the hub (i.e. grid supply and electric power produced by the cogeneration).

$$\left(v_5 + v_8 + v_9 + v_{10} + v_{11} + v_{12} + v_{13}\right) \cdot P_{grid}^{in_{\max}} \leq P_{grid}^{in} + \left(\eta_{CHP}^{g2e} \cdot P_{gas}^{in_{\max}} \cdot v_4\right) \tag{2.36}$$

The dispatch factors v_1 to v_4 represent the percentage of the natural gas use as input in the equipment, compared with the maximum amount of gas. The sum of these factors cannot exceed the maximum quantity that can be supplied by the network and thus, equation (2.37) is confirmed.

$$v_1 + v_2 + v_3 + v_4 \leq 1 \tag{2.37}$$

The total heat that is consumed by the absorption machines together with the energy that is used to fulfill the heating demand cannot exceed the total energy that is produced by the cogeneration and the three boilers.

$$P_{heat1} + P_{heat1} + L_{total}^{heat} \leq \sum_{i=1}^{4} Q_i \tag{2.38}$$

Calculation of the converter´s operation bounds:

Finally, the operation bounds of the equipment can be expressed as inequality in terms of their energy input, as presented in (2.39).

$$\begin{bmatrix} L_{boiler1}^{\min} \\ L_{boiler2}^{\min} \\ L_{boiler3}^{\min} \\ L_{CHP}^{\min} \\ L_{AC1}^{\min} \\ L_{AC2}^{\min} \\ L_{EC1}^{\min} \\ L_{EC2}^{\min} \\ L_{EC3}^{\min} \\ L_{EC4}^{\min} \\ L_{EC5}^{\min} \\ L_{EC6}^{\min} \end{bmatrix} \leq \begin{bmatrix} P_{gas}^{in_{\max}} \cdot v_1 \cdot \eta_{boiler1}^{g2t} \\ P_{gas}^{in_{\max}} \cdot v_2 \cdot \eta_{boiler2}^{g2t} \\ P_{gas}^{in_{\max}} \cdot v_3 \cdot \eta_{boiler3}^{g2t} \\ P_{gas}^{in_{\max}} \cdot v_4 \cdot \eta_{CHP}^{g2t} \\ P_{heat1} \cdot \eta_{AC1}^{h2c} \\ P_{heat2} \cdot \eta_{AC2}^{h2c} \\ P_{grid}^{in_{\max}} \cdot v_8 \cdot \eta_{EC1}^{e2c} \\ P_{grid}^{in_{\max}} \cdot v_9 \cdot \eta_{EC2}^{e2c} \\ P_{grid}^{in_{\max}} \cdot v_{10} \cdot \eta_{EC3}^{e2c} \\ P_{grid}^{in_{\max}} \cdot v_{11} \cdot \eta_{EC4}^{e2c} \\ P_{grid}^{in_{\max}} \cdot v_{12} \cdot \eta_{EC5}^{e2c} \\ P_{grid}^{in_{\max}} \cdot v_{13} \cdot \eta_{EC6}^{e2c} \end{bmatrix} \leq \begin{bmatrix} L_{boiler1}^{\max} \\ L_{boiler2}^{\max} \\ L_{boiler3}^{\max} \\ L_{CHP}^{\max} \\ L_{AC1}^{\max} \\ L_{AC2}^{\max} \\ L_{EC1}^{\max} \\ L_{EC2}^{\max} \\ L_{EC3}^{\max} \\ L_{EC4}^{\max} \\ L_{EC5}^{\max} \\ L_{EC6}^{\max} \end{bmatrix} \tag{2.39}$$

2.6 Conclusions

The energy hub concept presents a promising concept in terms of energy efficiency, as it provides a way of interpreting complex energy infrastructures as a unique interconnected system. Additionally, it permits to analyze the infrastructure of the system and its energy flow in terms of robustness, reliability and capacity, allowing to study and evaluate stable operation strategies for the system´s management.

The main contribution of this chapter is the presentation of a methodology for the analysis of the energetic infrastructure of a multi-carrier energy system, as well as its mathematical formulation in terms of system interconnections, energy restrictions, as well as operation bounds and energy availability. The obtained equations guarantee that the system is working into the engineering boundaries, avoiding operation anomalies that can be caused by unsatisfied energy requirements or overload of the infrastructure.

This methodology has been used for the analysis of the system of a car manufacturing plant, which has been used as test bench for the evaluation and validation of the hypotheses of this dissertation.

3.Energy Demand Forecasting

3.1 State of the art

With the continuously growing demand of the energy, it is getting more important to develop systems capable to optimize the energy use. Energy management is nowadays a subject of great importance because of the facing emerging problems of the global warming and fossil fuel shortage. In the industrial sector, the energy management systems have focused so far on the monitoring and the off-line management of energy, as outlined in [34]. The typical energy management systems are based on the real time collection of information about the plant's operation using energy meters and sensors. Those systems help to monitor the operation of the installations, collect data and generate reports to identify the possible critical points of the processes and consumptions. However, intelligent systems can improve the operation of the energy management systems, offering further and more advanced functionalities such as supervision and fault diagnosis, predictive maintenance, energy optimization and energy forecasting. All of the above functionalities have a common core: They use information of the consumption's historical behaviors by means of mathematical models, in order to predict their future patterns under known conditions. This information is even more important when advanced control actions that take into consideration the future conditions are implemented into the system, where the demand profiles are those that define the operation strategies. Thus, the accuracy of the demand forecasts is crucial for the operation of the system, as it can alter the demand pattern in the prediction horizon.

On this topic, several approaches have been studied over the past years to analyze and study the demand patterns based on historical data of the loads. For instance, different implementations of ANNs were presented in [35], [36] and [37], focused on the modeling and prediction of the load behavior in electrical distribution systems. Furthermore, the consideration of fuzzy logic as a forecasting tool for predicting a short-term load demand was investigated in [38], comparing its accuracy with ANN models. On the other hand, an application that uses traditional neuronal networks was presented in [39], in which it faces multi-input-multi-output applications with single input and output networks. A combination of support vector regression and differential evolution algorithms was used in [40], trying to deal with building energy consumption forecasting.

An ANFIS implementation for energy prediction of regional electrical loads in Taiwan was presented in [41], comparing its performance with other similar techniques (i.e., regression models, ANN-based models, genetic algorithms and hybrid ellipsoidal fuzzy systems). A cellular multi-grid genetic algorithm was presented in [42] to face balancing problems in assembling lines. Techniques based on cultural algorithms were presented in [43] to resolve complex mechanical design optimization problems in an efficient and effective method.

On this line of approaches, Section 3.2 presents a combination of Genetic Algorithms and Adaptive Neuro-Fuzzy Inference Systems as modeling and prediction algorithm, as well as the proposed methodology of their operation, with aim to generate high accuracy customizable mathematical models for different consumptions in order to obtain short-term demand forecasts that will be used in the energy hub optimization strategy.

Figure 3.1 depicts the block diagram of the proposed method, in which the GA is being used to determine the best training inputs of the ANFIS structure for an optimized data learning.

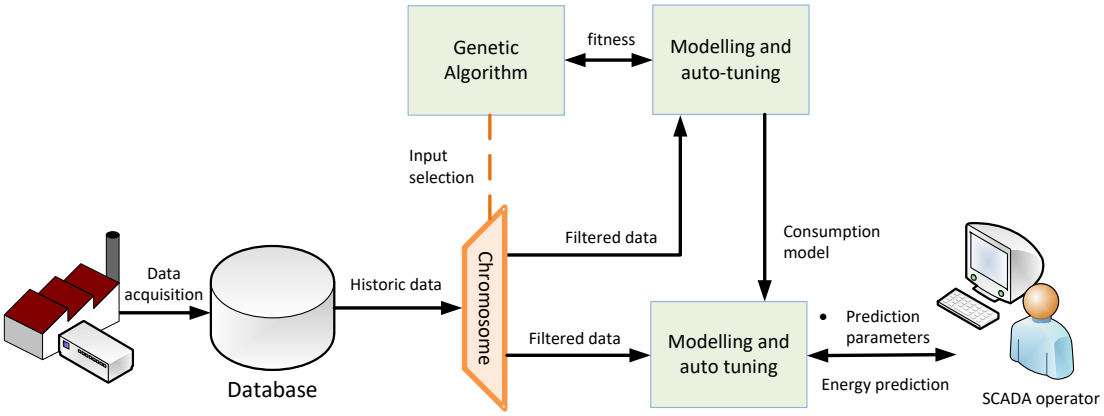

Figure 3.1: Block diagram of the proposed demand modelling and prediction method.

3.1.1 ANFIS

ANFIS is based on systems of Takagi-Sugeno type, combining fuzzy logic and neural networks. It was developed on 1993 by Rogen Jang [44] as a technique, able to overcome the shortcoming of the existed ANNs and fuzzy systems, whose major disadvantage was the inability to give any explicit knowledge or causal relationships for a system [45]-[46]. One of the main advantages that ANFIS presents is its flexibility over the training datasets. It can be adapted in different time intervals and prediction horizons, being able to model and accurately predict the dynamics that present the studied signals. This flexibility in adaptation is what it makes it a great tool for use in industrial consumptions, where infrequent and varying patters are very commons.

The fuzzy part of the ANFIS is constructed by means of input and output variables, membership functions (MF), fuzzy rules and inference method. The inputs consist of data that are correlated with the output as, for example, for the case energy consumptions, the scheduled production (related to the load), the climatic condition and the day of the week, among others [47]. The MFs of the system are the functions that define the fuzzy sets [48]. Finally, the fuzzy rules have a form of if-then rule and define how the output must be calculated for a specific value of membership of its inputs [49].

Figure 3.2 depicts the general architecture of an ANFIS model, which consists of multiple inputs *x* and one output *z*.

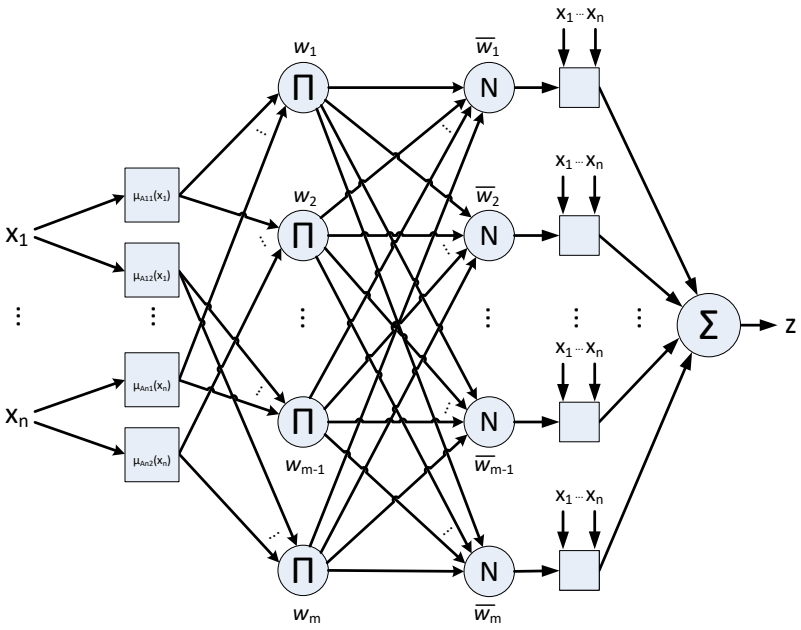

Figure 3.2: ANFIS architecture with two inputs, four rules and one output.

where n describes the number of the ANFIS inputs, m describes the number of the adaptive nodes (where $m = n^2$ for two linguistic terms per input) , $A_{ij}(X_i)$ is the linguistic label associated with the MF μ of input i, w_i is the product of all the incoming signals of node i and $\overline{w}_i$ describes the normalized firing strength of node i.

The typical ANFIS architecture consists of five layers. The first layer executes the fuzzification process on the inputs in order to convert them to fuzzy values through some membership functions μ. In the proposed method, a bell-shaped membership function has been selected with maximum equal to 1 and minimum equal to 0, as described in (3.1).

$$\mu_{Aij}(x_i) = \frac{1}{1 + \left| \frac{x_i - c_i}{a_i} \right|^{2b_i}} \quad , \quad j = 1, 2 \tag{3.1}$$

where c_i, a_i and b_i are the premise parameters and define the bell center, width and fuzzification factor of node i, respectively. Figure 3.2 presents an example of the membership function for different values of fuzzification factor.

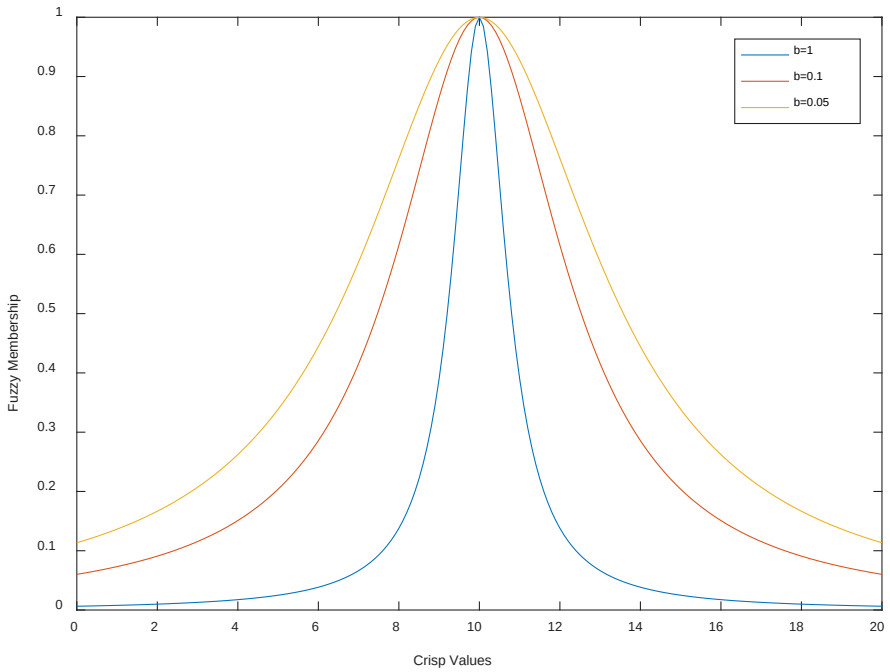

Figure 3.3: Fuzzy membership function with modified fuzzification factor (a=0.8, c=10).

The second layer calculates the fire strength of the rule, performing the AND operator of the incoming signals.

$$w_i = \prod_{i=1}^{m} \mu_{Aij}(\mathrm{X}_i) \quad , \quad j = 1, 2 \tag{3.2}$$

The third layer normalizes the membership functions, calculating the ration of the *i*-th rule's firing strength to the sum of all rules' strengths [50], applying the equation of (3.3).

$$\overline{w_i} = \frac{w_i}{\sum_{i=1}^{m} w_i} \tag{3.3}$$

The fourth layer executes the consequent part of the fuzzy rules by performing the Takagi-Sugeno fuzzy reasoning method, described in (3.4). During the execution, the consequent parameters k_i of each node are calculated.

$$\overline{w} * f_i = \overline{w} * (k_{i0} + k_{i1} * X_1 + k_{i2} * X_2 + \cdots + k_{in} * X_n) \tag{3.4}$$

Finally in layer 5, the only neuron computes the overall output of the incoming signals:

$$z = \sum_{i=1}^{m} w_i \cdot f_i \tag{3.5}$$

The same steps are used in both modelling and prediction operations. Their main difference is that in the modelling process, the objective is to train the consequent and premises parameters of the nodes by using known operation conditions (cases with known inputs and outputs), while in the prediction process, the objective is to obtain the output by using only known inputs (known values of the trained parameters).

In this architecture, the first and fourth layers contain the parameters that can be modified during the training (premises and consequent parameters respectively). There are two stages for the learning process. The forward path and the backward path. In the course of the forward path, the premises parameters are being set in steady state, while a recursive least square estimator method is applied to repair the consequent parameters. Next, after the consequent parameters are obtained, the input data are passed back to the ANFIS inputs and the generated output is compared with the actual one. During the backward path, the consequent parameters are set in a steady state and the error that occurred during the comparison

between the outputs (generated and actual) is propagated back to the first layer, by updating the premises parameters using the back propagation method [51].

Table IV. Training process procedure of ANFIS.

	FORWARD PATH	Backward path
Premise parameters	*Fixed*	*Gradient descent*
Consequent parameters	*Least-square estimator*	*Fixed*
Signals	*Node outputs*	Error signals

3.1.2 Genetic Algorithms

Genetic algorithms consist of a heuristic method that is based on the mechanism of natural selection and natural genetics, inspired by the Darwin's theory of evolutions, Mendelian's genetics and Weizmann's species selection theory [52]. A GA allows a population that is composed of many individuals (chromosomes) to evolve under specified selection rules to a state that maximizes the fitness. One of its main characteristics is that evaluates multiple solutions at the same time rather than a single one per iteration. It uses arithmetic operations, such as selection, mating and mutation, to perform organized but random information exchanges of the evaluated solutions, with objective to inherit the individuals that present high fitness value and eliminate the low ones [53]-[54]. The operation of the genetic algorithm consists of the following steps.

Generation of the initial population: In this step, the initial population is generated with individuals that are typically created with random values of the permitted domain range. Alternatively, their values are obtained by applying calculation methods that are determined by the problem domain.

Fitness calculation: In this step, all the individuals of the current population are evaluated in terms of a fitness measure, and are being classified based on their fitness rank.

Evaluation of criteria: In this step, the algorithm evaluates the established termination criteria and determines whether the process can end or proceed to the next generation.

Application of operators: In case the process continues, the algorithm generates a new population by selecting some of the current best individuals based on their fitness rank. Then, this new population is completed by applying the genetic operators of crossover and mutation to the new individuals [55]. Depending on the case, some implementations extend the current

population by adding new individuals in the current population, omitting the elimination of the least fit ones. Other implementations create a completely new population of individuals by applying the genetic operators to the current population. Moreover, there are GAs that do not use generations at all, but they use continuous replacements [56].

Finally, the process is repeated from *step b* until the satisfaction of any of the predefined termination criteria. The following figure depicts the flowchart with the steps of the genetic algorithms' process.

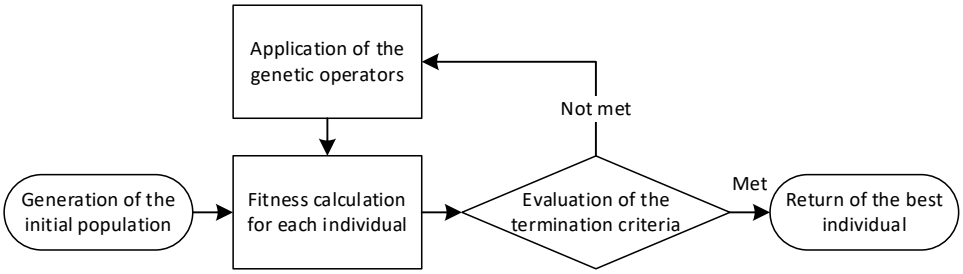

Figure 3.4: Simplified flowchart of the Genetic Algorithms' process.

Compared to other search procedures, the genetic algorithm present the following important advantages:

- The formulation and execution of the algorithm permits to optimize problems with both continuous and discrete variables;
- It doesn't require derivative information through the evaluation of the solutions and is able to search simultaneously a wide sampling of the cost surface;
- It is capable of dealing with problems that contain a large number of variables and complex cost surfaces (solutions with multiple local minimums);
- It provides a list of optimum variables than just a single solution.

These advantages produce good results in problems where traditional optimization approaches fail. Nevertheless, GA is not the best way to solve every problem, such as in convex analytical functions of few variables, where the traditional methods are tuned to quickly find the solution. In such cases, the calculus-based methods outperform the GA in terms of computational effort and time response. Considering all the above, the combination of GA and ANFIS can result to a powerful tool for the autonomous determination of the optimal training inputs for the demand modelling, as well as to enhance the flexibility on adapting to different consumption patterns with irregular behavior.

3.2 Energy Modeling and Prediction

This section presents a short-term load forecasting methodology based on adaptive neuro-fuzzy inference systems and genetic algorithms, which uses historical data from the consumptions' operation as well as other operation parameters that can influence on the demands' behavior. Despite that other data-driven modelling techniques can be suitable for this task, the combination of ANFIS and GA has been selected due to its flexibility on adapting easily in data patterns with irregular and infrequent behavior, while maintaining high accuracy results. These characteristics makes it suitable for applications in industrial processes, where auto-adjustment tasks and tuning actions have to be made periodically.

Nevertheless, independently of the modelling technique to be used, a series of preprocessing tasks have to be applied over the acquired data to equalize and adequate them for the data modelling process.

The proposed methodology consists of two main parts, as described in the following subsections:

i. The training and auto-tuning algorithm for the mathematical modelling of a consumption's pattern based on its historical behavior and its operation conditions;
ii. The prediction algorithm that forecasts the short-term future energy demand of a modelled consumption, for known operation conditions.

3.2.1 Modelling Process

In the modelling and auto-tuning process, the genetic algorithm is used for the identification of the best training inputs of the model with objective to obtain the maximum possible prediction accuracy by minimizing the forecast error. During the operation, the genetic algorithm evaluates several combination of training inputs, which are being used to train the ANFIS structure. This process consists of 10 steps, as presented in Figure 3.9, which are described below.

Step 1: GA initialization

In the fists step of the process, the initial population of the genetic algorithm is formed by generating random chromosomes of bit patterns. The populations is formed as a $N_{pop} \times N_{bits}$ matrix, where N_{pop} defines the number of individuals to be created and N_{bits} defines the

maximum number of training candidates to be considered for the modelling of the consumption.

$$population = \|P\| \quad , \qquad P \in \Re^{N_{pop} \times N_{bits}} , P \in \{0,1\} \tag{3.6}$$

Figure 3.5 describes the structure of the chromosome in connection with the training candidates of the model.

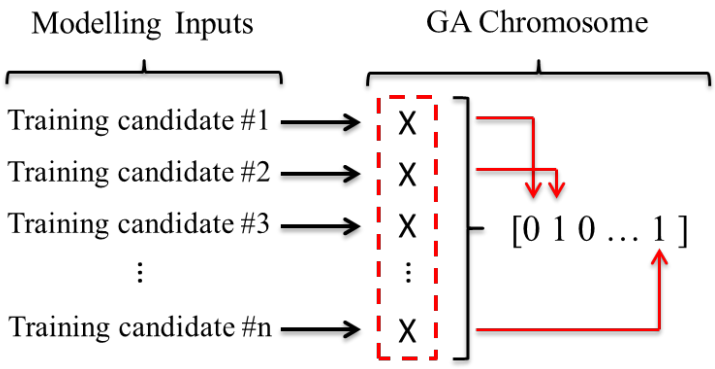

Figure 3.5: Codification of the chromosomes.

Step 2: Input filtering

During the second step of the process, the evaluated chromosome is used as a selector for the training candidates of the models, by filtering the inputs that correspond to the 0 bits, as depicted in Figure 3.5. In case of chromosomes that contain only 0 values, they are automatically rejected and replaced with new ones.

For the initial selection of the training input candidates, correlation analysis can be applied between the studied signal and the candidates. Most frequently, the input candidates can be selected based on the user's experience, the demand's energy type and the periodicity of the signal's pattern.

The following list presents the variables that have been selected as the most potential training candidates for the modelling of the energy consumptions of the industrial plant that has been used for the validation of the hypotheses of this dissertation.

- **Day of week:** Variable that takes values from 1 to 7, and correspond to the weekdays. This variable helps to identify energy patterns that can be related to specific days of the week and are repeated in weekly cycles.

- **Time of day**: Variable that indicates the daily time reference of the consumption, expressed in minutes (from 1 to 1440). It permits to identify patterns that are related to specific time periods during the day, such as daytime work periods and day shifts.
- **External temperature:** Variable that indicates the external temperature at the time of the consumption measurement. It permits to identify the effect of the temperature monomial in the energy consumption.
- **Scheduled production:** Variable that indicates the operation condition of the plant, in terms of production, at the time of the consumption measurement.
- **Historical reference of the consumption:** Variable that indicates the energy consumption of the studied load on a past moment (i.e. 1 day ago, 2 days ago, and 1 week ago). This information permits to identify patterns that are repeated in weekly cycles but are not day-dependent.

Step 3: ANFIS Configuration

During this step, the datasets for the training and the evaluation of the consumption's model are generated by splitting the input matrix (formed in the previous step) in two parts. The splitting proportions of the datasets depend on the configuration of the ANFIS and are typically the 2/3 and 1/3 for the training and evaluation sets, respectively.

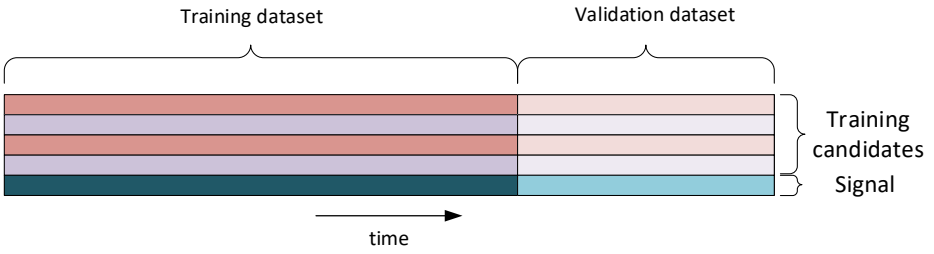

Figure 3.6: Schematic depiction of the training and validation datasets.

In case that any of the historical references of the consumption is being used as input, the corresponding samples of the signal vector, in the beginning of each dataset, are being dismissed and do not take part neither in the training nor in the validation process of the model. This occurs due to the necessity of using a part of samples of the signal as input (historical reference) and thus it cannot be used as reference. Similarly, all the input's data of the same time-series are discarded. Figure 3.7 presents an example of this case, whereas *s* is defined the consumption value of a time instant *t*, while as *m* is defined the time offset that corresponds to the maximum historical reference that has been selected as input (e.g. 1 day, 2 days or 1 week).

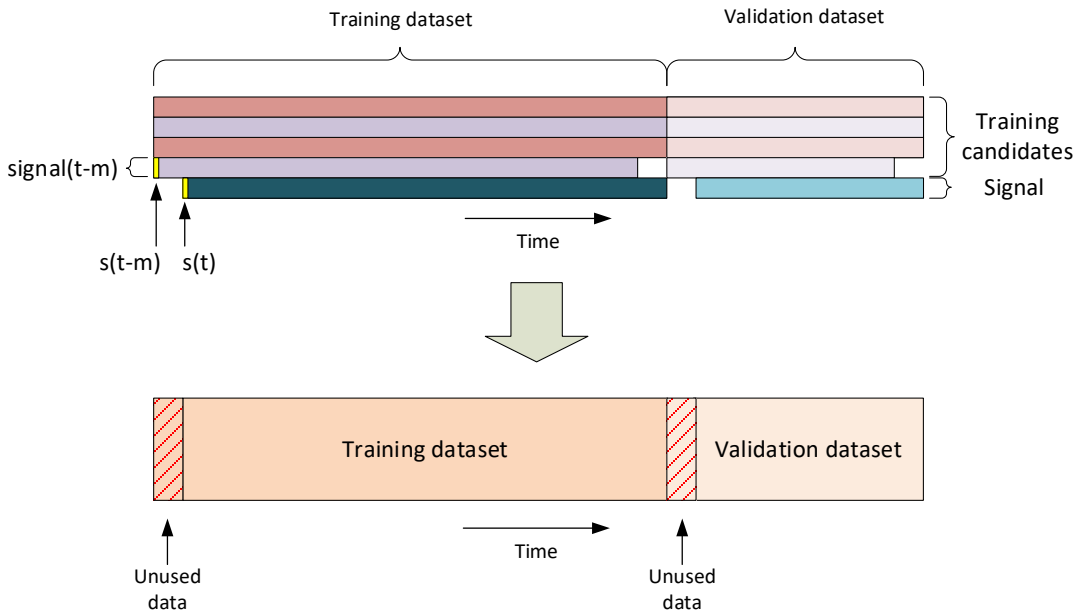

Figure 3.7: Depiction of unused data due to the use of historical signal references as inputs.

Typically, the database is split based on a chronological order (chronological splitting), using the most recent information as validation dataset. Nevertheless, this method presents mayor inefficiencies when parameters that are related to time are being used as inputs (e.g. external temperature). In such cases, the validation dataset may contain operation conditions that are not included in the training data (e.g. values of winter season in the training dataset and values of spring season in the checking dataset) and thus, they do not represent all the cases that are intended to be emulated. Thus, the behavior of the signal for some cases may be unknown for ANFIS. This has as a consequence to obtain bad performance indices for the trained model, even if the selected training inputs are the most adequate for the model. In order to handle this problem, the proposed methodology creates the training and validation datasets from different parts of range of the database as shown in Figure 3.8. The number of data splits to be made (successive splitting), varies on each model depending on the nature and range of its inputs.

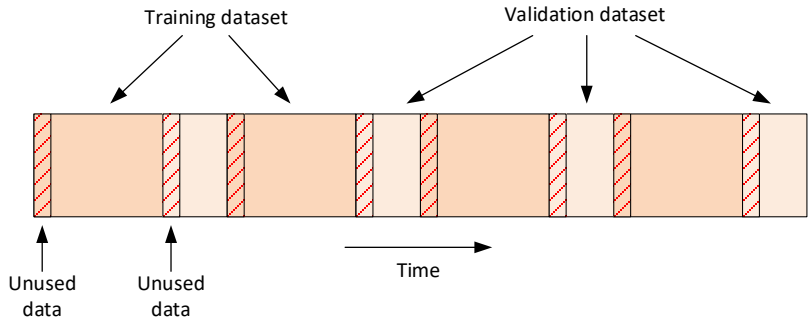

Figure 3.8: Creation of the training and validations datasets from several parts of the database.

The disadvantage of this approach is that, in case of use of any historical reference as input, the part of the database that is being dismissed as signal reference, increases with the number of data splits. Nevertheless, this disadvantage can be easily solved by incrementing the samples to be used during the modelling process. Furthermore, this approach reduces both the overfitting and under fitting errors, as it separates the data homogeneously in different periods, to assure that at least a part of all the possible trends of the signal are considered during training.

Step 4: Model Training

During this step, the training process of the ANFIS structure takes place, based on the procedure of Section 3.1.1. The algorithm applies a combination of the least-squares method and the back-propagation gradient descent method, in order to train the FIS membership function and emulate the given training data set.

Step 5: Model Training

After the finalization of the training process, the validation data are evaluated, applying an over fitting model validation. The evaluation of the forecast accuracy is made by the use of three statistical indicators that permit to calculate and interpret the prediction errors, as well as to compare the evaluated models under different training candidates. The selected performance evaluation indicators are the mean absolute percentage error, the symmetric mean absolute percentage error, as well as the root mean squared error, as defined in (3.7)-(3.9) respectively.

The mean absolute percentage error (MAPE) is one of the most widely used measure indicators for the forecast accuracy, having as main advantages the interpretability of the error and a non-scale dependency with the data. It is expressed in percentage terms, allowing to easily interpret the magnitude of the forecasting error. Nevertheless, MAPE should be only computed with positive data vectors, due to it presents infinite or undefined values when data are close to zero or have zero values [57].

$$MAPE = \frac{1}{n} \cdot \sum_{i=1}^{n} \left| \frac{y_i^{real} - y_i^{pred}}{y_i^{real}} \right| \tag{3.7}$$

The Symmetric mean absolute percentage error (SMAPE) is a variation on the MAPE that is calculated using the average of the absolute value of the actual and the absolute value of the

forecast in the denominator. In comparison to the MAPE, it provides better results with data that contains outliers. Its main disadvantages is that it applies heavier penalties on negative forecast errors than on positive ones, as well it reaches its upper (or lower) error bound when forecast is zero.

$$SMAPE = \frac{\sum_{t=1}^{n} \left| y_i^{pred} - y_i^{real} \right|}{\sum_{t=1}^{n} \left(y_i^{real} + y_i^{pred} \right)} \tag{3.8}$$

Even though, the disadvantages that present MAPE and SMAPE indicators, they have been selected for the evaluation of the prediction's performance, as the energy consumption data contains only positive values.

Finally, the root mean squared error (RMSE) has the advantage that gives disproportionate weight to very large errors.

$$RMSE = \sqrt{\frac{\sum_{i=1}^{n} \left(y_i^{pred} - y_i^{real} \right)^2}{n}} \tag{3.9}$$

whereas n is defined the number of fitted points, as y_i^{real} a vector with the real consumption values and as y_i^{pred} the forecasted consumption values.

The process between steps 2 to 5 is being repeated for the whole number of population.

Step 6: Genetic Algorithm Decision

In the sixth step, the performance values of the model of the evaluated chromosome are stored and are used for the comparison with the models of the rest of the population. In case that the optimization criteria have not been reached, the algorithm proceeds to apply the genetic operation in the population (steps 7 to 9) and the process is repeated from Step 2. In case that any of the criteria has been met, the process ends, and the chromosome that results in the best performance is returned.

Step 7 to 9: Genetic Algorithm Operations

In this step, the selection, the mutation and the crossover process are applied in order to define the new population that will be evaluated in the next iteration.

During the selection process, random chromosomes are being selected in order to be used for the mating and crossover operations, as well as to directly continue to the next population. In the mating process, a random part of 2 chromosomes are selected and be combined in order to form two new chromosomes. The same process is repeated for a pre-defined number of pairs of chromosomes. Finally, the mutation process is made of a uniform way, where the algorithm selects a fraction of the vector entries of an individual and replaces it with a random number from the entry´s range.

Step 10: Selection of the Best Training Candidates

Finally the de-codification of the chromosome vector is made, defining the optimal data input configuration for the training of the consumption model.

Figure 3.9 presents the flowchart of the proposed modelling procedure, indication the different steps that compose it.

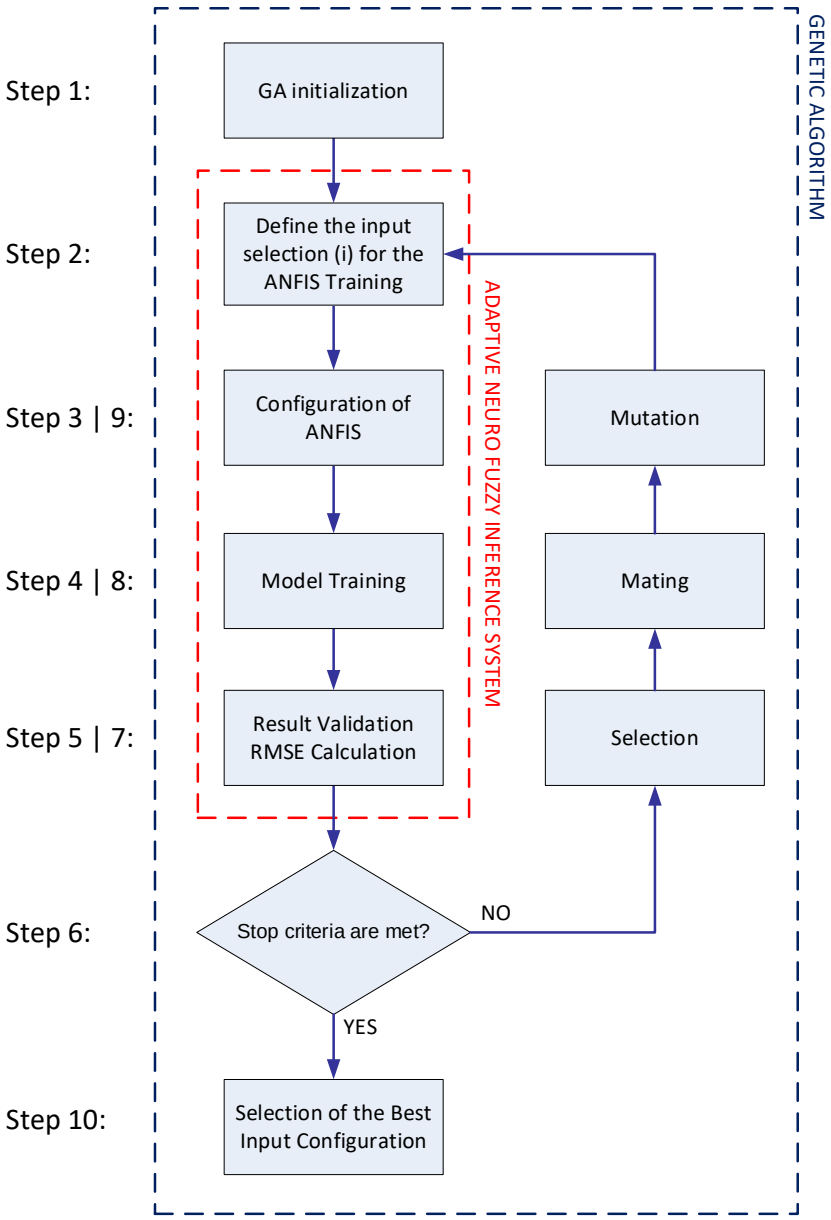

Figure 3.9: Flowchart of the modelling and tuning process.

3.2.2 Prediction Process

For the prediction of the demand, the ANFIS model is applied, taking into account the FIS structure of the trained model as well as the optimal identified chromosome during the training process.

Initially, the algorithm prepares an input matrix that contains the future values of the input candidates for the whole prediction horizon. Then, the input matrix is being filtered, remaining only the parameters that coincide with the model's chromosome. Furthermore, the FIS structure that contains the premise and consequent parameters as well as the membership functions and rules, stored into the model, are being read by the algorithm. Finally, the calculation of the energy demand takes place, by processing the input data through the layers of the ANFIS structure.

Figure 3.10 presents the block diagram of the prediction process.

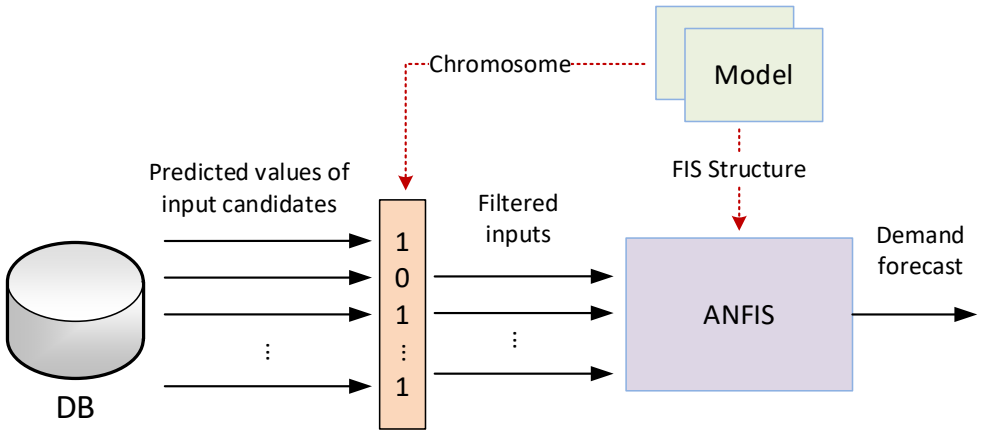

Figure 3.10: Block diagram of the prediction method.

3.3 Implementation and Results

The presented methodology has been implemented and tested under the real operation conditions of the automotive factory plant described in Section 2.4. The evaluation has been carried out for 14 cases of consumptions, which represent the most significant loads in terms of manufacturing processes, power and load profiles. The selected cases include the global energy consumption loads of the plant (i.e. electric and heating), as well as 2 electric and 2 heating consumptions of each one of the manufacturing processes (i.e. body shop, painting and assembling).

For the training process, as described in subsection 3.2.1, seven variables have been selected as the most potential candidates, which are: Day of week, time of day, external temperature, scheduled production, historic consumption of 7 days, historic consumption of 2 days and historic consumption of 1 day.

The following figure presents the structure of the chromosome, describing the parameter that corresponds to each gene.

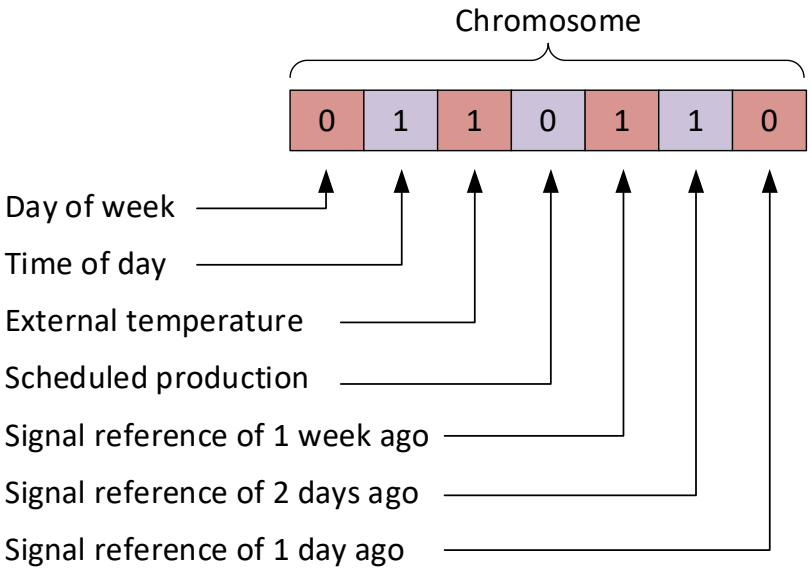

Figure 3.11: Description of the chromosome´s genes.

Based on the number of the training candidates, it results that the Genetic Algorithm can form chromosomes with seven bits, which produce 127 possible binary combinations (2^7-1) lying between value *0000001* and *1111111*.

The following part presents the detailed validation process and the obtained results of the proposed methodology applied on the total electric demand of the automotive manufacturing

process. All the consumption quantities are expressed as per-units to preserve confidentiality and to generalize the results.

For the evaluation of the methodology applied on this case, a historical database with a total of 9 months has been used. It consists of samples of 15 minute intervals, containing energy consumption data, as well as operation variables that can affect, with a direct or indirect way, the energy profile.

Figure 3.12 presents the energy consumption profile for the complete period of 9 months that contains 25920 data samples.

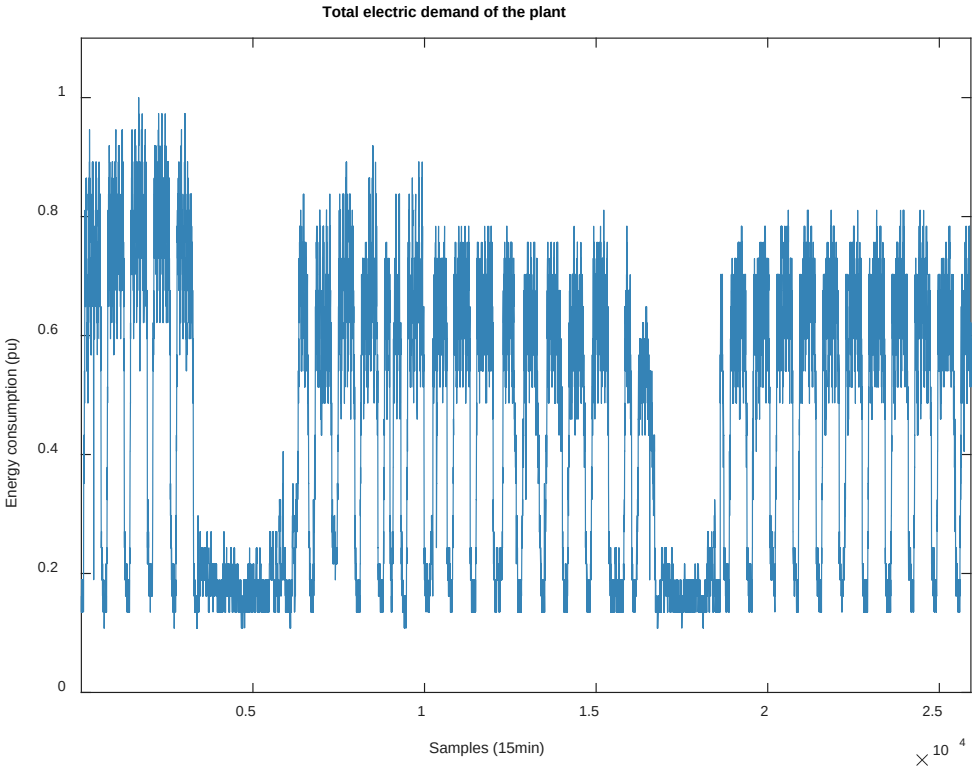

Figure 3.12: Consumption profile of the total electric demand of the plant for a period of 9 months.

During the evaluation of the algorithm, the training process has been executed in a total of nine times (one execution per month), completing each time its existing database with the dataset from the following month. The genetic algorithm was configured empirically after a series of evaluations with a population of 20 individuals per generation.

Figure 3.13 presents the part of training and evaluation dataset that were used in each case, depicted in red and green colors respectively. As it can be observed in the figure, a successive data splitting has been applied to use the 2/3 of every 2880 samples (1 month) for the training set, while the remaining 1/3 is used for the model's validation.

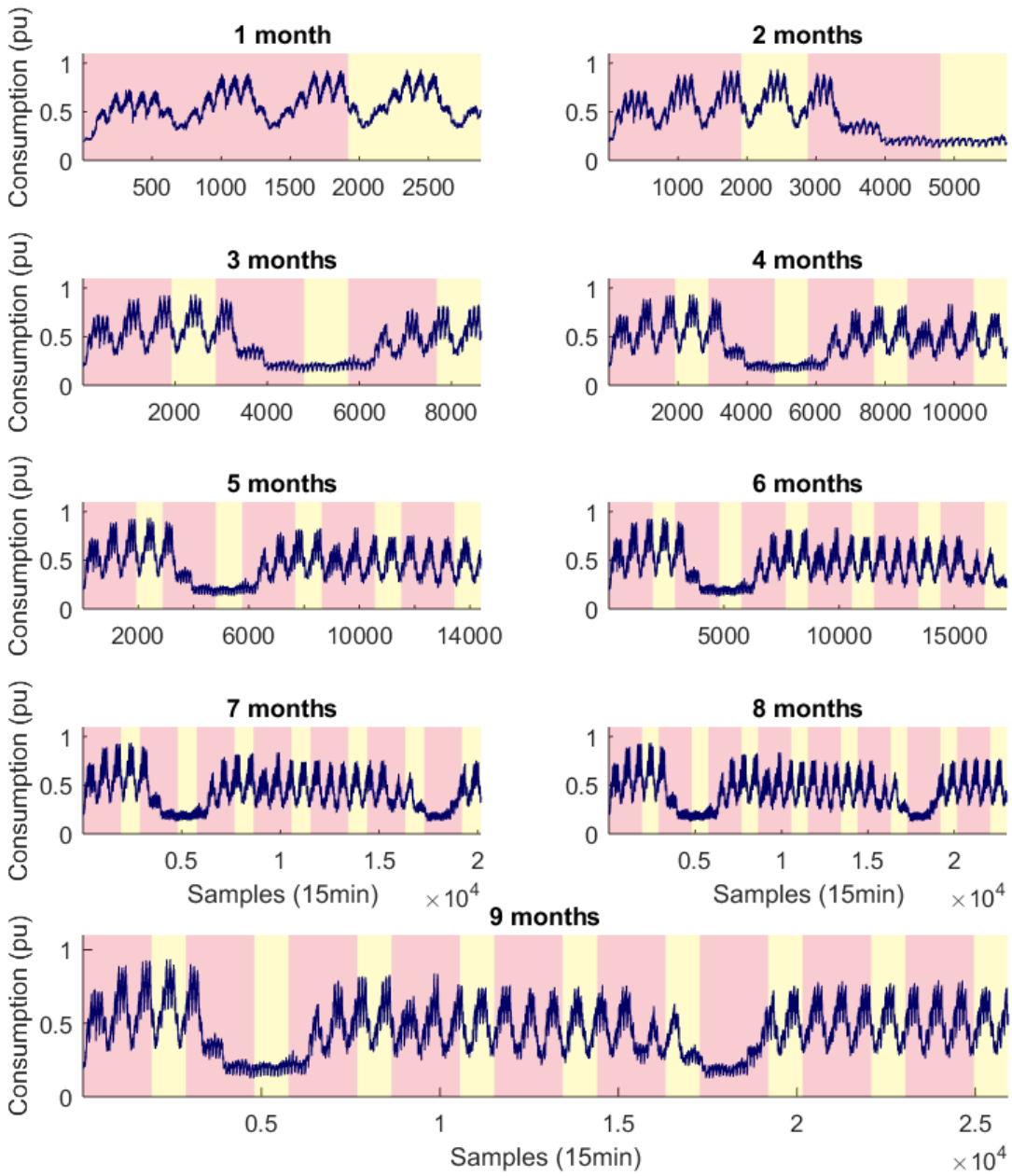

Figure 3.13: Consumption profile for the different execution periods. Red: training dataset; Yellow: validation dataset.

Figure 3.14 depicts the optimal chromosomes that were selected by the GA in each period by using the successive data splitting approach, while Figure 3.15, Figure 3.16 and Figure 3.17 present the performance indices of the model in terms of MAPE, SMAPE and RMSE, respectively, for both approaches (i.e. successive splitting and chronological splitting).

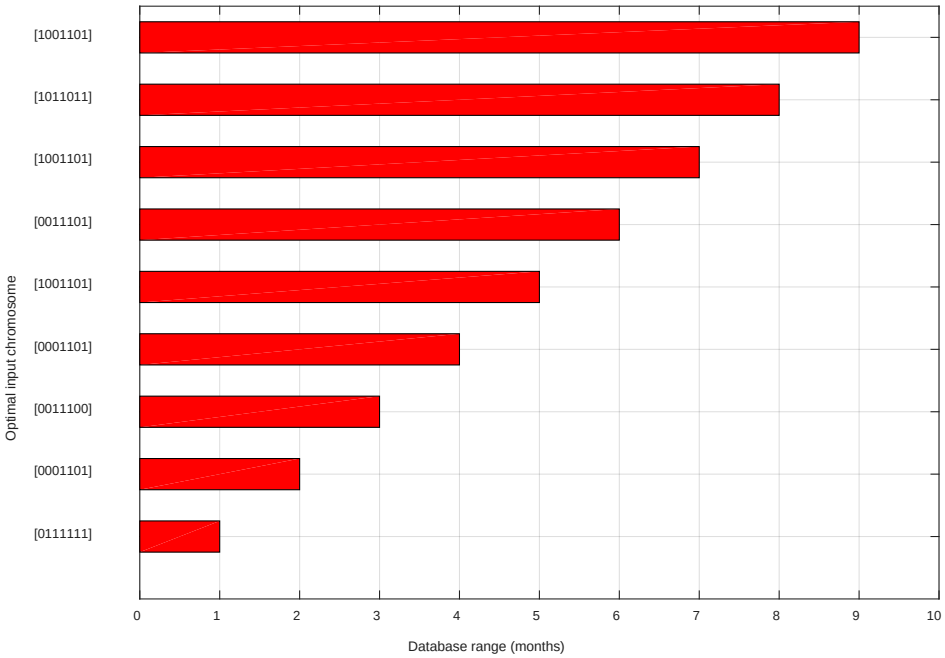

Figure 3.14: Optimal chromosome for each training period.

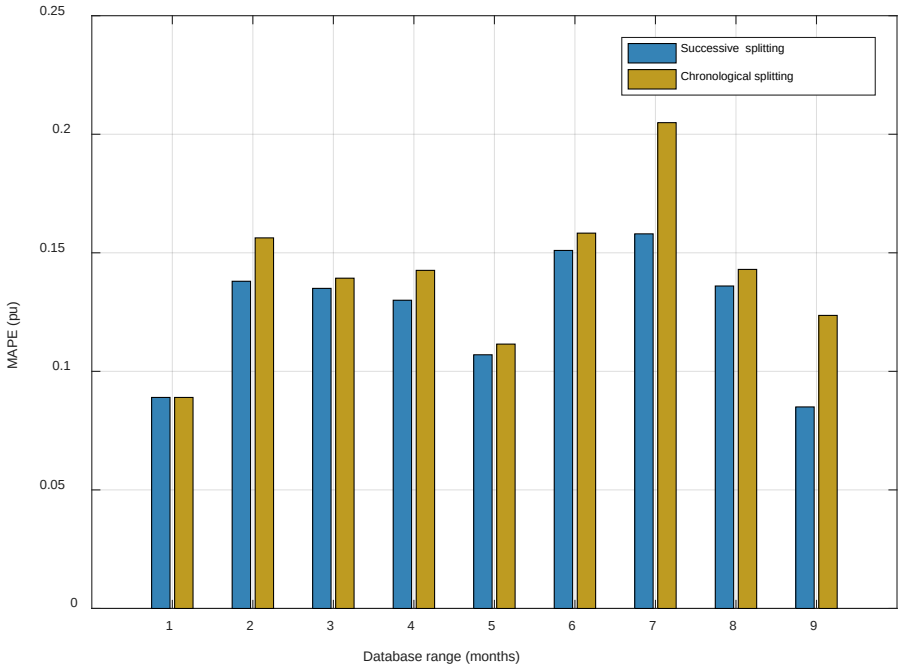

Figure 3.15: MAPE indices for each training period using the two data splitting approaches.

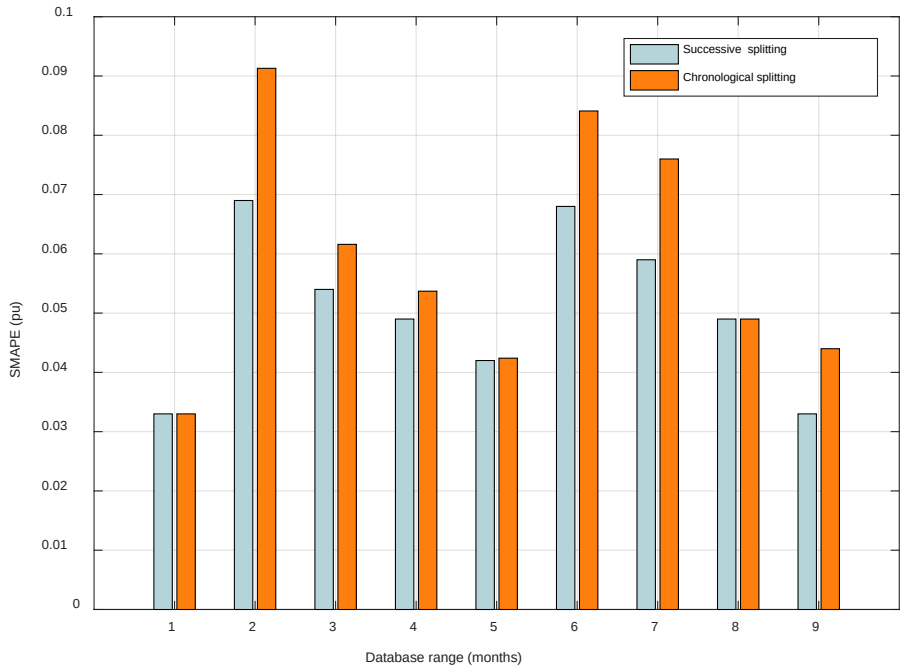

Figure 3.16: SMAPE indices for each training period using the two data splitting approaches.

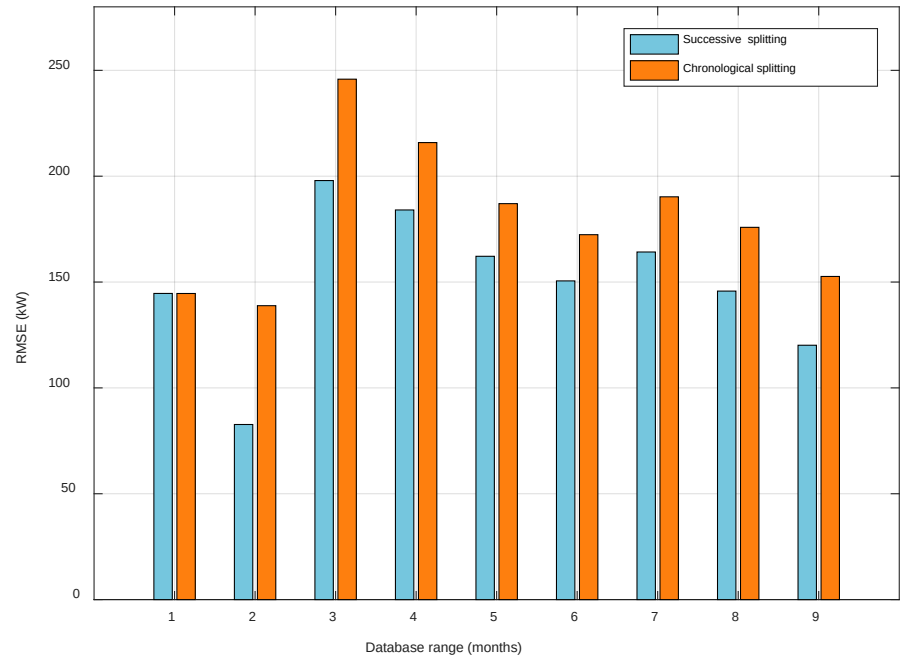

Figure 3.17: RMSE indices for each training period using the two data splitting approaches.

As it can be observed by comparing the results of the two modelling approaches, for all the testing periods, the performance indices are better when the successive splitting approach is applied on the data. This occurs due to the premise and consequent parameters are trained with samples from all the time range of the database, rather than from one part that could

contain partial information of the consumption´s operation. The following table presents the numerical values of the performance indices, as well as the percentage of their improvement by using the successive data splitting approach.

Table V. Energy performance indices for the two data splitting approaches.

TRAINING PERIOD	SUCCESSIVE APPROACH			CHRONOLOGICAL APPROACH			IMPROVEMENT		
	MAPE	SMAPE	RMSE	MAPE	SMAPE	RMSE	MAPE	SMAPE	RMSE
1 month	*0,089*	*0,033*	*144,6*	*0,089*	*0,033*	*144,6*	*0%*	*0%*	*0%*
2 months	*0,138*	*0,069*	*82,71*	*0,156*	*0,091*	*138,8*	*11,7%*	*24,4%*	***40,4%***
3 months	*0,135*	*0,054*	*197,9*	*0,139*	*0,061*	*245,8*	*3,08%*	*12,3%*	*19,4%*
4 months	*0,130*	*0,049*	*184,0*	*0,142*	*0,053*	*215,8*	*8,83%*	*8,75%*	*14,7%*
5 months	*0,107*	*0,042*	*162,1*	*0,111*	*0,042*	*187,0*	*4,03%*	*0,94%*	*13,2%*
6 months	*0,151*	*0,068*	*150,5*	*0,158*	*0,084*	*172,8*	*4,61%*	*19,1%*	*12,6%*
7 months	*0,158*	*0,059*	*164,1*	*0,204*	*0,076*	*190,2*	*22,8%*	*22,3%*	*13,7%*
8 months	*0,136*	*0,049*	*145,7*	*0,143*	*0,049*	*175,8*	*4,89%*	*0%*	*17,1%*
9 months	*0,085*	*0,033*	*120,1*	*0,123*	*0,044*	*152,6*	***31,2%***	***25,0%***	*21,2%*

On the other hand, in order to evaluate the efficiency of the results of the presented algorithm, each selected chromosome was used to train all the different sets of data (dataset from one month till nine months, split with the successive approach) in order to calculate the performance indicators that result in each case. Table VI presents the results of this evaluation. The solution that presents the best indices for each training period has been marked in bold, indicating the optimal input configuration (chromosome) of each case.

Table VI. Energy performance indices for the different training periods.

TRAINING PERIOD	0111111			0001101			0011100		
	MAPE	SMAPE	RMSE	MAPE	SMAPE	RMSE	MAPE	SMAPE	RMSE
1 month	***0,089***	***0,033***	***144,6***	*0,090*	*0,033*	*147,9*	*0,102*	*0,037*	*284,6*
2 months	*0,182*	*0,092*	*107,8*	***0,138***	***0,069***	***82,71***	*0,159*	*0,079*	*93,63*
3 months	*0,169*	*0,073*	*733,6*	*0,149*	*0,062*	*235,0*	***0,135***	***0,054***	***197,9***
4 months	*0,598*	*0,230*	*1037*	***0,130***	***0,049***	***184,0***	*0,160*	*0,065*	*227,2*
5 months	*0,165*	*0,072*	*240,6*	*0,131*	*0,050*	*192,1*	*0,134*	*0,052*	*188,4*
6 months	*0,287*	*0,086*	*310,7*	*0,207*	*0,069*	*221,5*	*0,178*	*0,076*	*236,3*
7 months	*0,219*	*0,078*	*217,7*	*0,204*	*0,070*	*195,1*	*0,193*	*0,076*	*1381*
8 months	*0,189*	*0,064*	*201,7*	*0,141*	*0,050*	*166,5*	*0,149*	*0,054*	*183,7*
9 months	*0,107*	*0,045*	*150,1*	*0,093*	*0,038*	*138,3*	*0,108*	*0,046*	*173,5*
TRAINING PERIOD	1001101			0011101			1011011		
	MAPE	SMAPE	RMSE	MAPE	SMAPE	RMSE	MAPE	SMAPE	RMSE
1 month	*0,095*	*0,036*	*238,7*	*0,092*	*0,034*	*152,5*	*0,094*	*0,035*	*396,2*
2 months	*0,139*	*0,073*	*86,82*	*0,139*	*0,069*	*152,5*	*0,171*	*0,079*	*113,9*
3 months	*0,149*	*0,064*	*270,2*	*0,168*	*0,063*	*238,3*	*0,182*	*0,080*	*312,0*
4 months	*0,424*	*0,136*	*1904*	*0,261*	*0,091*	*235,6*	*0,170*	*0,062*	*411,4*
5 months	***0,107***	***0,042***	***162,1***	*0,150*	*0,062*	*233,7*	*0,181*	*0,085*	*234,7*
6 months	*0,154*	*0,076*	*183,7*	***0,151***	***0,068***	***150,5***	*0,296*	*0,090*	*288,3*
7 months	***0,158***	***0,059***	***164,1***	*0,219*	*0,079*	*235,4*	*0,234*	*0,081*	*209,5*
8 months	*0,146*	*0,058*	*151,0*	*0,152*	*0,056*	*191,7*	***0,136***	***0,049***	***145,7***
9 months	***0,085***	***0,033***	***120,1***	*0,094*	*0,040*	*146,7*	*0,095*	*0,039*	*150,2*

From the obtained results, it can be observed that in all the cases the chromosome of the training data is changing during the time. This happens because the consumption´s behavior depends on different variables that vary during the time. Analyzing the genes of the chromosomes that are selected in each case, it results that the most important training inputs for the selected consumption is the scheduled production, the historical consumption of a day and the historical consumption of a week. The following table highlights the selection of the input candidates during the nine months of operation, as well as the total number of their use.

Table VII. Results of the optimal training candidates for the different periods.

Training Period	Genes of the Chromosome						
	1	2	3	4	5	6	7
1 month	*0*	*1*	*1*	*1*	*1*	*1*	*1*
2 months	*0*	*0*	*0*	*1*	*1*	*0*	*1*
3 months	*0*	*0*	*1*	*1*	*1*	*0*	*0*
4 months	*0*	*0*	*0*	*1*	*1*	*0*	*1*
5 months	*1*	*0*	*0*	*1*	*1*	*0*	*1*
6 months	*0*	*0*	*1*	*1*	*1*	*0*	*1*
7 months	*1*	*0*	*0*	*1*	*1*	*0*	*1*
8 months	*1*	*0*	*1*	*1*	*0*	*1*	*1*
9 months	*1*	*0*	*0*	*1*	*1*	*0*	*1*
Times of selection	*4*	*1*	*4*	*9*	*8*	*2*	*8*

Figure 3.18 to Figure 3.26 depict the comparison between the real consumption and the predicted one for the validation datasets of the 9 cases, applying the optimal input configurations.

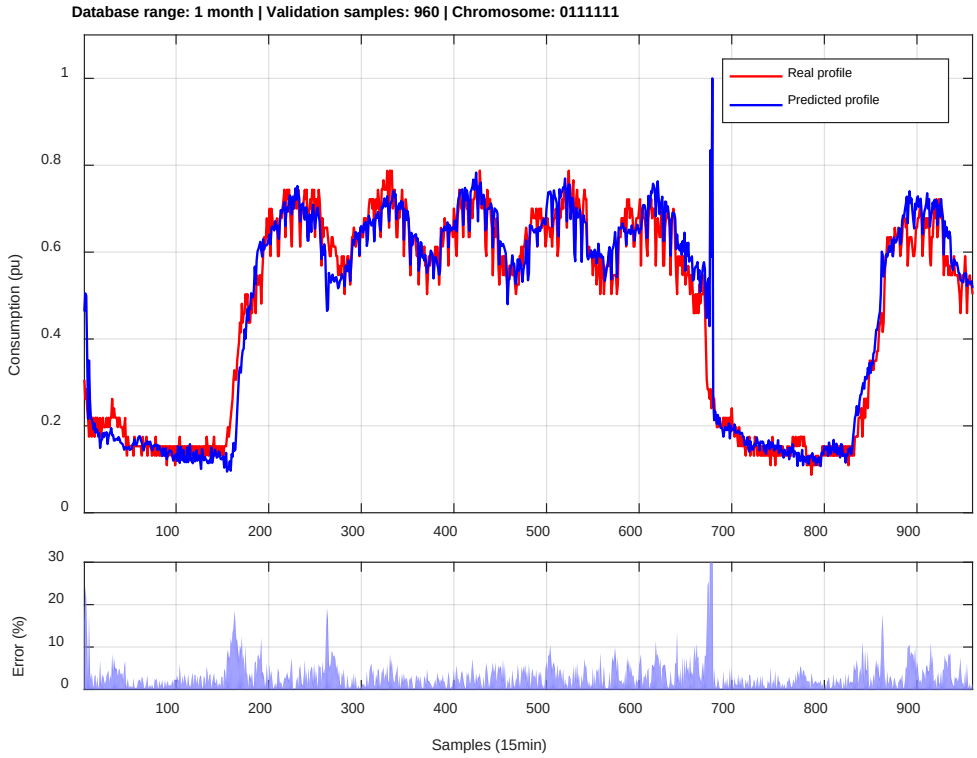

Figure 3.18: Comparison between real and predicted consumption for a database range of 1 month.

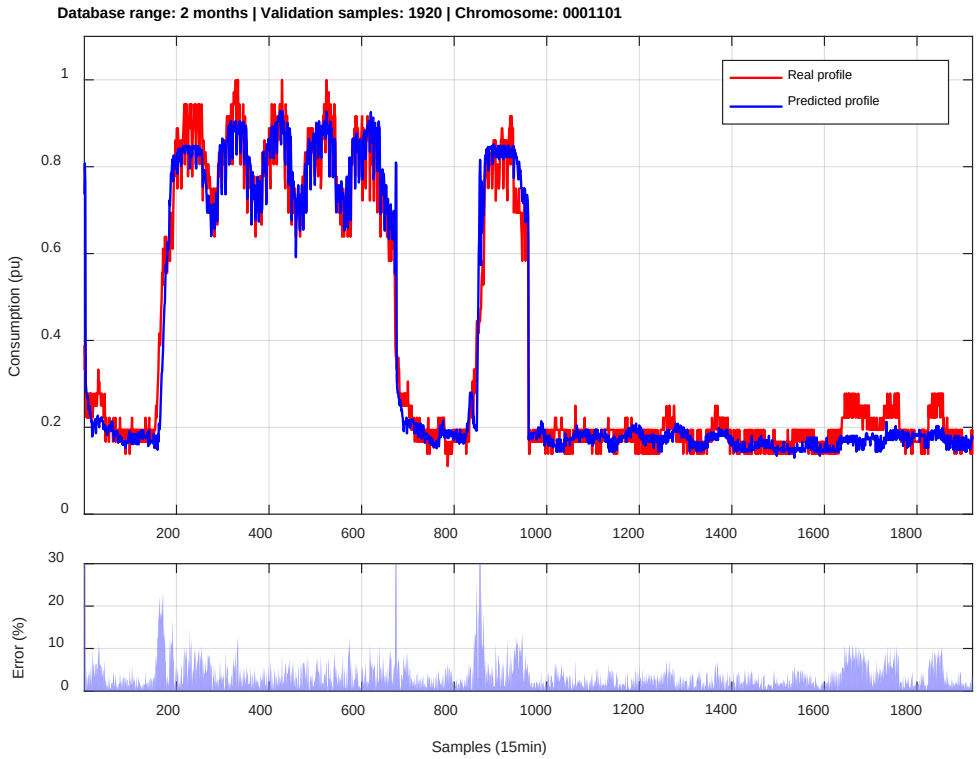

Figure 3.19: Comparison between real and predicted consumption for a range of 2 months.

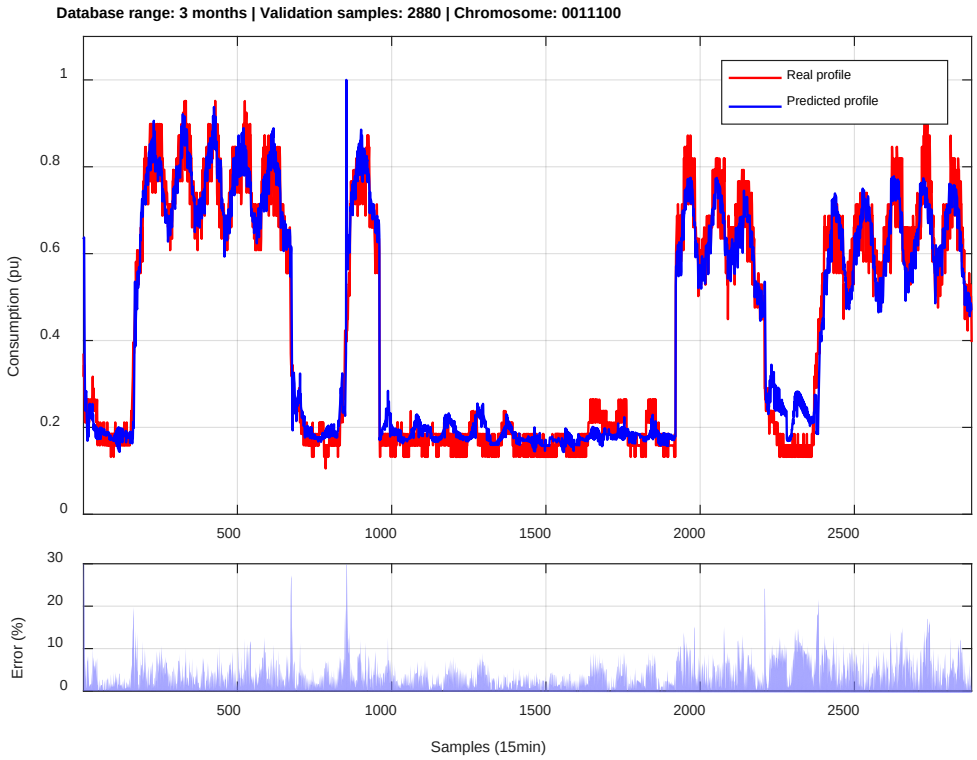

Figure 3.20: Comparison between real and predicted consumption for a range of 3 months.

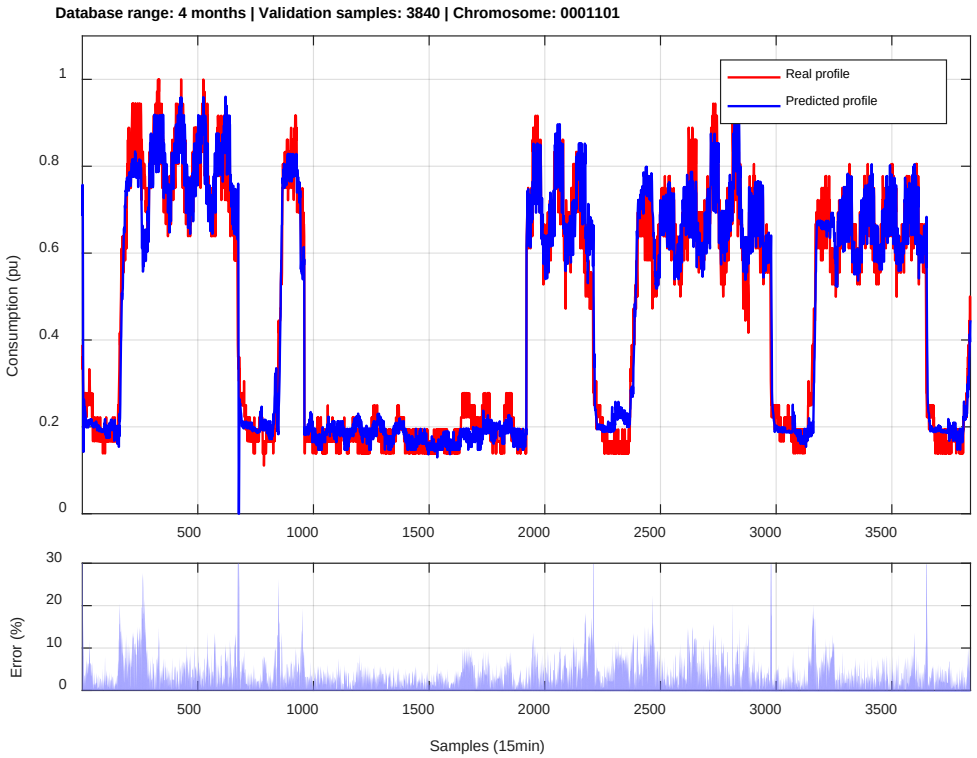

Figure 3.21: Comparison between real and predicted consumption for a range of 4 months.

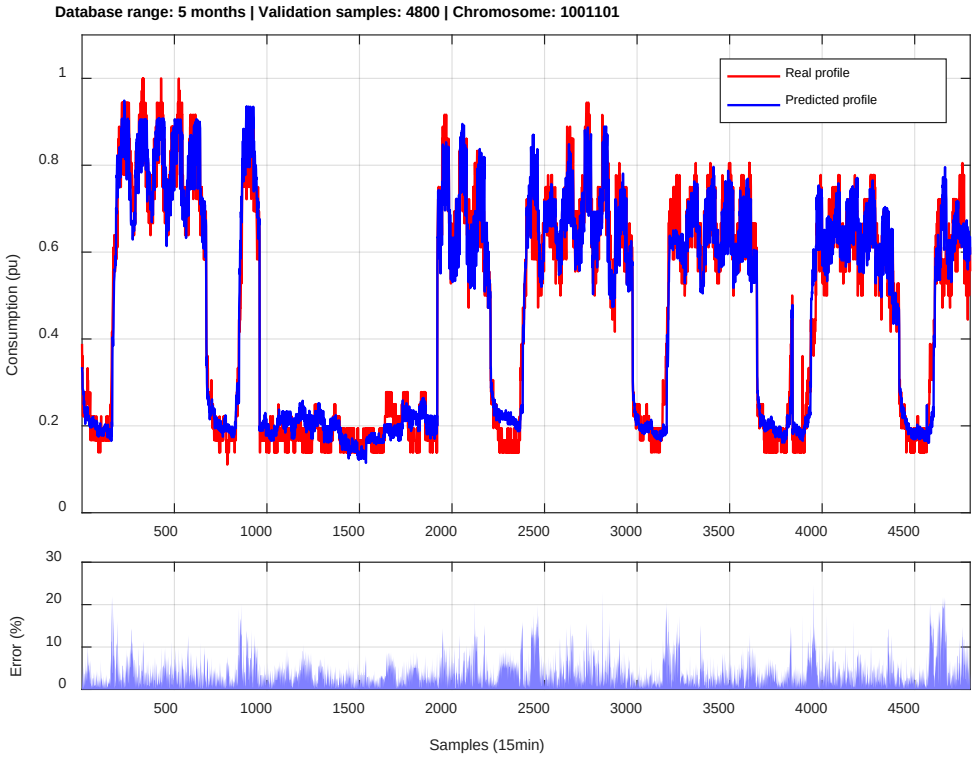

Figure 3.22: Comparison between real and predicted consumption for a range of 5 months.

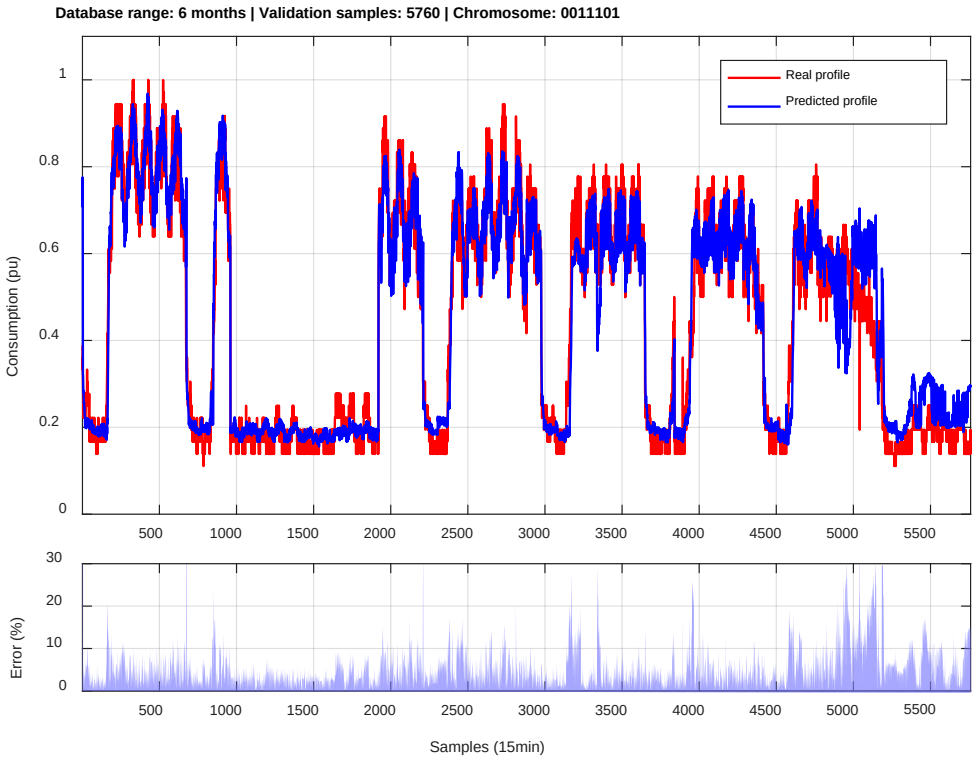

Figure 3.23: Comparison between real and predicted consumption for a range of 6 months.

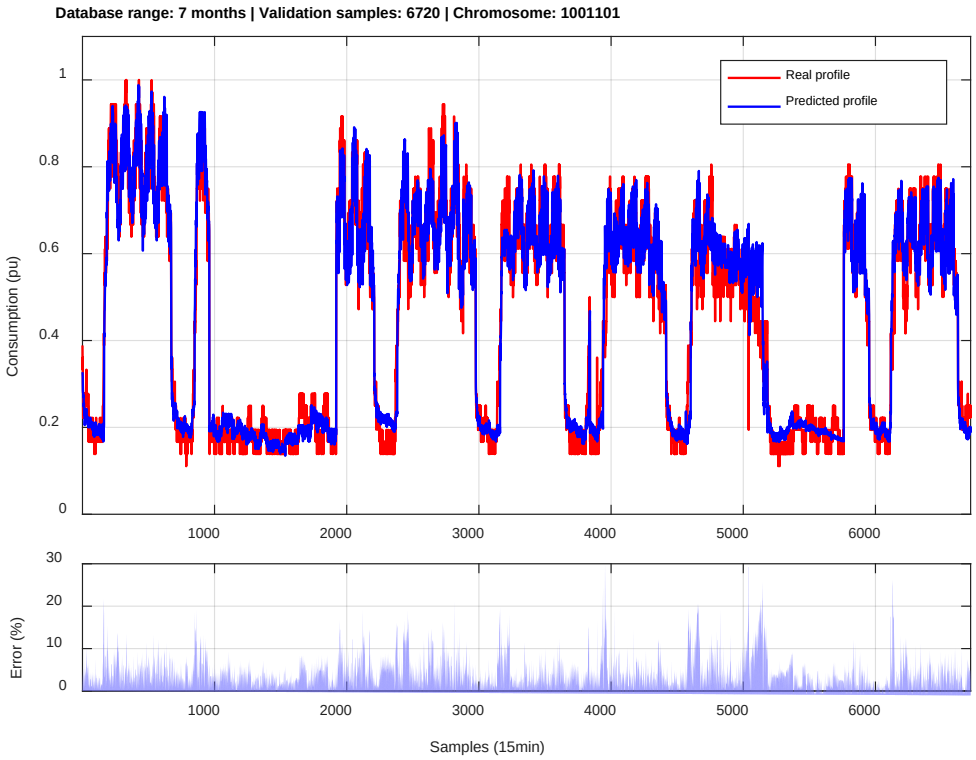

Figure 3.24: Comparison between real and predicted consumption for a range of 7 months.

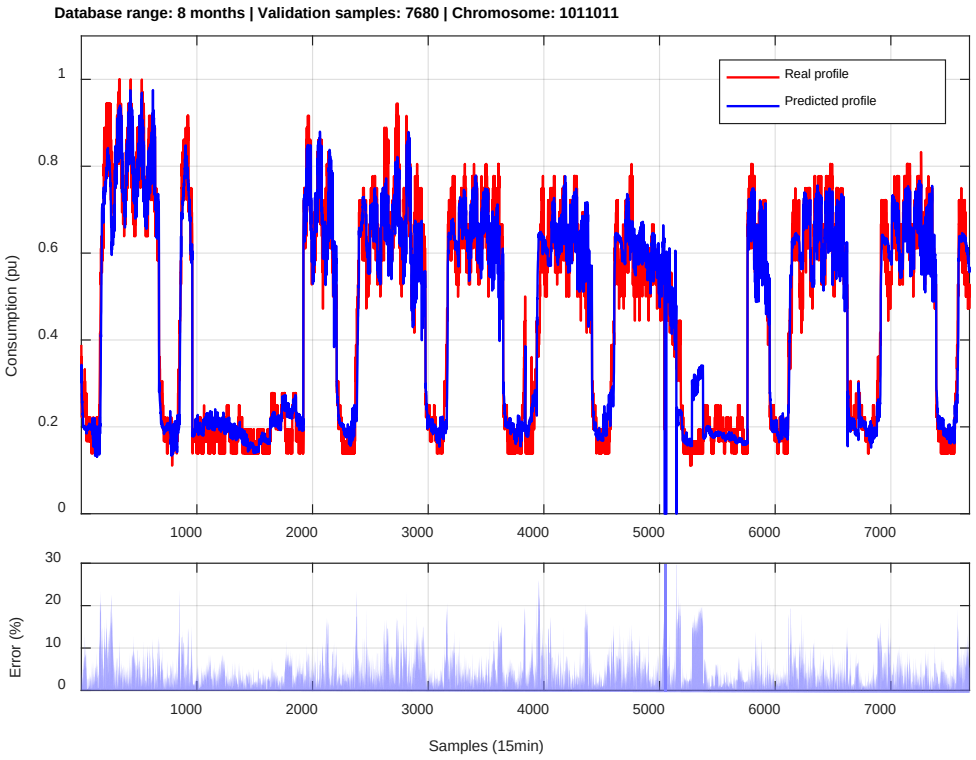

Figure 3.25: Comparison between real and predicted consumption for a range of 8 months.

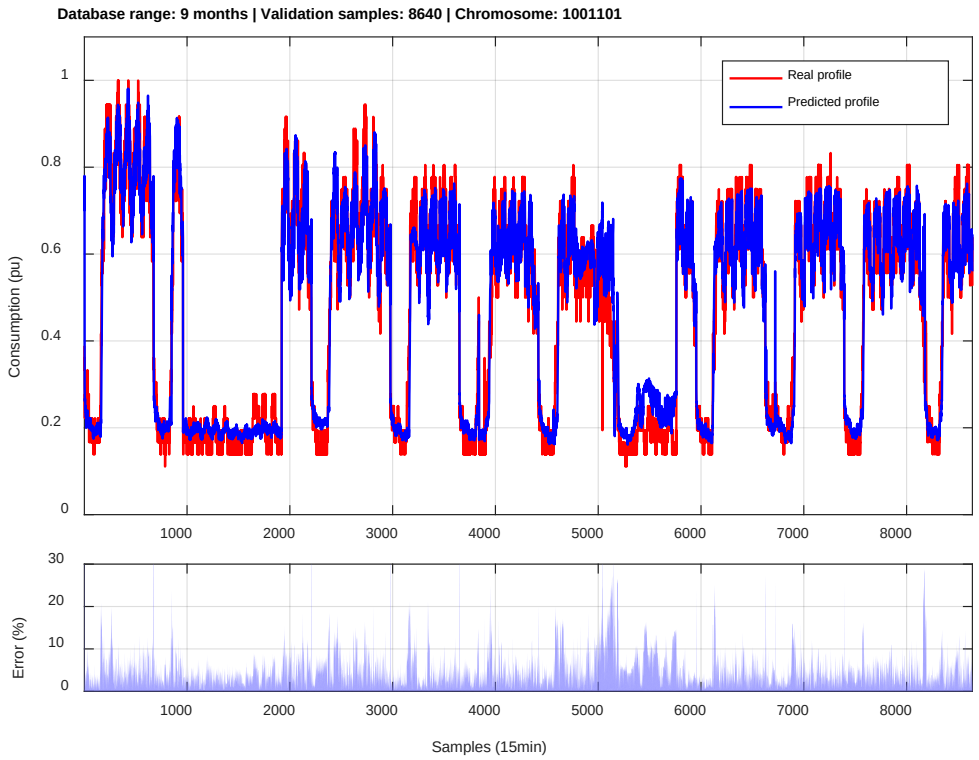

Figure 3.26: Comparison between real and predicted consumption for a range of 9 months.

Finally, Table VIII presents an overview of the performance evaluation indices that resulted from the testing of the modelling and prediction methodology on the 14 different consumptions.

Table VIII. Performance evaluation indices of the demand forecasting for the validation cases.

TITLE	MANUFACTURING PROCESS	MAPE(PU)	SMAPE(PU)	RMSE (%)
Total electric demand of the plant	*Global*	*0,085*	*0,033*	*6,22%*
Total heating demand of the plant	*Global*	*12,00*	*5,37*	*7,49%*
Total electric demand of workshop 1	*Body Shop*	*16,89*	*6,89*	*6,33%*
Total heating demand of workshop 1	*Body Shop*	*36,81*	*11,40*	*11,48%*
Total electric demand of workshop 1A	*Body Shop*	*21,31*	*6,94*	*11,39%*
Total heating demand of workshop 1A	*Body Shop*	*32,99*	*16,35*	*10,80%*
Total electric demand of workshop 2	*Painting*	*5,14*	*2,13*	*4,77%*
Total heating demand of workshop 2	*Painting*	*30,82*	*14,22*	*9,52%*
Total electric demand of workshop 4	*Painting*	*6,34*	*2,46*	*5,56%*
Total heating demand of workshop 4	*Painting*	*30,17*	*15,26*	*11,52%*
Total electric demand of workshop 9	*Assembling*	*7,11*	*2,45*	*5,76%*
Total heating demand of workshop 9	*Assembling*	*21,97*	*10,03*	*7,27%*
Total electric demand of workshop 10	*Assembling*	*4,45*	*1,88*	*3,64%*
Total heating demand of workshop 10	*Assembling*	*25,55*	*11,23*	*11,08%*

Appendix A1 contains validation cases of energy prediction, applied on 8 of the above consumptions (1 per manufacturing process and energy type), for prediction horizons of 24 hours.

As it can be observed in the figures, there are cases in which the trained mathematical model fails to predict accurately the energy consumption even if the selection of the energy inputs has been optimized by the genetic algorithm.

This is presented mainly on consumptions that are strongly influences by parameters that tend to vary on time (e.g. external temperature, scheduled production, etc.), having as a consequence, the premise and consequent parameters of the FIS model to be trained for multiple operation conditions at ones (e.g. workdays and holidays, seasons of year, production variations, etc.), resulting to large offsets between the signal points and the trained parameters (e.g. during the least squares fitting).

In order to handle this problem and increase the prediction accuracy, a multi-model training approach is proposed and described in the following section.

3.4 Smart Multi-Model Training Approach

Despite the possible performance improvements that can be obtained during the training of a model by using the successive database splitting, it has been concluded that in many cases the resulted prediction accuracy is not satisfactory, mainly in short-term demand forecasts where the prediction requirements are high.

In order to handle this problem, a multi-model training approach is proposed, in which multiple models are developed for a single signal, based on a hierarchical clustering of similar load behaviors [58]. This approach is able to identify the necessary number of models to be trained, based on the operation conditions and the profile of the consumption.

The clustering analysis takes place in step 3 of the modelling process (depicted in Figure 3.9), where the training and validation datasets are being created. In this step, the signal profile is being compared in terms of similarity, and is classified into clusters based on a predefined minimum distance. Once the distance indicator of each sample is calculated, pairs of data are merged iteratively until only one cluster remains, using the linkage algorithm. The sequence of states defined by the iterative algorithm represents a binary, hierarchical cluster tree. The branches of the tree that violate the working constraints are removed so that only maximum N clusters of minimum distance D remain.

Finally, the subsets of data that are identified by the clusters are assembled and converted back into time-series, creating the individual databases that include different operation patterns of the signal. Then each database is treated individually, defining the training and validation dataset for the model and proceeding to step 4 of the modelling process.

The following part present the proposed multi-model approach applied to the energy consumption of Figure 3.12. The configuration of the algorithm has been set for a maximum number of 10 clusters (N = 10) and a minimum distance of thirty percent (D = 0.3).

The classification obtained by the clustering process is depicted in Figure 3.27 and Figure 3.28 where they present dendrograms with the maximum number of the identified clusters and the final selection of clusters based on the defined maximum distance limit, respectively.

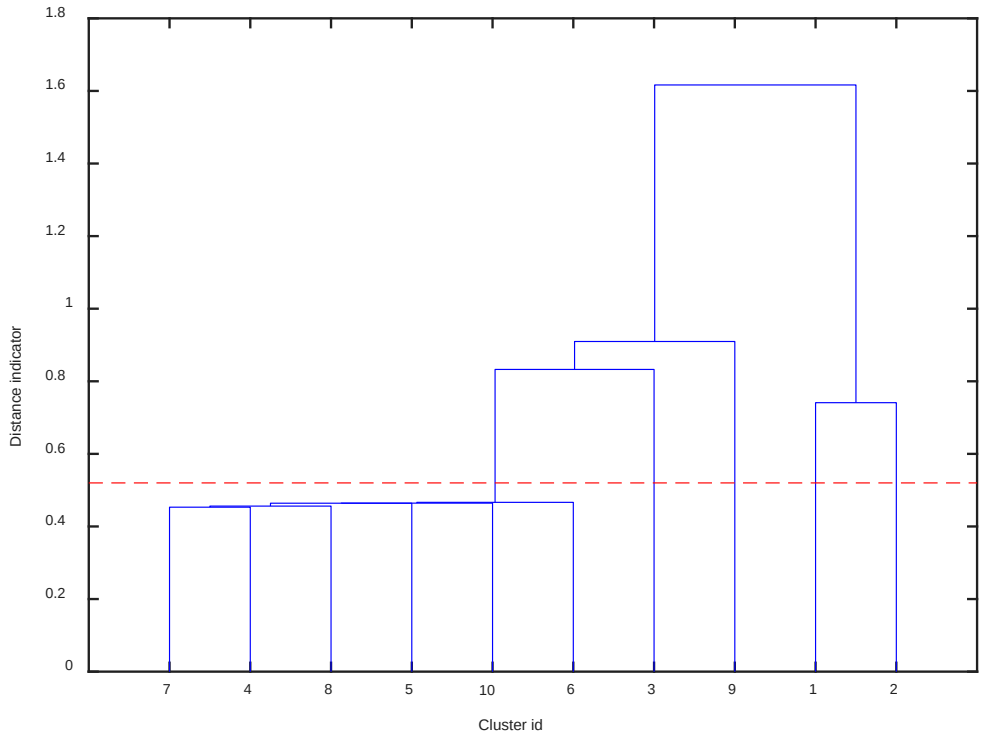

Figure 3.27: Dendogram that presents the maximum number of the identified clusters.

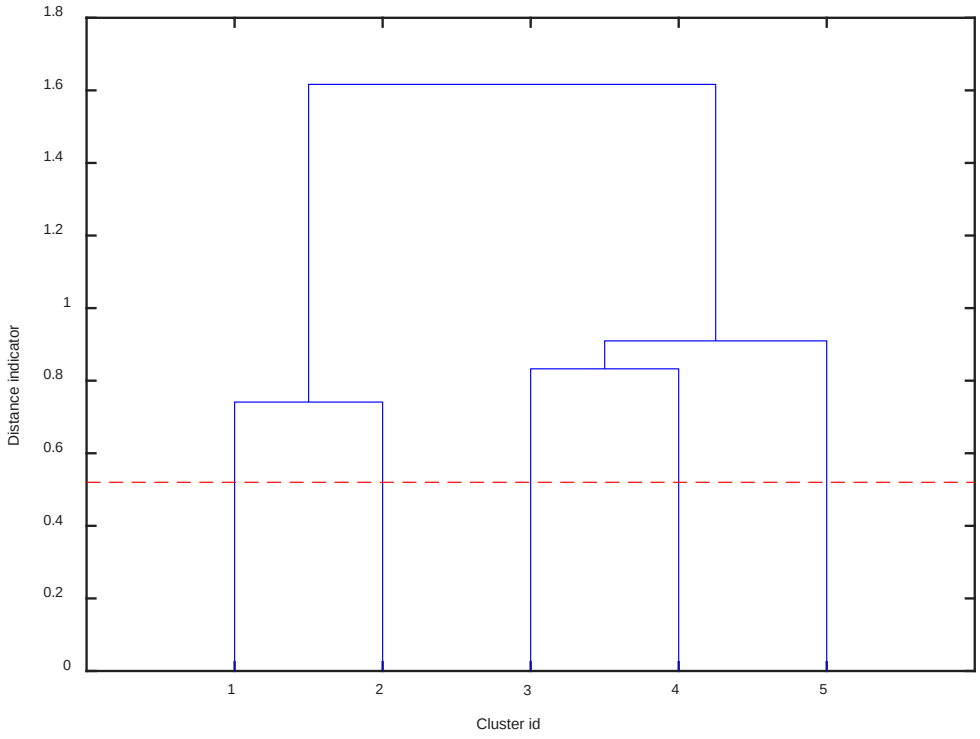

Figure 3.28: Dendogram that presents the resulted clusters of the database.

Once the clusters are identified, the database is filtered using the cluster id, as depicted in Figure 3.29. Then the training process continues with the generation of the different models for each database, following the steps that are described in section 3.2.

As it can be observed in the following figure, 5 different clusters (consumption profiles with similar patterns) have been identified and presented in different colors.

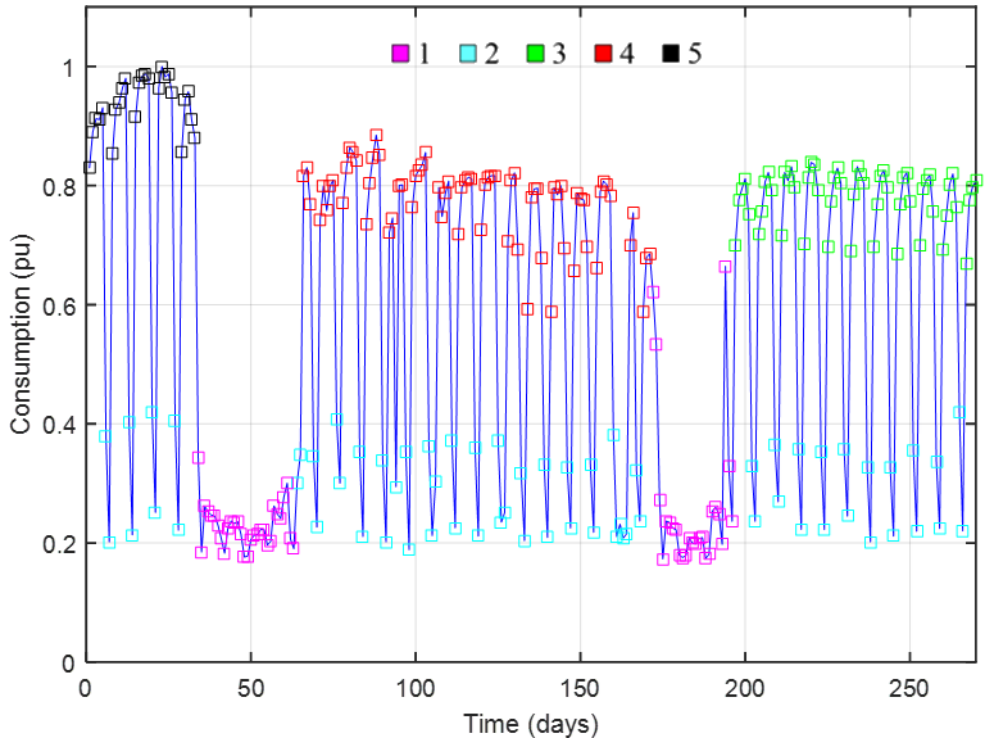

Figure 3.29: Energy consumption profile classified by cluster id.

Table IX presents a comparison of the forecasting and maximum obtained errors between the single model approach, using successive data splitting and the multi-model training approach, using hierarchical clustering.

Table IX. Comparison of forecasting performance indices between the single model and multi-model approach.

Cluster ID	RMSE (%)		Max Error (%)	
	Single Model	Multi-model	Single Model	Multi-Model
1		*7,87*		*46,10*
2		*4,03*		*21,85*
3	*6,22*	*3,80*	*34,84*	*14,52*
4		*4,16*		*27,93*
5		*4,75*		*29,43*
Avg	*6,22*	*4,92*	*34,84*	*27,97*

It can be observed that an important accuracy improvement is achieved in most of the subsets, specifically an average (Avg.) 21% of RMSE reduction and a 20% of maximum error reduction. On the other hand, it can be observed that there are cases where the calculated error is worse than the single models' (i.e. id 1). Such cases typically correspond to operation periods with complex patterns, that are mainly influenced by the human behavior and are difficult to predict based on data models (e.g. holidays, maintenance periods, etc.).

The following table shows the optimal training chromosomes that were identified by the genetic algorithm during the training process of each cluster.

Table X. Results of the optimal training candidates for the different clusters.

CLUSTER ID	GENES OF THE CHROMOSOME						
	1	2	3	4	5	6	7
1	*1*	*0*	*1*	*0*	*0*	*0*	*1*
2	*0*	*1*	*0*	*1*	*1*	*0*	*1*
3	*1*	*1*	*0*	*1*	*1*	*0*	*1*
4	*0*	*1*	*1*	*1*	*1*	*0*	*1*
5	*0*	*1*	*1*	*1*	*0*	*0*	*1*
Total	*2*	*4*	*3*	*4*	*3*	*0*	*5*

As it can be observed, a different training input combination has been resulted as the optimal one for all of the clusters, and thus, it can be concluded that the use of a GA-ANFIS training methodology gives rise to potential increase of the forecasting accuracy.

The following figures depict the comparison between the real consumption and the predicted one for a period of 2 days, obtained for the models of cluster 3, 4 and 1, which correspond to the cases with the **best, medium and worst forecasting performance**, respectively.

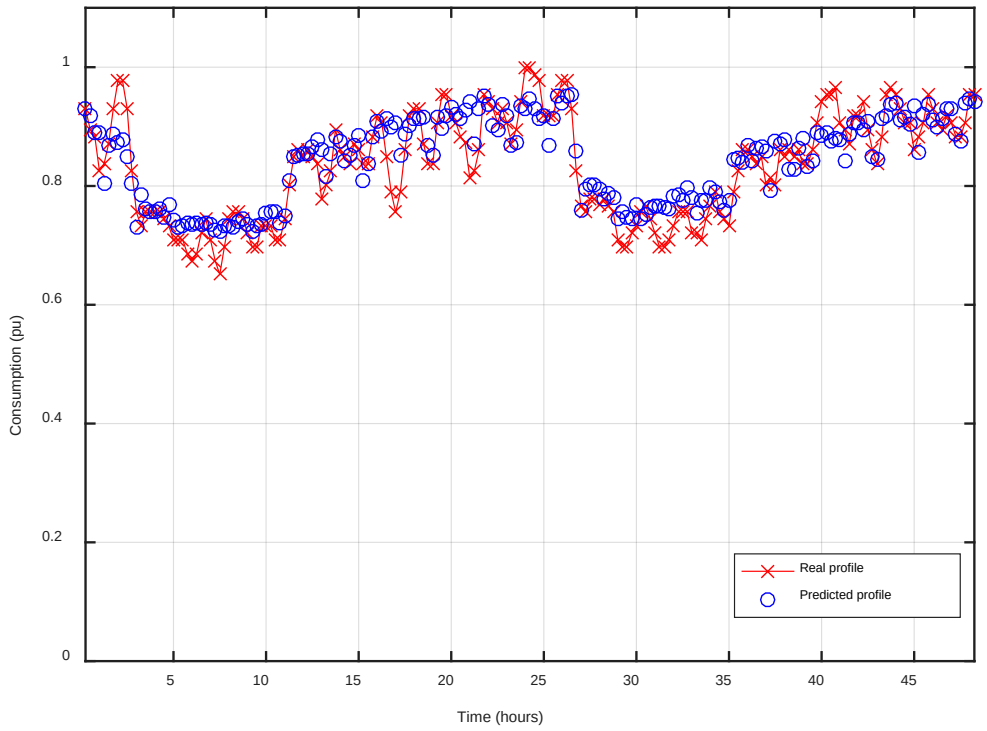

Figure 3.30: Comparison between real profile and prediction for cluster id: 3.

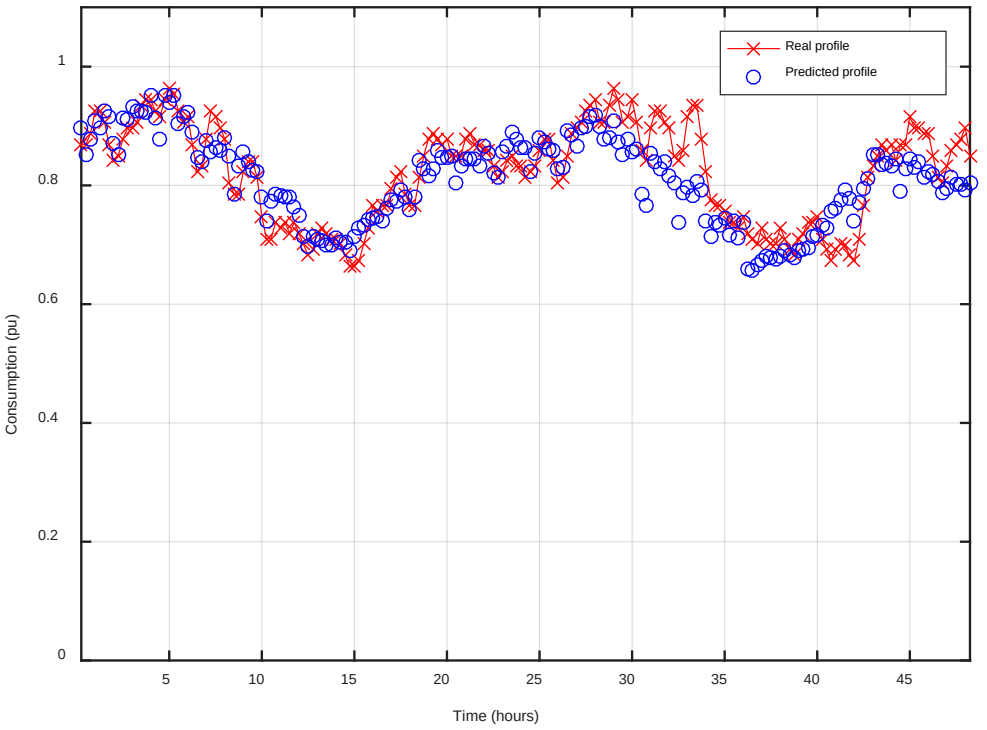

Figure 3.31: Comparison between real profile and prediction for cluster id: 4.

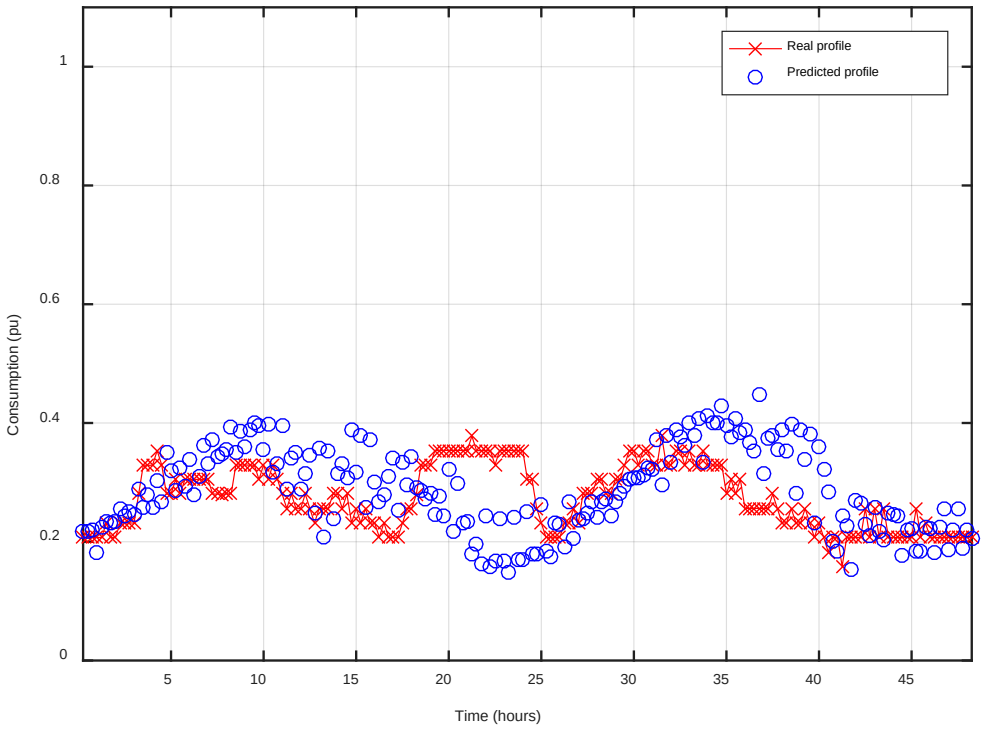

Figure 3.32: Comparison between real profile and prediction for cluster id: 1.

3.5 Conclusions

The main contribution of this chapter is the presentation of a methodology for the modeling and energy forecasting using a combination of Genetic Algorithms and Adaptive Neuro-Fuzzy Inference Systems, with aim to generate high accuracy customizable mathematical models for different consumptions in order to obtain short-term demand forecasts that are used in the energy hub optimization strategy.

In the proposed methodology, the ANFIS is used to train the mathematical model of the consumption and to provide a short-term load forecast while the GA is responsible for analyzing the database and the possible correlations between the demand and the input candidates and evaluate which are the optimal ones to be used as inputs in the training and the prediction process.

Although there are many approaches for the load forecasting, in the presented methodology, the use of ANFIS has been selected due to the capacity of the algorithm to model different time series patterns without the need of any modifications in its structure, making it ideal for implementation on multi-carrier energy systems, where different type of consumptions are present. That results to an algorithm that requires few configurations for its operation and it can be integrated easily into an industrial application. Furthermore, the combination of GA-ANFIS, permits to evaluate periodically the accuracy of the predictions, and update (if necessary) the training inputs of the models. Thus, in this methodology, the genetic algorithm has a fundamental role in the performance of the energy modelling, as it identifies changes in the load's behavior and always selects the best training candidates based on correlation analyses. Additionally, the use of a successive splitting filtering of the database for the definition of the training and checking data has proved to present better result than the chronological one, being advantageous for the training of consumptions of which the future behavior and profile is unknown.

On the other hand, a multi-model training approach is presented, which increases even more the modelling performance and the prediction accuracies by clustering the database into separate datasets, based on the consumption patterns. Since the initially complex modeling problem is split into a set of smaller problems, it is easier for the algorithm to train each group, as its members present a similar behavior, and so it helps the training algorithm converge faster. Also, the proposed methodology accomplishes a forecast response that adapts better to the different dynamics of the load demand signal.

Another important advantage of this system is that it welcomes parallelization during the input selection and training process. On a single model approach, the training algorithm usually needs to run on a single machine. But once the patterns have been identified and classified by the system, the data subsets can be trained by different nodes or even in cloud computing services. In addition, each set of data can take advantage of the different cores of the node and run multiple input selection search scenarios of the genetic algorithm concurrently, reducing even more the processing time.

Simulations and experimental validations have been carried out to verify the performance of the proposed methodology under different conditions and for several consumptions of an automotive manufacturing plant. From the obtained results, it can be observed that the use of the GA to evaluate the training data can offer an improvement in the prediction results, as it detects modifications in the consumption´s behavior and selects always the input dataset that presents the best performance.

Finally, it has to be mentioned that the proposed forecasting methodology can be implemented to any energy load profile, of both the industrial and tertiary sector, due to its flexibility and easy adaptation over existing databases. Thus, it is a suitable methodology for real time application, which require to determine accurately and rapidly the prediction operating profiles of different type of consumptions.

4. Energy Flow Optimization

4.1 State of the art

Since energy can be produced by using different technology or capacity mixes, it is important that the energy infrastructure adopt that flexibility to meet the energy demand patterns at maximum efficiency and minimum cost. To achieve that, optimization techniques can be implemented, taking into consideration several conditions and multiple variables simultaneously, such as the demand profiles (of the entire optimization horizon), the infrastructure restrictions, the energy availability, the equipment's operation bounds as well as the resulting impact of each strategy.

Up to now, different applications and algorithms have been used in order to optimize multivariable problems. For simple systems the optimization can be done by differentiating the equations with respect to each parameter in turn, setting the set of partial differential equations to zero and solving this set of simultaneous equations. However, in more complicated cases, it may be impossible to differentiate the equations, or very difficultly soluble non-linear equations may result.

The available methods for constrained optimization can be divided into two main categories: the deterministic and the stochastic ones. Based on the literature review of this field, the generalized reduced gradient methods and the sequential quadratic programming methods are two of the best deterministic local optimization methods. These gradient-based methods

always look for the optimum, which is located closest to the starting point of the search, whether it is a local or a global one [58]. Although there are several methods for the solution of constrained nonlinear programming problems, there is not any known method able to determine the global minimum with certainty in the general non-linear programming problem [60].

In the cases of optimal power flow, and given the increased complexity of the resulting objective function, an appropriate strategy would require employment of efficient optimization algorithms in order to determine the distributed generation capacity. Traditional linear programming, mixed-integer linear programming and mathematical programming have been the most widely applied methods for the optimization problem of linear formulations, aiming at minimizing the discounted investment and operational costs associated with meeting energy demand [61]-[62]. While a linear algorithm is well suited for optimization of a system described by a linear model, the nonlinear programming approach is also commonly employed when nonlinear formulations and logistical constrains are applied to the energy production or energy conversion equipment [63].

Algorithms such as particle swarm optimization, sequential quadratic programming, and Lagrangian relaxation were used successfully in applications of power dispatch as published in [64]-[66], respectively. Solutions addressing the forecasting problem in optimization, often account for the random-like behavior of the load and price using stochastic and fuzzy methods. In the stochastic approach, mean values for electric power and heat are estimated by taking the randomness in electricity and heat demand into account [67]-[68]. Other iterative evolutionary algorithms have been employed by several authors to maximize social utility to the customers and minimize operational costs [69], or to minimize costs and GHG emissions [70]. The use of genetic algorithms has been presented in [71] with objective to minimize the generation and environmental costs of an electric distribution system, taking into consideration its operation and maintenance costs as well. Some other proposed methods which deal with the multiobjective optimization of energy hubs, include the “jump and shift” technique [72] to solve each objective at a time until they converge to a single solution, and the scalarization technique as presented in [73] and [74].

On this line of approaches, this chapter presents a new methodology for the dynamic optimization of multi-carrier energy systems, combining demand forecasting (based on the GA-ANFIS approach, presented in Chapter 3) and nonlinear mixed-integer programming. The energy flow of the system is being optimized by means of a multiobjective genetic algorithm

with objectives to satisfy the energy demands, to minimize the total operation costs and energy, and to minimize the generated CO_2 emissions. Furthermore, the methodology takes into account the dynamic system response, expressed as thermal inertias of the energy production equipment, to calculate its effect to the equipment's operation bounds during the multi-time period optimization.

Figure 4.1 depicts the block diagram of the proposed method, in which the GA is being used to determine the best training inputs of the ANFIS structure for an optimized data learning.

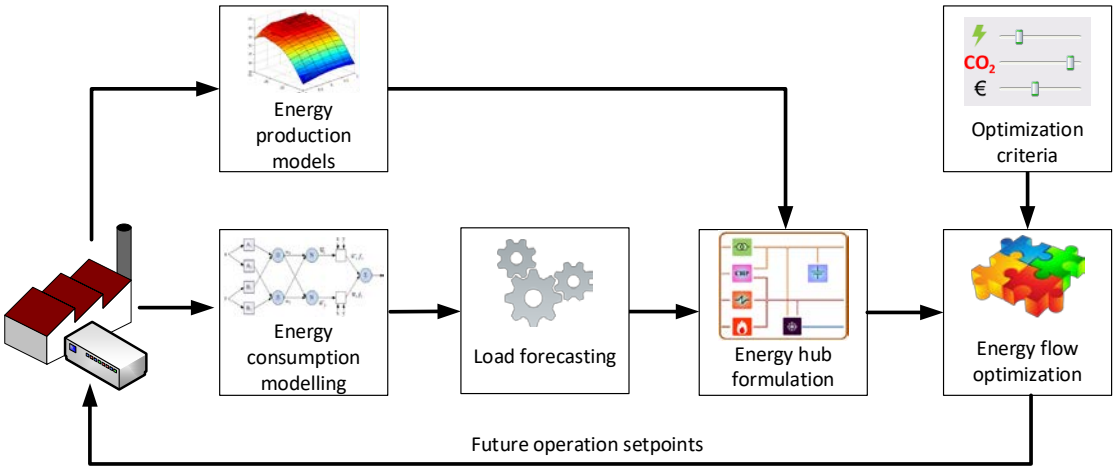

Figure 4.1: Structure of the proposed optimization process.

4.2 Mathematical Formulation

Depending on the structure of the multi-carrier energy system as well as the type of technologies and equipment that contains, the mathematical formulation of the problem can vary between continuous linear, continuous nonlinear, mixed-integer linear and nonlinear, as well as multi-period continuous and multi-period mixed integer problems [75]-[77]. The following sections describe the general formulas of these cases.

4.2.1 Continuous Linear or Nonlinear Problems

Linear and nonlinear programming problems with continuous optimization variables x can be formulated mathematical as follows:

$$\begin{aligned} \text{Minimize} \quad & f(x) \\ \text{subject to} \quad & g(x) = 0 \\ & h(x) \le 0 \end{aligned} \tag{4.1}$$

where

- $x = (x_1, \dots, x_{N_x})$ is the $1 \times N_x$ vector of continuous optimization variables, $x \in S \subset \Re^{N_x}$;
- $f(x): \Re^N \to \Re$ is a scalar-valued objective function;
- $g(x): \Re^{N_x} \to \Re^v$ is the $v \times 1$ vector of equality constraints;
- $h(x): \Re^{N_x} \to \Re^w$ is the $w \times 1$ vector of inequality constraints.

4.2.2 Mixed-Integer Linear or Nonlinear Problems

The mixed-integer programming problems include both continues variables x, as well as discrete variables y, and can be formulated as follows:

$$\begin{aligned} \text{Minimize} \quad & f(x, y) \\ \text{subject to} \quad & g(x, y) = 0 \\ & h(x, y) \le 0 \end{aligned} \tag{4.2}$$

where

- $x = (x_1, \dots, x_{N_x})$ is the $1 \times N_x$ vector of continuous optimization variables, $x \in S \subset \Re^{N_x}$;
- $y = (y_1, \dots, y_{N_y})$ is the $1 \times N_y$ vector of discrete optimization variables, $y \in D \subset Z^{N_y}$;
- $f(x,y): \{\Re^{N_x}, Z^{N_y}\} \to \Re$ is a scalar-valued objective function;
- $g(x,y): \{\Re^{N_x}, Z^{N_y}\} \to \Re^v$ is the $v \times 1$ vector of equality constraints;
- $h(x,y): \{\Re^{N_x}, Z^{N_y}\} \to \Re^w$ is the $w \times 1$ vector of inequality constraints.

4.2.3 Multi-Period Continuous Problems

The multi-period optimization consists in the calculation of an optimal solution taking into account multiple time periods $t \in \{1, 2, \text{K}, N_t\}$ instead of one instance of the problem. In the continuous case, multi-period problems are generally stated as:

$$\begin{aligned} &\text{Minimize} && \sum_{t=1}^{N_t} f^t(x) \\ &\text{subject to} && g^t(x) = 0 \quad \forall t \\ & && h^t(x) \le 0 \quad \forall t \end{aligned} \tag{4.3}$$

where

- $x \in \Re^{(N_x \cdot N_t)}$ is the $1 \times (N_x \cdot N_t)$ vector of continuous optimization variables;
- $t \in \{1,2, \dots, N_t\}$ is the $1 \times N_t$ vector of the optimization time instants;
- $f^t(x): \Re^{(N_x \cdot N_t)} \to \Re$ is a scalar-valued objective function, reflecting the result for the time instant t;
- $g^t(x): \Re^{(N_x \cdot N_t)} \to \Re^v$ is the $v \times 1$ vector of equality constraints at instant t;
- $h^t(x): \Re^{(N_x \cdot N_t)} \to \Re^w$ is the $w \times 1$ vector of inequality constraints at instant t.

4.2.4 Multi-Period Mixed-Integer Problems

The multi-period mixed-integer problems are the ones that represent the most the operation of the multi-carrier energy systems due to the discrete operation of the energy production equipment. These problems can be formulated mathematically as follows:

$$\begin{aligned} &\text{Minimize} && \sum_{t=1}^{N_t} f^t(x,y) \\ &\text{subject to} && g^t(x,y)=0 \quad \forall t \\ & && h^t(x,y)\le 0 \quad \forall t \end{aligned} \tag{4.4}$$

where

- $x \in S \subset \Re^{(N_x \cdot N_t)}$ is the $1\times(N_x \cdot N_t)$ vector of continuous optimization variables;
- $y \in D \subset Z^{(N_y \cdot N_t)}$ is the $1\times(N_y \cdot N_t)$ vector of discrete optimization variables;
- $t \in \{1,2,\dots,N_t\}$ is the $1\times N_t$ vector of the optimization time instants;
- $f^t(x,y): \left\{\Re^{N_x}, Z^{N_y}\right\} \to \Re$ is a scalar-valued objective function, reflecting the result for the time instant t;
- $g^t(x,y): \left\{\Re^{N_x}, Z^{N_y}\right\} \to \Re^v$ is the $v\times 1$ vector of equality constraints at instant t;
- $h^t(x,y): \left\{\Re^{N_x}, Z^{N_y}\right\} \to \Re^w$ is the $w\times 1$ vector of inequality constraints at instant t.

4.2.5 Multi-Carrier Power Flow

The multi-carrier optimal power flow can be defined as the determination of an optimal operating strategy of an energy system and its complete state, including transmission and conversion of multiple energy carriers within security constraints.

Mathematically, a multi-carrier optimal power flow can be formulated as a linear or nonlinear constrained optimization problem, which as presented in (4.5) it consists of the mathematical expressions that describe i) the cost function of the problem (subject of minimization or maximization), ii) the energy flow of the system in terms of the available energy carriers, iii) the energy system's restrictions and iv) the equipment's operation bounds.

$$\begin{aligned} &\text{Minimize} && f=\sum_{t=1}^{N_t} f^t\left(P_i^t, v_{i\alpha k}\right) && \\ &\text{subject to} && L_i-\eta_i\cdot P_i=0 && \forall i\in H \\ & && \underline{P_{i\alpha}} \le P_{i\alpha} \le \overline{P_{i\alpha}} && \forall \alpha \in \mathrm{E} \\ & && \underline{P}_{i\alpha k} \le \vartheta_{i\alpha k}\cdot P_{i\alpha} \le \overline{P}_{i\alpha k} && \forall i\in H, \forall \alpha\in \mathrm{E}, \forall k\in \eta_{i\alpha} \\ & && 0\le \vartheta_{i\alpha k}\le 1 && \forall i\in H, \forall \alpha\in \mathrm{E}, \forall k\in \eta_{i\alpha} \end{aligned} \tag{4.5}$$

where

- $\alpha, \beta, \gamma, \dots, \omega \in E$ is a set of primary energy sources;
- $i, j \in H = \{1,2, \dots, N_H\}$ is a set of hubs;
- $k \in \eta_{i\alpha} = \{1,2, \dots, N_{\eta_{i\alpha}}\}$ is a set of converters η_i of hub i; the subset $\eta_{i\alpha} \subseteq \eta_i$ contains all the elements of hub i, which convert energy α into another carrier;
- $\underline{P}_i$ and $\overline{P}_i$ are the power limitation vectors of the hub inputs P_i (lower and upper limits respectively).

4.3 Optimization Criteria

In contrast to single-objective problems, in multi-objective optimization, the fitness function consists of several criteria that have to be evaluated simultaneously in order to determine whether a proposed solution presents better score than others and thus tends to optimum. The criteria might be of qualitative or quantitative nature (e.g. the cost of an energy source can be numerically measured while the comfort rating could be subjectively describe as high, medium or low) and they depend on the problem to be resolved. In the case of the multi-carrier power flow, the fitness function requires quantitative information about scores of each criterion, which as described above, are i) minimization of the input energy use, ii) minimization of the energy costs and iii) minimization of the equivalent carbon dioxide emissions (CO_{2eq}).

Thus, for the formulation of the criteria, the total energy use (f_1) can be calculated by aggregating the energy amount of the system´s inputs for all the time instants of the optimization horizon.

$$f_1^t = \sum_{\alpha} \sum_{t} P_{Tot,t}^{in,a} \tag{4.6}$$

Similarly, the energy cost of the system (f_2) can be calculated as the product of the consumed energy and its corresponding price as described in (4.7).

$$f_2^t = \sum_{\alpha} \sum_{t} P_{Tot,t}^{in,a} \cdot \lambda_t^{\alpha} \tag{4.7}$$

Finally, the total emissions (f_3) can be calculated considering the product of the total consumed energy amount and the greenhouse gas equivalencies.

$$f_3^t = \sum_{\alpha} \sum_{t} P_{Tot,t}^{in,a} \cdot e^{a} \tag{4.8}$$

where

- P_{Tot}^{in} represents the total input energy of the hub;
- α is the index of the hub´s input energy carriers [1 : *A*];
- *t* is the index for the optimization time instants [1 : *T*];
- λ_t^{α} describes the energy price of energy carrier *α* at time instant *t*;
- e^{α} describes the emission factor of the input energy carrier *α*.

Among the different quantitative methods to handle multi-criteria decisions (e.g. value and utility analysis, ideal point method, outranking method, analytical hierarchy process, etc.), one of the most commonly used is the weighted summation (weighted global criterion method), in which all the objective functions are combined to form a single one. In this method, the score of the fitness function is obtained by aggregating the individual normalized scores of the criteria, which have been previously multiplied by an assigned weight (4.9).

$$ff = \sum_{j=1}^{O} f_j^{trans} \cdot w_j \tag{4.9}$$

whereas *ff* is described the fitness function of the optimization problem, *j* is the index for optimization criteria [1 : *O*] and as f_j^{trans} and w_j are described the normalized score and assigned weight of criterion *j*, respectively. The normalization process of the criteria´s scores is made in order to remove dimensions or possible balance magnitude differences that may exist between the criteria. Equation (4.10) present the transforming approach that has been selected to normalize the criteria´s scores, as it is considered one of the most robust [78], regardless of the objectives´ original ranges.

$$f_j^{trans} = \frac{f_j(x,y) - f_j^o}{f_j^{\max} - f_j^o} \tag{4.10}$$

In this approach, the values of f_j^{trans} typically lies between zero and one depending on the accuracy of values $f_j^{\max}$ and f_j^0, which describe the maximum and minimum fitness scores of criterion *j,* respectively, for the case in which the problem is resolved as single objective.

4.4 Optimization Process

The proposed optimization process consists of 8 steps that can be classified in 3 main blocks (Figure 4.2): the demand prediction for the optimization horizon; the mathematical description of the problem, formulated as an intertemporal optimization problem, taking into account the conditions and restrictions of the system; and finally, the calculation of the optimum energy flow to satisfy the energy demands. The detailed characteristics of the method's steps are discussed next.

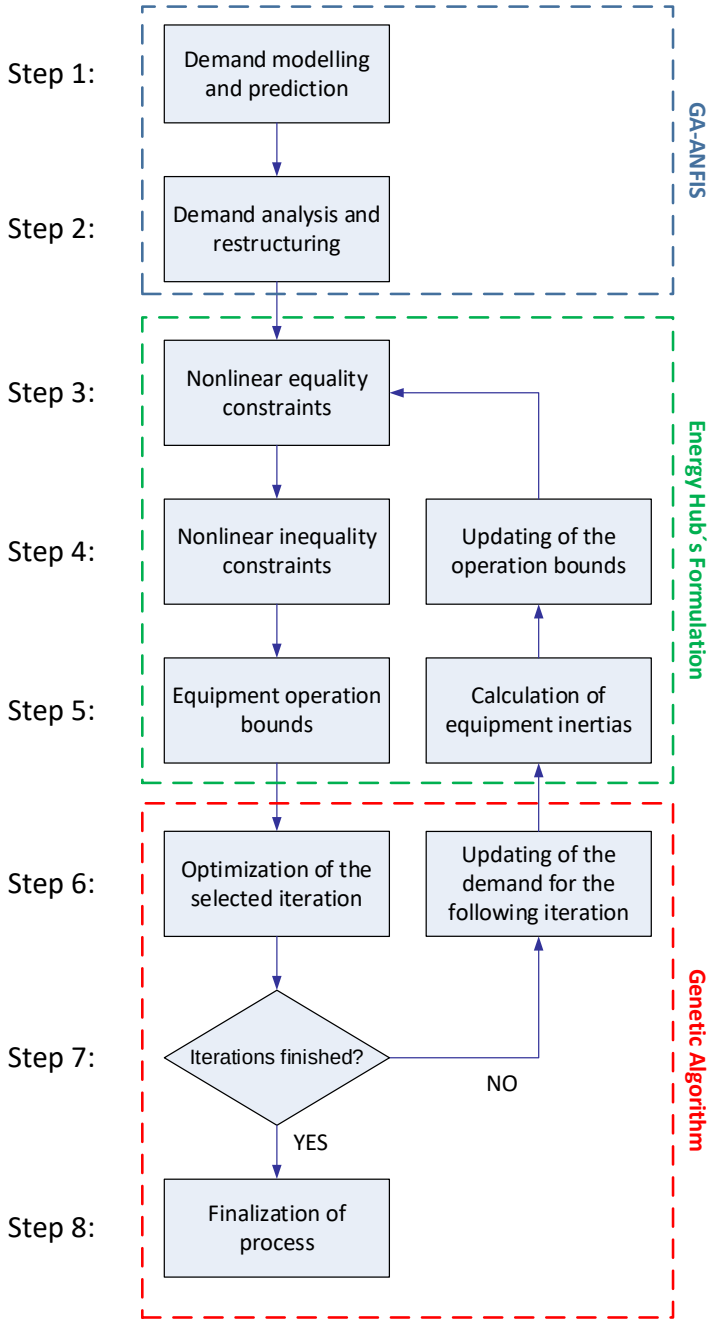

Figure 4.2: Dataflow of the optimization process.

Step 1: Demand Modelling and Prediction

The demand modelling and prediction tasks, as described in Chapter 0, are performed by means of a combination of an ANFIS of Takagi-Sugeno type and genetic algorithms, with objective to train the mathematical models of the system's energetic requirements, referenced to operation conditions and external parameters (e.g. climate conditions, time, etc.). The GA is used to select the training inputs for the model, while ANFIS calculates the relationships and the inference rules between the selected inputs and the demands, training the mathematical model.

The training and evaluation process is repeated for all the input combinations of the models and the most accurate ones are kept. Once all of the mathematical models are obtained, they are used by the same algorithm to forecast the energy demands of the system for a predefined optimization horizon and time intervals (e.g. 10 seconds, 1 minute, 15 minutes, etc.). In this step, current and future data for the model's inputs are used, obtained by different sources (e.g. information given by a user, data gathered from a weather service, etc.).

Step 2: Demand Analysis and Restructuring

In this step, the algorithm analyses the total energetic requirements of the system for the complete prediction (and optimization) horizon and applies a descending sorting to the demand vectors. Thus, the vectors are converted from time-ordered to descending-ordered, permitting to evaluate initially the time instants that present the higher energetic needs, calculating the optimal operation of the equipment and their settling times. In this way, the algorithm analyses and evaluates each time instant individually but it takes into account the operation of the equipment at the rest of the evaluated time instants (past and future) in order to recalculate (if necessary) the equipment's operation bounds. This evaluation process has as objective to calculate initially the optimal operation of the energy production equipment and carriers (e.g. cogeneration, boilers, grid supply, etc.) for the higher demand periods (before evaluating the lower ones), to guarantee that the required demand of the system, even for the peak demands, will be entirely fulfilled and the system will operate in an optimal manner.

In this context, Figure 4.3 presents an example of an energy profile that consists of 20 time-instants. The figure depicts both the time order of the demand that appears at the top x-axis, as well as the evaluation order (descending-order, depicted at the bottom x-axis), which is

used by the algorithm to optimize each one of the time instants individually till completing the entire horizon. In the following paradigm, the algorithm begins by optimizing the time instant that is located at time *t*=11 and corresponds to the higher demand point of the prediction horizon. Then the evaluation continues with time-instants: *t*=10, *t*=12, *t*=13, and so on, following the depicted evaluation order. The axes of the figure depict both the time order of the signal, as well as the evaluation order of the signal, depicted in the upper and lower axis respectively.

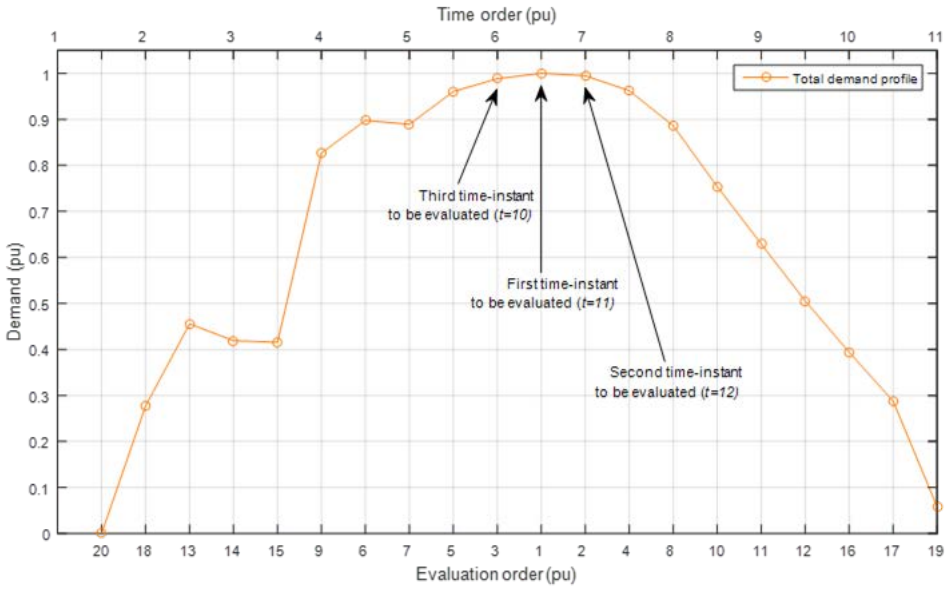

Figure 4.3: Example of the evaluation order of the time instants, based on descending-order.

Figure 4.4 presents graphically a comparison between the original and reconstructed demand vector of Figure 4.3, depicting the initial time ordered demand vector, calculated by the GA-ANFIS algorithm, and the restructured descending ordered demand vector, which is finally used as reference for the energy flow optimization of the system.

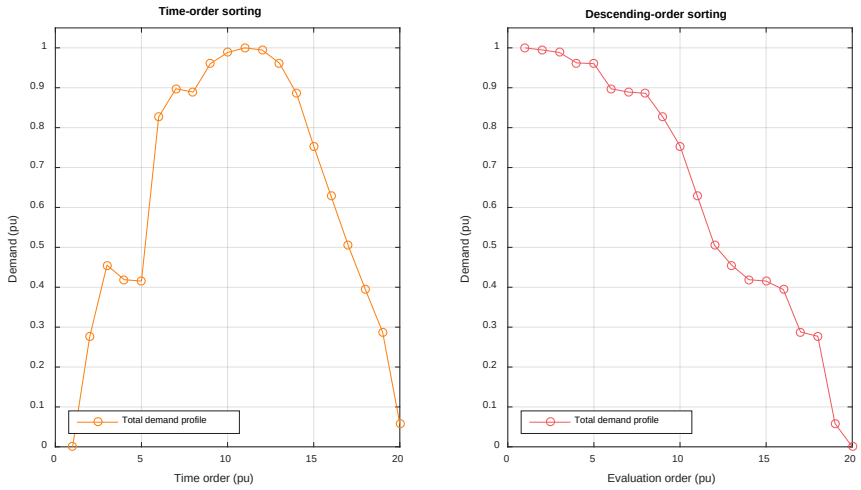

Figure 4.4: Comparison between time-ordered demand vector and descending-order demand vector.

Step 3: Coefficient of Performance Constraints

During this step, the algorithm calculates the coefficient of performance of the energy production equipment along time, which can be constant or its values can vary depending on the type of equipment and the operating conditions, as well as the energy demand of the evaluated time instant in order to formulate the system´s equality constrains.

In the case of a variable COP, the calculation is made by use of mathematical models of the equipment, which characterize the operation of the equipment in different operation states. In the case of static ones, the equipment's efficiency remains constant in spite of its operation conditions, which can typically be obtained by the manufacturer technical sheets.

As expressed in (4.11), the equality constraints state the available energy carriers between the primary energy sources and demands, which represent the hub inputs and hub outputs, respectively.

$$P_{ik,t}^{out,\beta} = P_{ik,t}^{in,\alpha} \cdot \eta_{i,t}^{\beta\alpha} \qquad \forall \alpha, \forall \beta, \forall i, \forall k \tag{4.11}$$

where

- $P_{ik,t}^{out,\beta}$ represents the output power (of type β) of the k^{th} energy converter of type i at the time instant t;
- $P_{ik,t}^{in,\alpha}$ represents the input power (of type α) of the k^{th} energy converter of type i at the time instant t;
- t is the index for the optimization time instants [1 : T];
- $\eta_{i,t}^{\beta\alpha}$ represents the efficiency of the energy convert of type i, at time instant t, for converting energy of carrier α to carrier β.

Step 4: Energy Supply Constraints

On the fourth step, the algorithm calculates the restrictions of the system and formulates the inequality constraint vectors. These restrictions can vary depending on the evaluated time instant and as shown in (4.12) and (4.13), they are related to the maximum available supply limits of the primary energies and the maximum limits of energy production by equipment.

$$\sum_i \sum_k P_{ik,t}^{in,\alpha} \le \overline{P}_{Tot,t}^{in,\alpha} \qquad \forall \alpha, \forall i, \forall k, \forall t \tag{4.12}$$

$$\sum_i \sum_k P_{ik,t}^{\text{out},\beta} / \eta_{i,t}^{\beta\alpha} \le \overline{P}_{i,t}^{in} \qquad \forall \alpha, \forall \beta, \forall i, \forall k, \forall t \tag{4.13}$$

where

- $P_{ik,t}^{in,\alpha}$ represents the input power (of type α) of the k^{th} energy converter of type i at the time instant t;
- $\overline{P}_{Tot}^{in,\alpha}$ represents the maximum supply limit of energy carrier α;
- $P_{ik,t}^{out,\beta}$ represents the output power (of type β) of the k^{th} energy converter of type i at the time instant t;
- $\eta_{i,t}^{\beta\alpha}$ represents the efficiency of the energy convert of type i, at time instant t, for converting energy of carrier α to carrier β;
- $\overline{P}_{i,t}^{in}$ represents the maximum input power for the energy converter of type i at the time instant t.

Step 5: Equipment´s Operating Bounds

This step is focused on the calculation of the equipment's operating bound vectors. The bound levels can be affected by the dynamic response of the equipment, as inertias and delays could be present while reaching the desired energy outputs from their current operating point. Thus, in order to obtain a feasible and stable operating strategy for the energy production equipment, which results to optimal power flow, the algorithm needs to consider the equipment´s inertias and dynamics, which are formulated as additional constraints in the optimization problem.

Furthermore, the algorithm takes into account the effects and implications of its decisions of each single time instant at the rest of the prediction horizon, as they can influence the future operating possibilities. Equation (4.14) presents the generic formulation of the equipment's operation bounds in relation to their energy production.

$$\underline{P}_{i,t}^{in,\alpha} \le P_{ik,t}^{in,\alpha} \le \overline{P}_{i,t}^{in,\alpha} \qquad \forall \alpha, \forall i, \forall k, \forall t \tag{4.14}$$

where

- $\underline{P}_{i,t}^{in,\alpha}$ represents the minimum input power for the energy converter of type i of energy carrier α at the time instant *t*;
- $P_{ik,t}^{in,\alpha}$ represents the input power (of type α) of the kth energy converter of type i at the time instant *t*;
- $\overline{P}_{i,t}^{in,\alpha}$ represents the maximum input power for the energy converter of type i of energy carrier α at the time instant *t*.

Step 6: Optimization of Time Instant

On this step the algorithm calculates the optimal energy flow of the multi-carrier energy system for the current time instant by means of the GA algorithm. Initially, the mixed-integer problem is solved for every criterion individually to obtain their minimum feasible points (utopia points) and their maximum values. These values are used for the normalization of the optimization criteria, when are being evaluated into the multiobjective weighted-sum function. Then the whole multi-objective problem is solved, normalizing the criteria values with the transforming approach of (4.10).

The execution of the genetic algorithm is based on the same evaluation steps, as depicted in Figure 3.4, applying also the three genetic operators that consist on i) the selection of the best chromosomes , ii) the mating of individuals and iii) the mutation of random genes.

During the generation of the initial population, the problem variables are being encoded in binary format in order to simplify their processing and the execution of the genetic operators. The mathematical formulation for the binary encoding of the *n*th variable *p* is presented in (4.16), while (4.15) describes the normalization process that is used to adapt equal quantization levels for all the variables that form part of the chromosome.

$$p_{norm} = \frac{p_n - p_{\min}}{p_{\max} - p_{\min}} \tag{4.15}$$

$$gene[m] = round\left(p_{norm} - 2^{-m} - \sum_{p=1}^{m-1} gene[p] \cdot 2^{-p} \right) \tag{4.16}$$

Similarly, before evaluating the fitness cost of the chromosomes, a decoding process takes place in order to restore the natural values of the variables. Equations (4.17) and (4.18) describe the decoding formulation.

$$p_{quant} = \sum_{m=1}^{N_{gene}} gene[m] \cdot 2^{-m} + 2^{-(M+1)} \tag{4.17}$$

$$q_n = p_{quant} \cdot (p_{\max} - p_{\min}) + p_{\min} \tag{4.18}$$

where

- p_{norm} represents the normalized variable with range [0, 1];
- $p_{\min}$ represents the minimum value of the evaluated variable;
- $p_{\max}$ represents the maximum value of the evaluated variable;
- $gene[m]$ represents the binary version of p_n;
- $round[\cdot]$ represents the round value of a number to the nearest integer;
- p_{quant} represents the quantized value of p_{norm};
- q_n represents the quantized version of p_n;
- N_{gene} defines the number of bits (*b*) that contains the chromosome;

Figure 4.5 depicts the generic structure of the chromosome's formulation, consisting of multiple encoded variables (genes).

$$chromosome = [\underbrace{101100110100011101}_{gene_1}\underbrace{}_{gene_2}\underbrace{}_{gene_3} \ldots \underbrace{111010}_{gene_n}]$$

Figure 4.5: Example of the chromosome structure, consisting of n-number genes.

Once the algorithm optimizes the operation of the time instant t $\{t \in \mathbb{N} \mid 1 \leq t \leq T\}$, the mathematical models of those equipment that present inertias, are used to calculate their maximum and minimum energy production bounds for the nigh time instants.

These bounds may vary from the minimum and nominal output powers of the equipment due to possible delays in their operation. Thus, the equipment bounds are recalculated (are reduced if necessary) for the time instants [t-1,...,t-m] and [t+1,…,t+n] (where t-m and t+n cannot exceed the values 1 and T, respectively) and are taken into account by the optimization algorithm during the evaluation of the following instants.

In this context, the following figures present an example of the step-by-step evaluation process of the algorithm, based on the demand case of Figure 4.3, which is considered as the heating demand of the energetic infrastructure of Figure 2.7. As stated previously, in the case of the following paradigm, the optimization process initializes by evaluating the demand and operations conditions of the time instant located at t=11, which corresponds to the higher demand point of the prediction horizon. In cases where the same demand value appears in more than one time instant, the algorithm make a chronological sort for their evaluation.

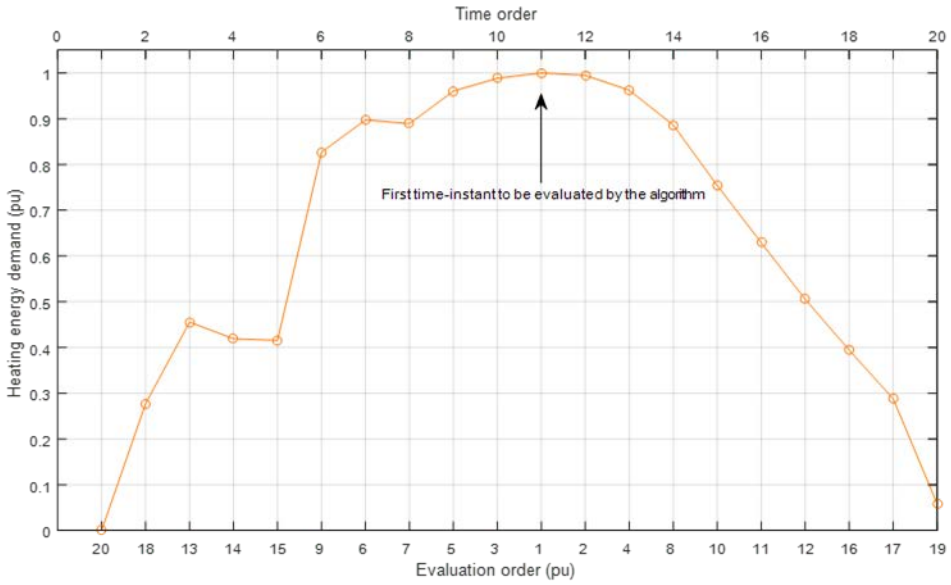

Figure 4.6: Example of the descending evaluation order of a heating energy demand vector.

At the initial iteration of the algorithm, there are no limitation on the operation bounds of the equipment (i.e. cogeneration and gas boilers) and thus, in terms of primary energy use, the corresponding constraints are formulated as follows:

$$\underline{P}^{in,gas,}_{CHP,t} \le P^{out,heat}_{CHP,t} \Big/ \eta^{g2h}_{CHP,t} \le \overline{P}^{in,gas}_{CHP,t} \quad , \quad t = 11 \tag{4.19}$$

$$\underline{P}^{in,gas,}_{boiler1,t} \le P^{out,heat}_{boiler1,t} \Big/ \eta^{g2h}_{boiler1,t} \le \overline{P}^{in,gas}_{boiler1,t} \quad , \quad t = 11 \tag{4.20}$$

$$\underline{P}^{in,gas,}_{boiler2,t} \le P^{out,heat}_{boiler2,t} \Big/ \eta^{g2h}_{boiler2,t} \le \overline{P}^{in,gas}_{boiler2,t} \quad , \quad t = 11 \tag{4.21}$$

$$\underline{P}^{in,gas,}_{boiler3,t} \le P^{out,heat}_{boiler3,t} \Big/ \eta^{g2h}_{boiler3,t} \le \overline{P}^{in,gas}_{boiler3,t} \quad , \quad t = 11 \tag{4.22}$$

Where the minimum energy supply values are equal to 0 and refer to a disconnected status, while the maximum energy supply values correspond to the required amount of gas to operate at nominal powers.

Once the current iteration is evaluated, the algorithm analyses the operation of the equipment and calculates the influence of their inertias at the nigh time instants. Considering as an example that the demand of time instant *t*=11 is fulfilled entirely by the cogeneration equipment with an operation point of 80% of its nominal power, then the algorithm uses the mathematical model of the equipment to recalculate the minimum operation bounds of the equipment at the previous time instants *t* = [1, 2,…, 10] and following time instants *t* = [12, 13,…, 20]. In this case, the following figure depicts an example of the inertia behavior, calculated by use of the space state model of Figure 4.7. It has to be mentioned that in terms of representation, Figure 4.7 depicts positive time units and negative time units for the cases where the equipment has to increase or decrease its output power, respectively.

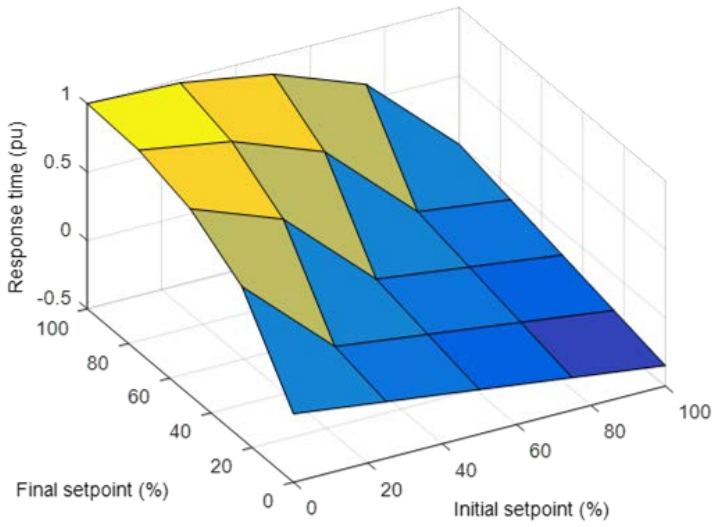

Figure 4.7: Example of the space state model of the equipment, indicating its response time to reach the final set point, based on its current operating condition.

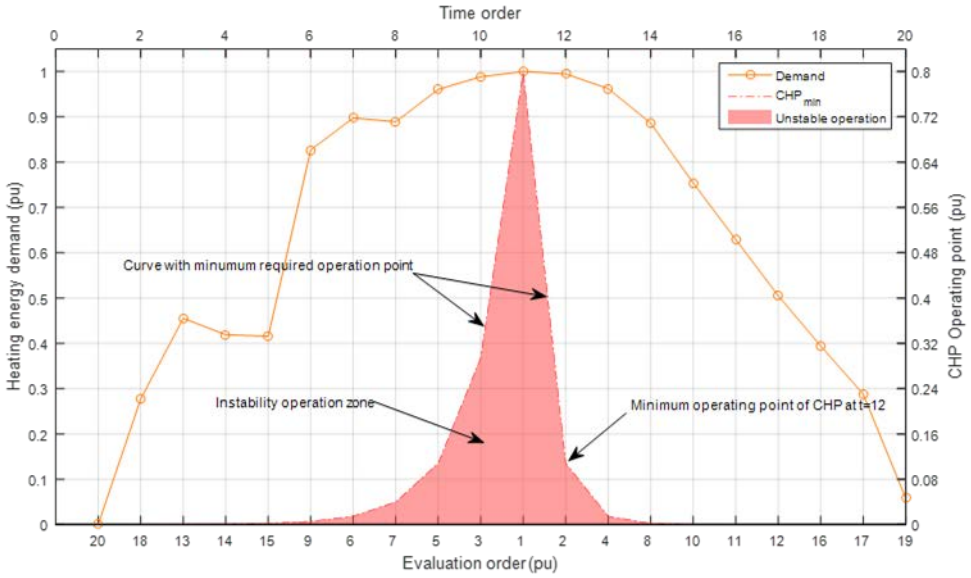

Figure 4.8: Example of the minimum operation bound curve of the equipment, based on its optimal operation of instant t=11.

The red curve indicates the minimum required operation point of the equipment in terms of produced power, in order to be able to achieve the optimum set-points that were calculated for time instant *t*=11. Thus, at the second iteration of the algorithm, which based on the example it corresponds to time instant *t*=12, the minimum operation bound of the CHP would be reestablished at the 11% of its nominal power (0.11pu) and would be formulated as follows.

$$\overline{P}_{CHP,t}^{in,gas} \cdot 0.11 \le P_{CHP,t}^{out,heat} \Big/ \eta_{CHP,t}^{g2h} \le \overline{P}_{CHP,t}^{in,gas} \quad , \quad t = 12 \tag{4.23}$$

Additionally, the figure depicts in red area the instability operation zone of the equipment, which refers to the operating zone, in which, due to the equipment's inertias, it will not be able to achieve its defined setpoint. Thus, it will not be able to predict the behavior of the energy system, if the energy demand will not be fulfilled.

With the same procedure, the algorithm continues optimizing the rest of the remaining time instants (with descending order), recalculating the possible limitation of the operation bounds for all of the equipment.

The following figure presents the bound restrictions of the cogeneration equipment after the second iteration, considering that based on the optimization strategy, at *t*=12 it produces only the 60 percent of the demand while the remaining is fulfilled by the rest of the equipment.

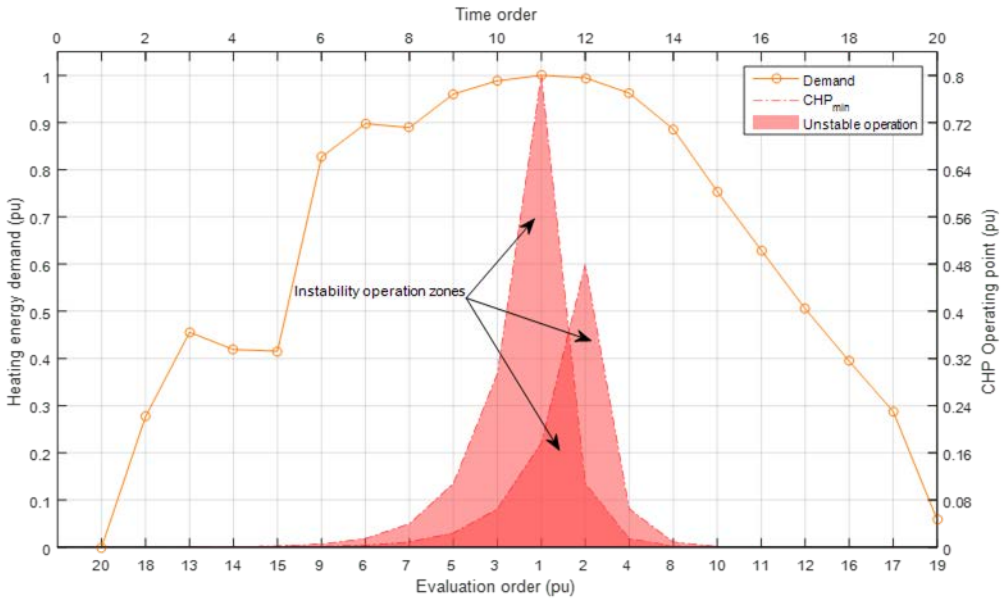

Figure 4.9: Example of the minimum operation bound curve of the equipment, based on its optimal operation scenario of time instants t = [11, 12].

Similarly as previous, at the third iteration (*t*=10), the minimum operation bounds would be recalculated focusing on the minimum required operating point of the equipment to reach the operating condition of *t*=11.

$$\overline{P}^{in,gas}_{CHP,t} \cdot 0.29 \le P^{out,heat}_{CHP,t} \Big/ \eta^{g2h}_{CHP,t} \le \overline{P}^{in,gas}_{CHP,t} \quad , \quad t = 10 \tag{4.24}$$

Figure 4.10 presents the results of the entire demand vector, depicting the operation points of the cogeneration equipment and the minimum operation point curve for each time instant, based on the inertia calculation of each iteration. As it can be observed in the figure, in order to fulfil the energy demand in *t=1*, the equipment has to be activated before the time instant *t=0*, where the optimization horizon begins.

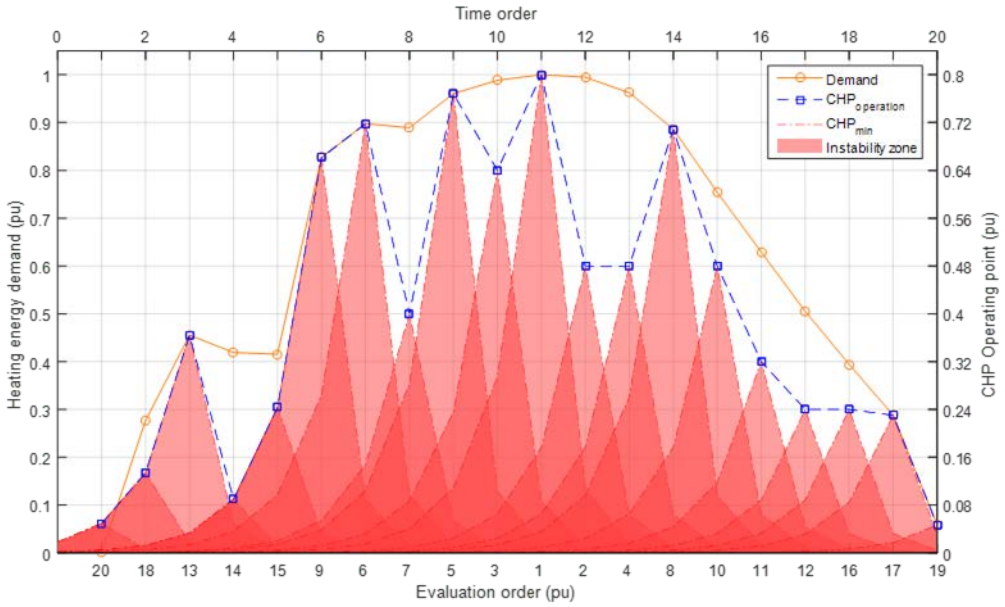

Figure 4.10: Example with the comparison between the operation strategy of the equipment and the minimum instability zones for the entire demand vector.

Finally, a comparison between the minimum operation bounds of the equipment and its final operation strategy can be observed in Figure 4.11, following the evaluation order of the time instants.

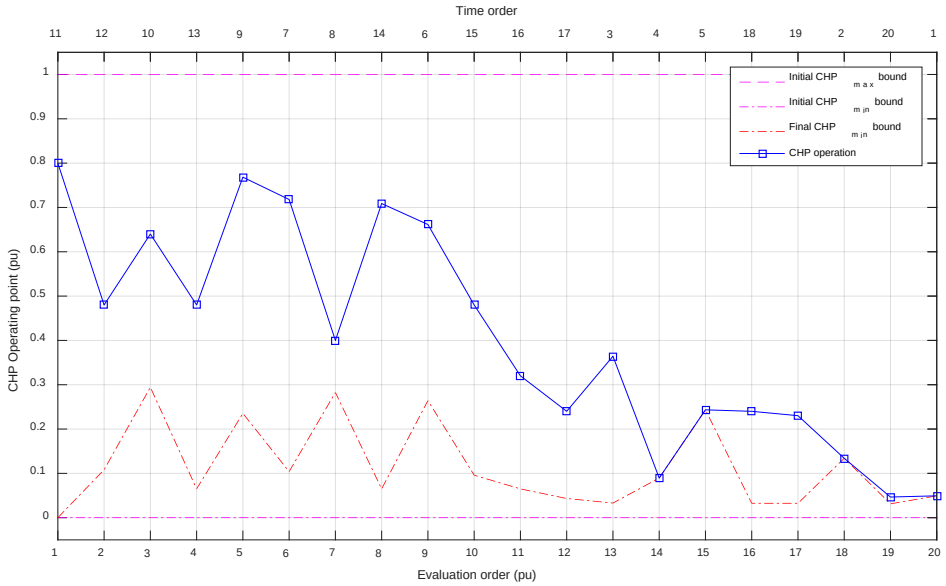

Figure 4.11: Evolution of the operation bounds of the equipment during the evaluation of the time instants.

As it can be observed by the example, the operation strategy of each equipment, at each time instant, can significantly affect the operation bounds of the rest optimization horizon, and thus affect the stability of the system.

Step 7: Evaluation and Updating of Conditions

In case that the optimization horizon has not yet evaluated completely, the algorithm continues to the next time instant, updating the entire problems values (i.e. demands, constraints, bounds, prices and emissions). Furthermore, the updating of the necessary upper and lower equipment bounds is made, based on the calculated inertias from the previous time instants. Then steps 3 to 6 are repeated.

Step 8: Optimization of Time Instant

When all the optimization horizon is evaluated, the algorithm restores the results' order to the natural one (time-referenced) and provides the obtained optimal solution for the optimization horizon.

4.5 Implementation and Results

This section presents the validation results of the proposed optimization methodology, applied at the energy hub structure that is depicted in Figure 2.7.

The testing period of the algorithm took place during a total of 3 months, evaluating the performance and impact of the algorithm compared with the real operating profiles of the industrial site. The following table presents the different periods of validation, indicating the climatic and production conditions of the site.

Due to confidentiality, the production conditions are represented as percentage, referred to the maximum production capacity of the production lines. Similarly, the energy consumption and energy production results that are presented in the following subsections, are depicted in per-unit values.

Table XI. Real case evaluation periods of the proposed optimization methodology.

Date Range	Temperature (°C)			Production (%)		
	Avg	Min	Max	Body shop	Painting	Assembling
01 – 31 January 2015	*8,71*	*0,3*	*19,7*	*73,5%*	*81,2%*	*73,3%*
01 – 28 February 2015	*8,86*	*0*	*20,8*	*90,7%*	*87,7%*	*88,8%*
01 – 31 March 2015	*13,25*	*3*	*26,9*	*91,7%*	*94,54%*	*91,1%*

The validation of the proposed methodology was made by applying different optimization criteria into the algorithm, using the actual energy demands of the site, which were monitored and acquired by the SCADA system. After that, a comparison of the real operation and the predicted one (calculated by the developed algorithm) was made in order to analyze the differences in terms of primary energy use, costs and CO_2 emissions and to evaluate the performance and the impact of the proposed methodology into the process. Specifically, the validation tests were made for two optimization criteria sets, as presented below.

a. Minimization of the use of primary energy sources and CO_2 emissions;
b. Minimization of primary energy sources, energy costs and the CO_2 emissions.

The following subsections present the description of the models of the energy production equipment of the plant, the detailed results of the proposed methodology for a period of 24 hours, as well as a long term validation analysis for the whole validation period of 3 months.

4.5.1 Energy Production Equipment Models

As commented in the previous chapters, the final objective of the proposed methodology is to model the behavior of a given multicarrier energy system and to optimize its energy flow. In order to achieve that, it is necessary to dispose the coefficients of performance of the equipment and their operating inertias. This information can be obtained by several ways, such as provided by the manufacturer, by applying measurements during the operation of the equipment, or by developing their mathematical models. In this case, the mathematical modelling of the energy production equipment were developed by the VTT Technical Research Centre of Finland in the framework of the FP7 EuroEnergest project. The design and the initial developments of the models have been done in the Apros software [79], permitting to analyze their operating behavior. After that, the models have been exported as Matlab functions in order to be used by the developed optimization algorithm. The models are based on mechanistic simulations, using physical dimensions of the processes and pipelines, as well as equipment-specific parameters. They utilize dynamic conservation equations of mass, energy and momentum to calculate flows, temperatures, concentrations and pressures in the systems. During their development, the obtained simulation results were compared with measured data from the real system and adequate adjustments were made in the models' structure and parameters to improve their accuracy. Nevertheless, it has to be mentioned that the proposed optimization method is not restricted to use mechanistic simulation models, but other type of models could be used as well (e.g. data-based models, stochastic, physical, etc.) maintaining a defined input-output structure.

A detailed description of the equipment's modelling process is presented in [80], discussing the modelling structure, the mathematical formulation and the obtained accuracy.

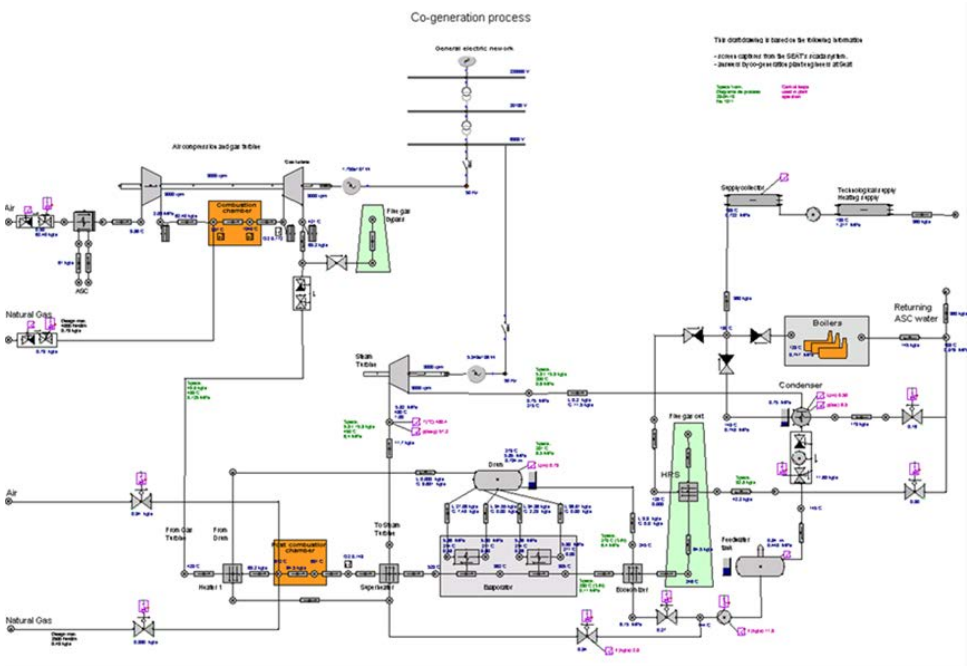

Figure 4.12: View of the Cogeneration diagram of Apros model, which includes the gas turbine, the steam processes and the heat recovery side of the superheated water system.

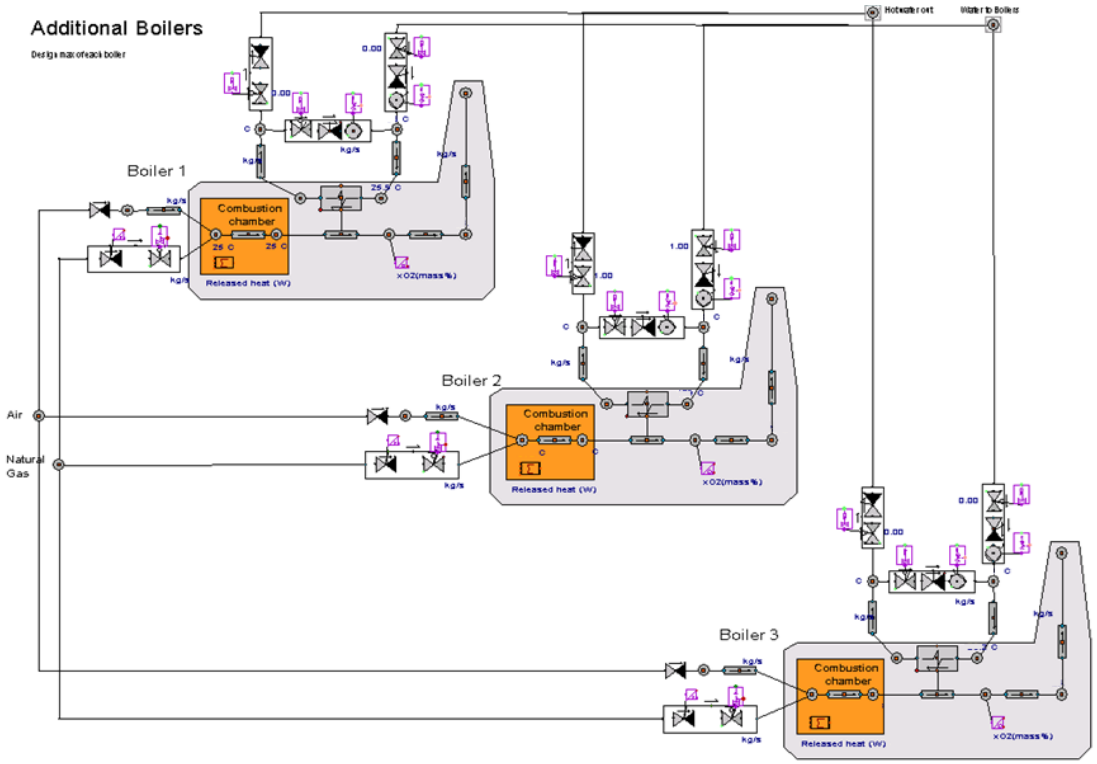

Figure 4.13: View of the Boilers' model, developed in Apros software by VTT.

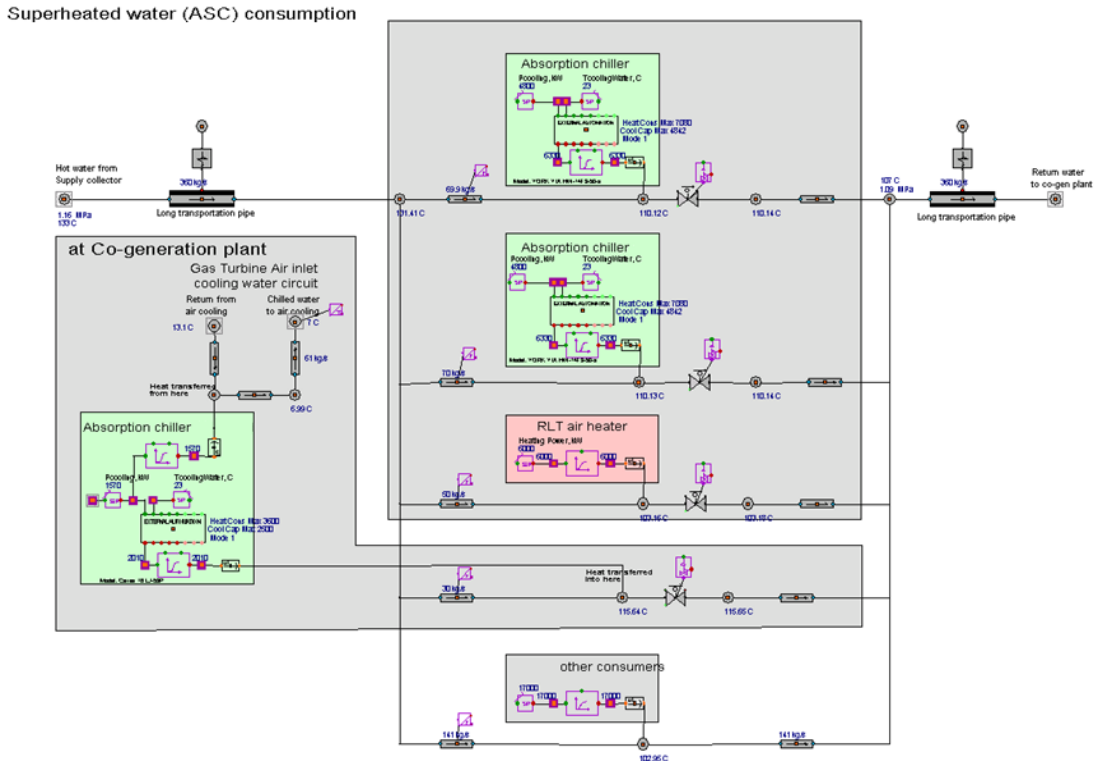

Figure 4.14: Example of the Chiller models, developed in Apros software by VTT.

It has to be highlighted that VTT maintains the property of the energy production equipment models of the industrial site that has been used for the experimental validation of the proposed optimization algorithm.

4.5.2 Validation Results

This subsection presents the performance of the optimization methodology for a validation period of 24 hours. Figure 4.15 depicts the energy demand profiles of the industrial site, which as described in Chapter 2.5, they consist of the total electric and total heating demands of the industrial site, as well as the cooling demands of 4 individual loads.

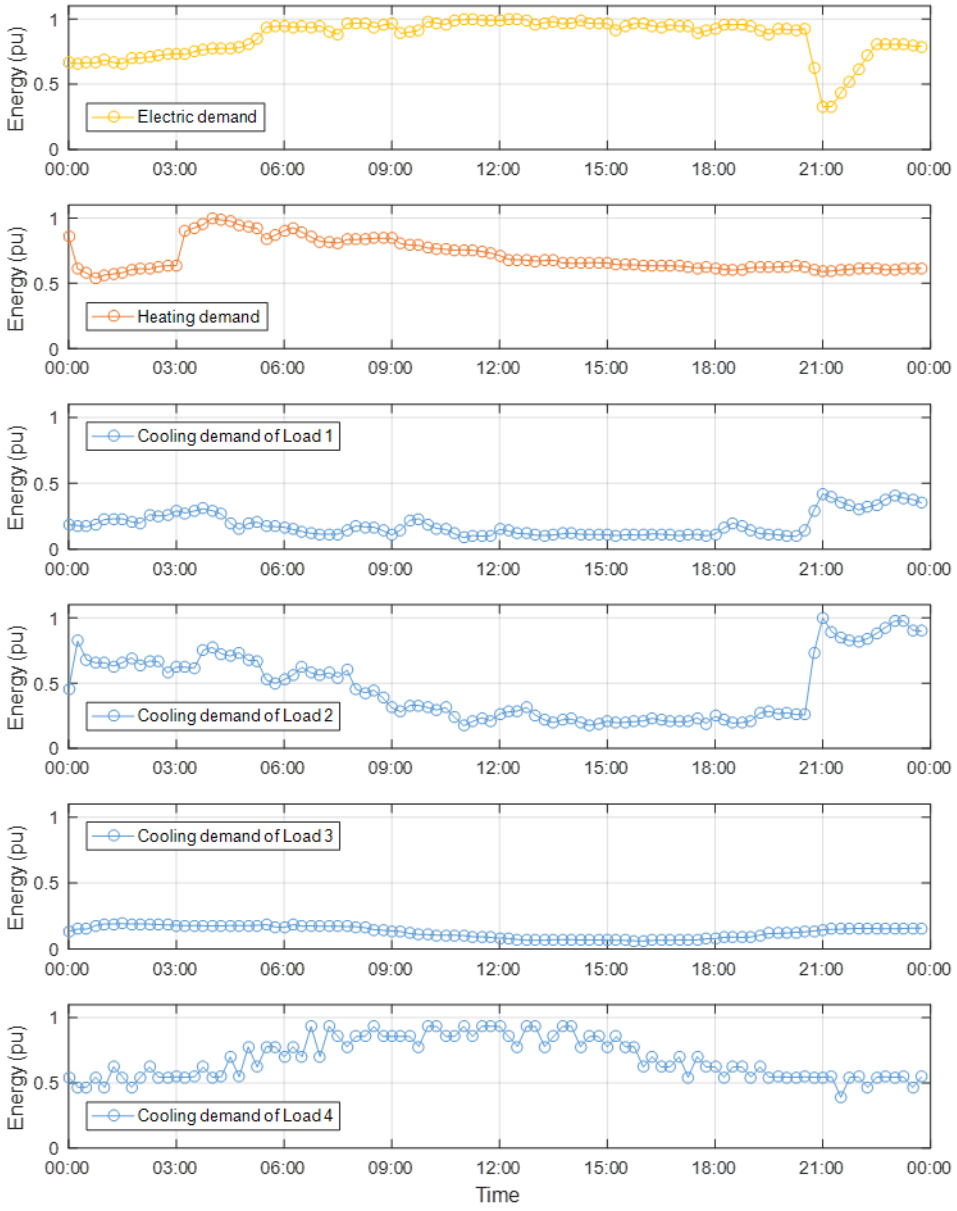

Figure 4.15: Energy demand profiles of the validation plant for a period of 24 hours.

In case of the cooling production, based on the available energy equipment and their interconnection with the rest of the system, the required energy is produced by 4 chiller groups that contains 2 equipment each; two absorption chillers and 6 electric chillers (Figure 4.16). For the case of the absorption chillers, their energy supply depends on the heating energy that is produced by the cogeneration and the boilers, and thus, their operation can affect significantly the whole operating strategy of the heating production process. For the case of the electric chillers, the energy supply has to be provided by the grid and the cogeneration's electricity production, and thus, this amount of energy has to be considered as an additional amount of the electric demand, used for the production of cool.

Thus, the optimization problem can be resolved separately for each production stage, which consist of the initial calculation of the optimal operation of the chiller equipment, which will result to the required heating and electric energy for their operation, and then the calculation of the optimal operating strategy of the heating equipment, considering the new updated demands. Figure 4.16 depicts the two separate production stages, indicating the energy interconnections between the equipment.

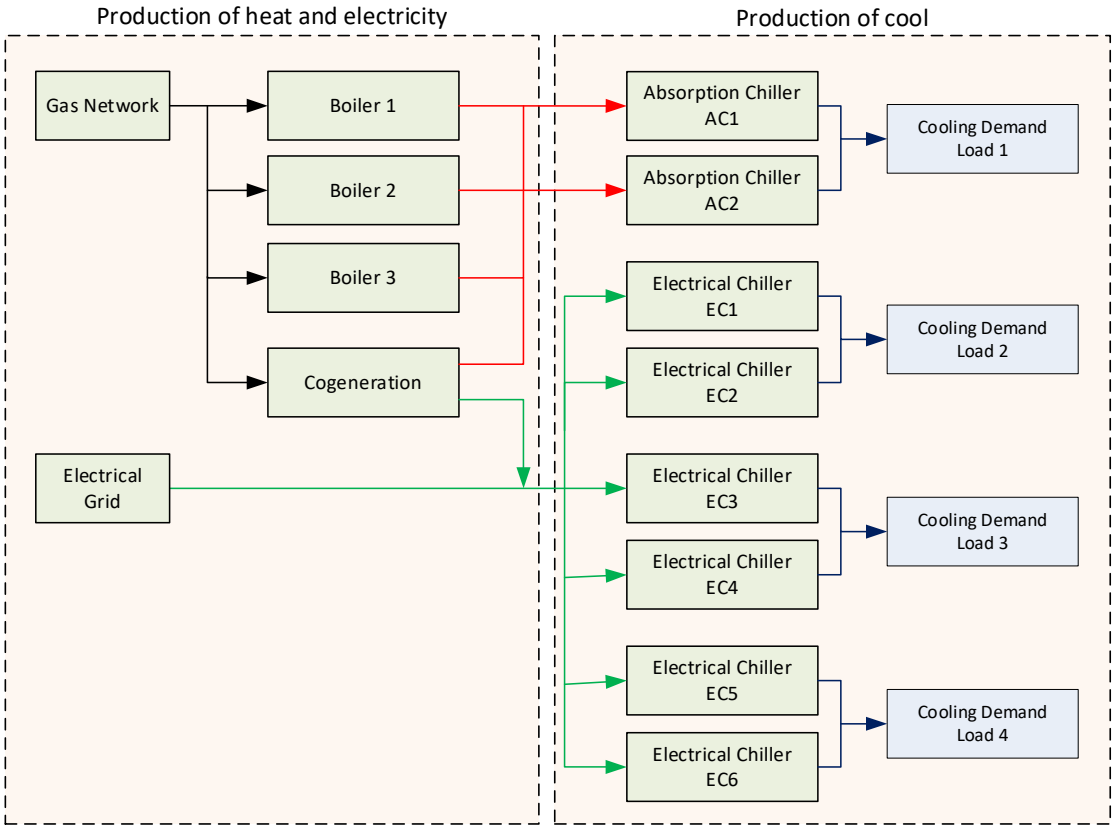

Figure 4.16: Energy production stages of the system.

Based on the mathematical formulation of the system, described in (2.34) to (2.39), the stage of the cooling production can be formulated as follows, where (4.25) describes the equality constraints of the problem, (4.26) to (4.27) the inequality constraints and (4.28) the operating bounds of the chillers.

$$\begin{bmatrix} L_{Load\,1,t}^{Cool} \\ L_{Load\,2,t}^{Cool} \\ L_{Load\,3,t}^{Cool} \\ L_{Load\,4,t}^{Cool} \end{bmatrix} = \begin{bmatrix} \eta_{AC1,t}^{h2c} & \eta_{AC2,t}^{h2c} & 0 & 0 & 0 & 0 & 0 & 0 \\ 0 & 0 & \eta_{EC1,t}^{e2c} & \eta_{EC2,t}^{e2c} & 0 & 0 & 0 & 0 \\ 0 & 0 & 0 & 0 & \eta_{EC3,t}^{e2c} & \eta_{EC4,t}^{e2c} & 0 & 0 \\ 0 & 0 & 0 & 0 & 0 & 0 & \eta_{EC5,t}^{e2c} & \eta_{EC6,t}^{e2c} \end{bmatrix} * \begin{bmatrix} P_{AC1,t}^{heat} \\ P_{AC2,t}^{heat} \\ P_{EC1,t}^{electricity} \\ P_{EC2,t}^{electricity} \\ P_{EC3,t}^{electricity} \\ P_{EC4,t}^{electricity} \\ P_{EC5,t}^{electricity} \\ P_{EC6,t}^{electricity} \end{bmatrix} \quad (4.25)$$

where the sum of the electric power consumption by the electric chillers cannot exceed the amount of available electric power that is provided by the grid and the maximum electric power that can be produced by the cogeneration equipment, minus the actual electric demand of the plant.

$$\sum_{i=1}^{6} P_{ECi,t}^{electricity} \leq P_{grid,t}^{in} + P_{CHP,t}^{electr_{\max}} - L_{total,t}^{electric} \quad (4.26)$$

Similarly, the amount of the heating energy that can be consumed by the absorption machines cannot exceed the amount of energy that can be produced by the cogeneration and the 3 boilers, minus the actual heating demand of the plant.

$$P_{AC1,t}^{heat} + P_{AC2,t}^{heat} \leq P_{gas,t}^{in_{\max}} \cdot (\eta_{boiler1,t}^{g2t} + \eta_{boiler2,t}^{g2t} + \eta_{boiler3,t}^{g2t} + \eta_{CHP,t}^{g2t}) - L_{total,t}^{heat} \quad (4.27)$$

Finally, the operating bounds of the equipment can vary between their minimum and maximum production levels, or if were the case, between the updated production limits, affected by the inertias of the equipment.

$$\begin{bmatrix} L_{AC1,t}^{\min} \\ L_{AC2,t}^{\min} \\ L_{EC1,t}^{\min} \\ L_{EC2,t}^{\min} \\ L_{EC3,t}^{\min} \\ L_{EC4,t}^{\min} \\ L_{EC5,t}^{\min} \\ L_{EC6,t}^{\min} \end{bmatrix} \leq \begin{bmatrix} P_{total,t}^{heat} \cdot \eta_{boiler1,t}^{g2t} \cdot v_1 \\ P_{total,t}^{heat} \cdot \eta_{boiler2,t}^{g2t} \cdot v_2 \\ P_{total,t}^{electricity} \cdot \eta_{EC1,t}^{e2c} \cdot v_3 \\ P_{total,t}^{electricity} \cdot \eta_{EC2,t}^{e2c} \cdot v_4 \\ P_{total,t}^{electricity} \cdot \eta_{EC3,t}^{e2c} \cdot v_5 \\ P_{total,t}^{electricity} \cdot \eta_{EC4,t}^{e2c} \cdot v_6 \\ P_{total,t}^{electricity} \cdot \eta_{EC5,t}^{e2c} \cdot v_7 \\ P_{total,t}^{electricity} \cdot \eta_{EC6,t}^{e2c} \cdot v_8 \end{bmatrix} \leq \begin{bmatrix} L_{AC1,t}^{\max} \\ L_{AC2,t}^{\max} \\ L_{EC1,t}^{\max} \\ L_{EC2,t}^{\max} \\ L_{EC3,t}^{\max} \\ L_{EC4,t}^{\max} \\ L_{EC5,t}^{\max} \\ L_{EC6,t}^{\max} \end{bmatrix} \quad (4.28)$$

Figure 4.17 presents the descending-order profile of the cooling demands, which indicates the evaluation order of the optimization algorithm.

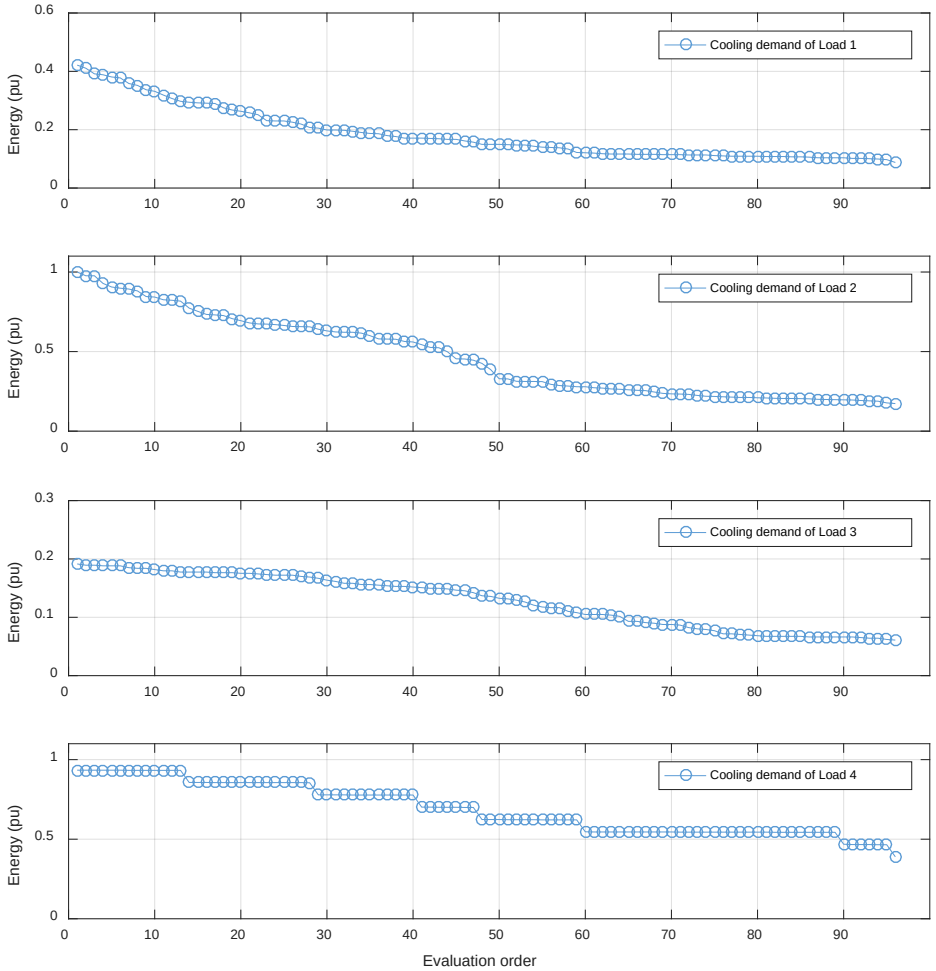

Figure 4.17: Evaluation order of the cooling demands.

As a result of the evaluation of the optimization criteria (described in (4.9)) for the entire demand profile, the following figure summarizes the fitness values of each criterion in quartiles, as well as their variability during the evaluated operating strategies.

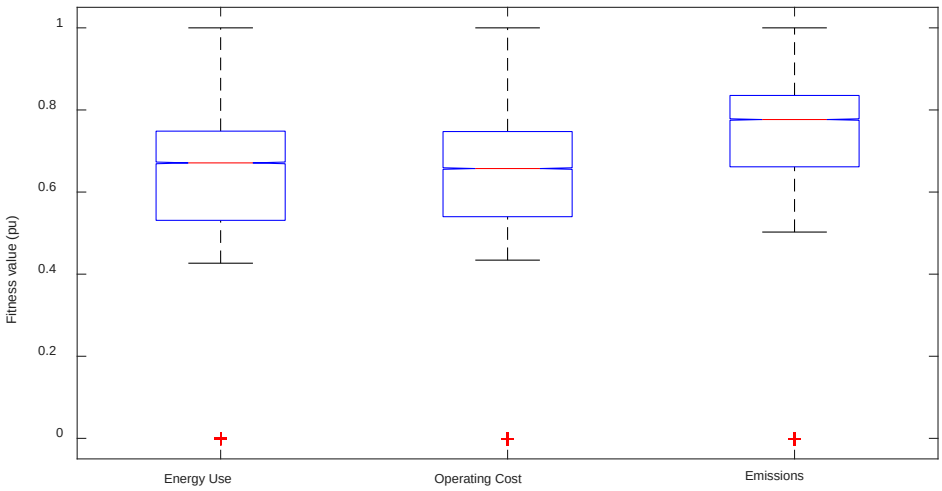

Figure 4.18: Comparison between cooling demand and production of the 4 loads.

Figure 4.19 presents a comparison between the demand profiles and the energy production of the absorption and electric chillers. Additionally, Figure 4.20 depicts the fitness results that were obtained by evaluating different combination of the criteria, applying similar weights.

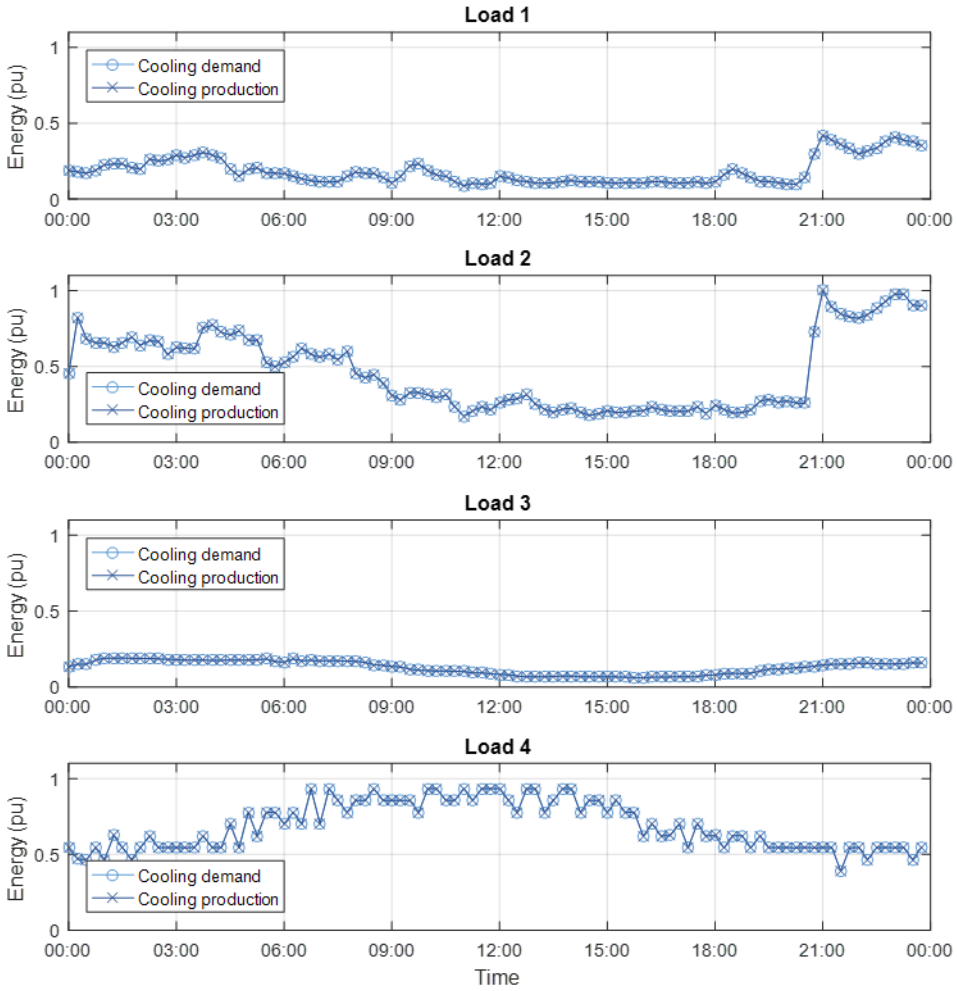

Figure 4.19: Comparison between cooling demand and production of the 4 loads.

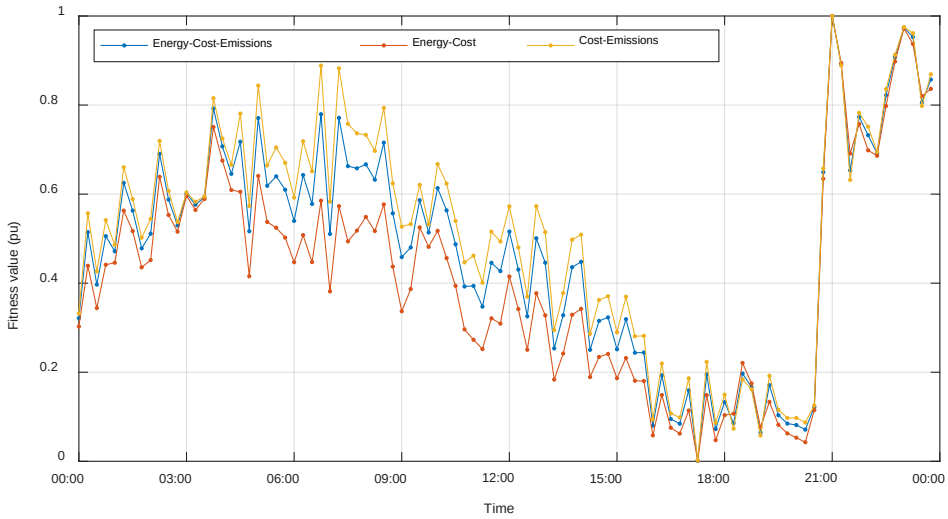

Figure 4.20: Fitness values of the optimization of the cooling process, applying different criteria combinations.

From the point of view of the chillers' production, Figure 4.21 to Figure 4.24 present the equipment's operations that result to the satisfaction of the cooling demands of load 1 to load 4, respectively.

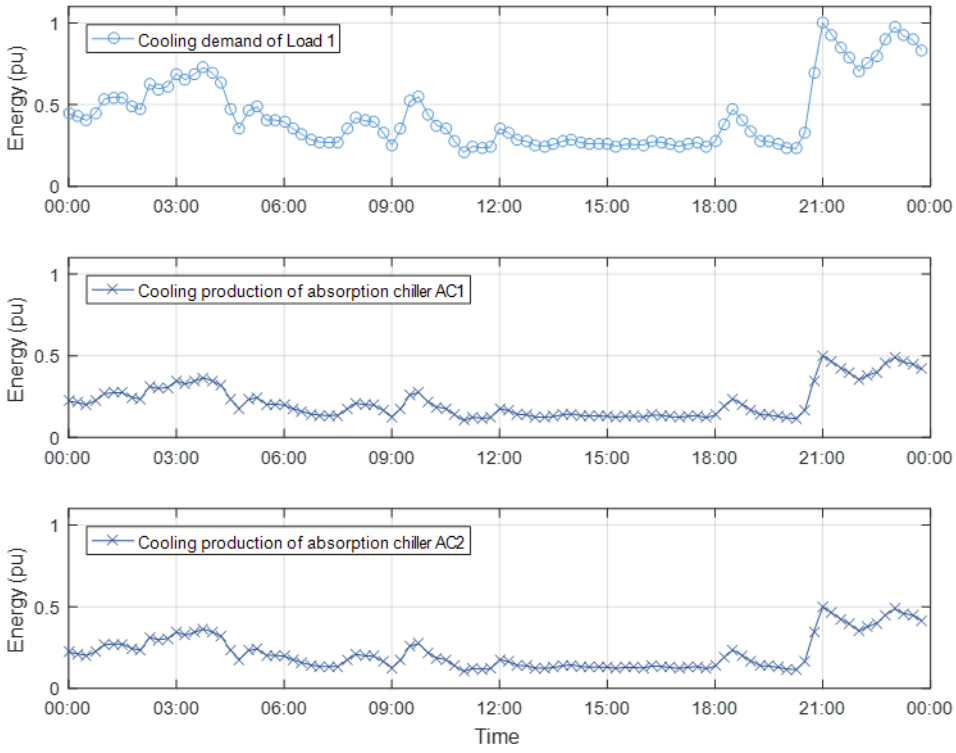

Figure 4.21: Comparison between the cooling demand of Load 1 and the production profiles of the absorption chillers.

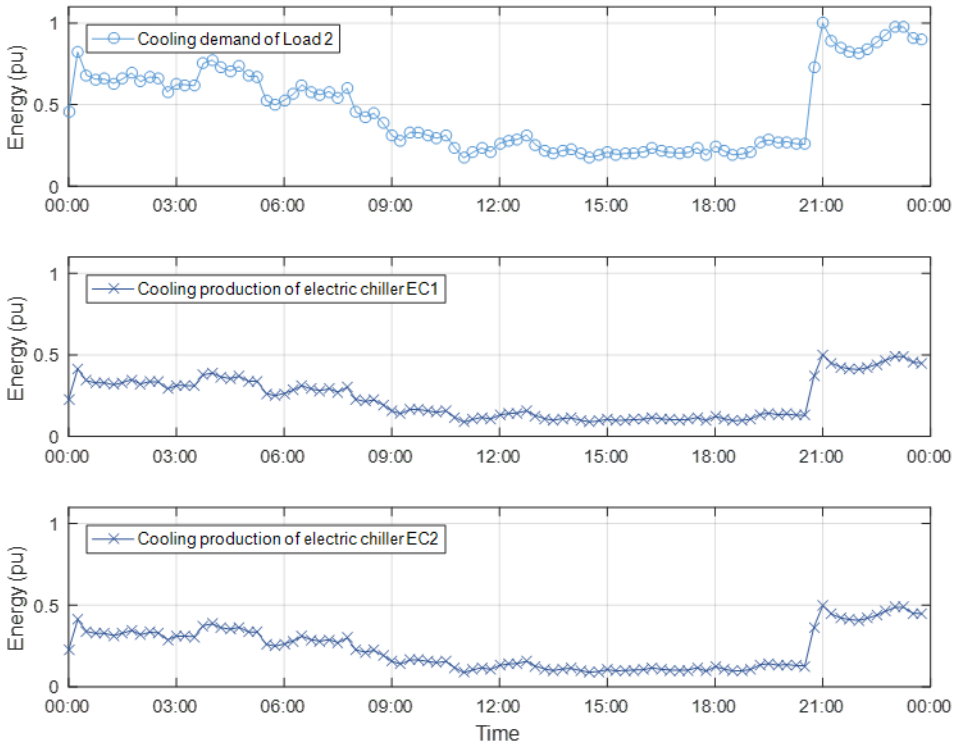

Figure 4.22: Comparison between the cooling demand of Load 2 and the production profiles of the electric chillers EC1 and EC2.

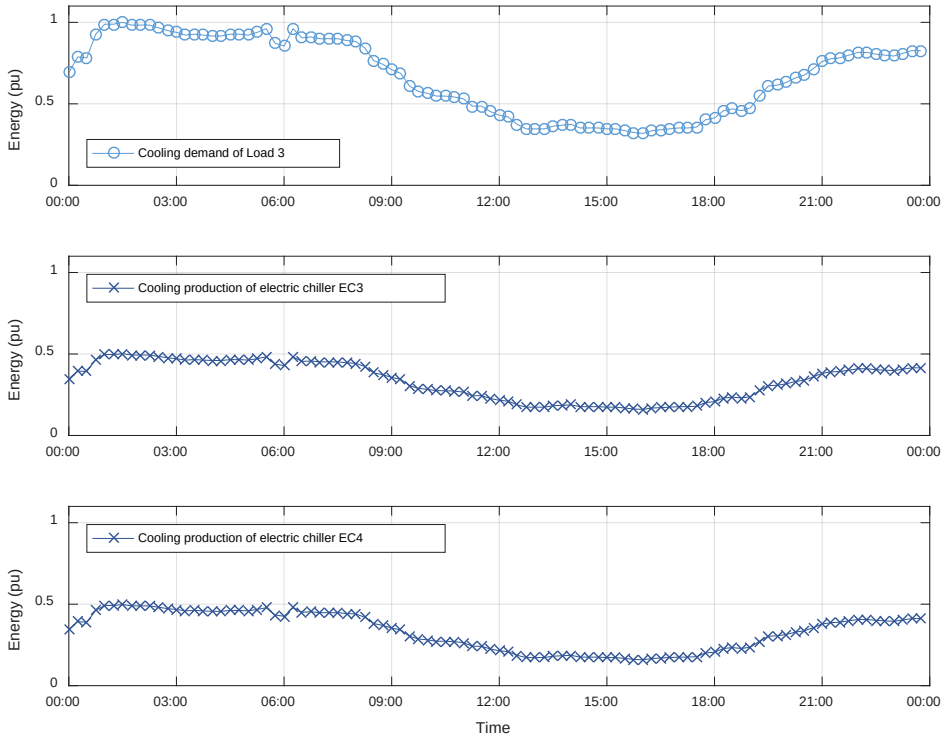

Figure 4.23: Comparison between the cooling demand of Load 3 and the production profiles of the electric chillers EC3 and EC4.

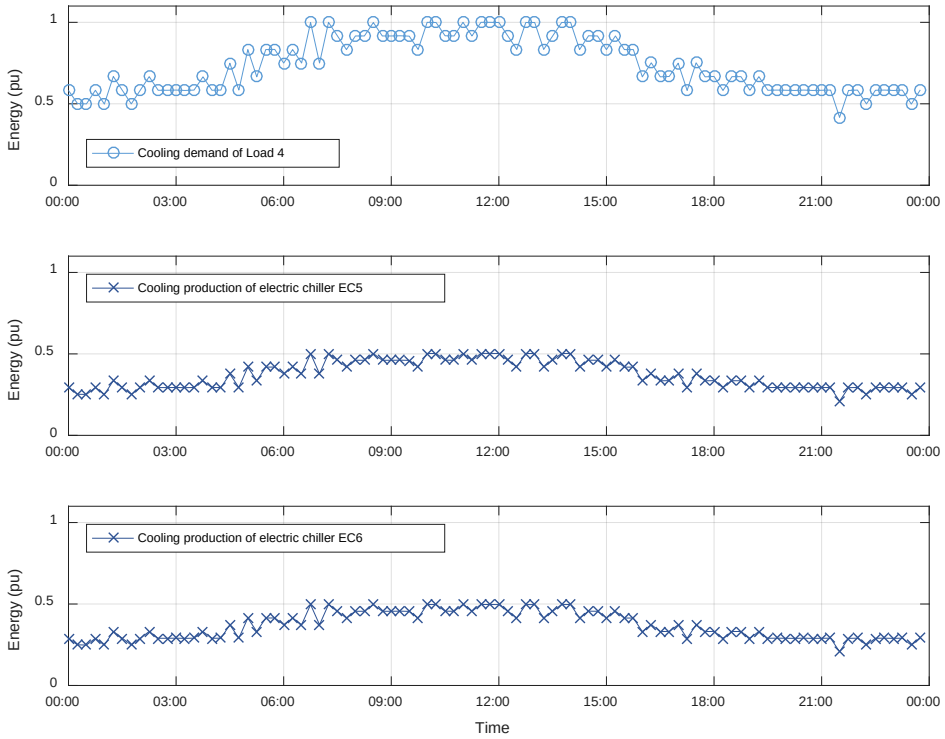

Figure 4.24: Comparison between the cooling demand of Load 4 and the production profiles of the electric chillers EC5 and EC6.

In terms of energy use for the operation of the absorption and electric chillers, Figure 4.25 depicts the heating and electricity amounts that were consumed by each equipment at the different time instants.

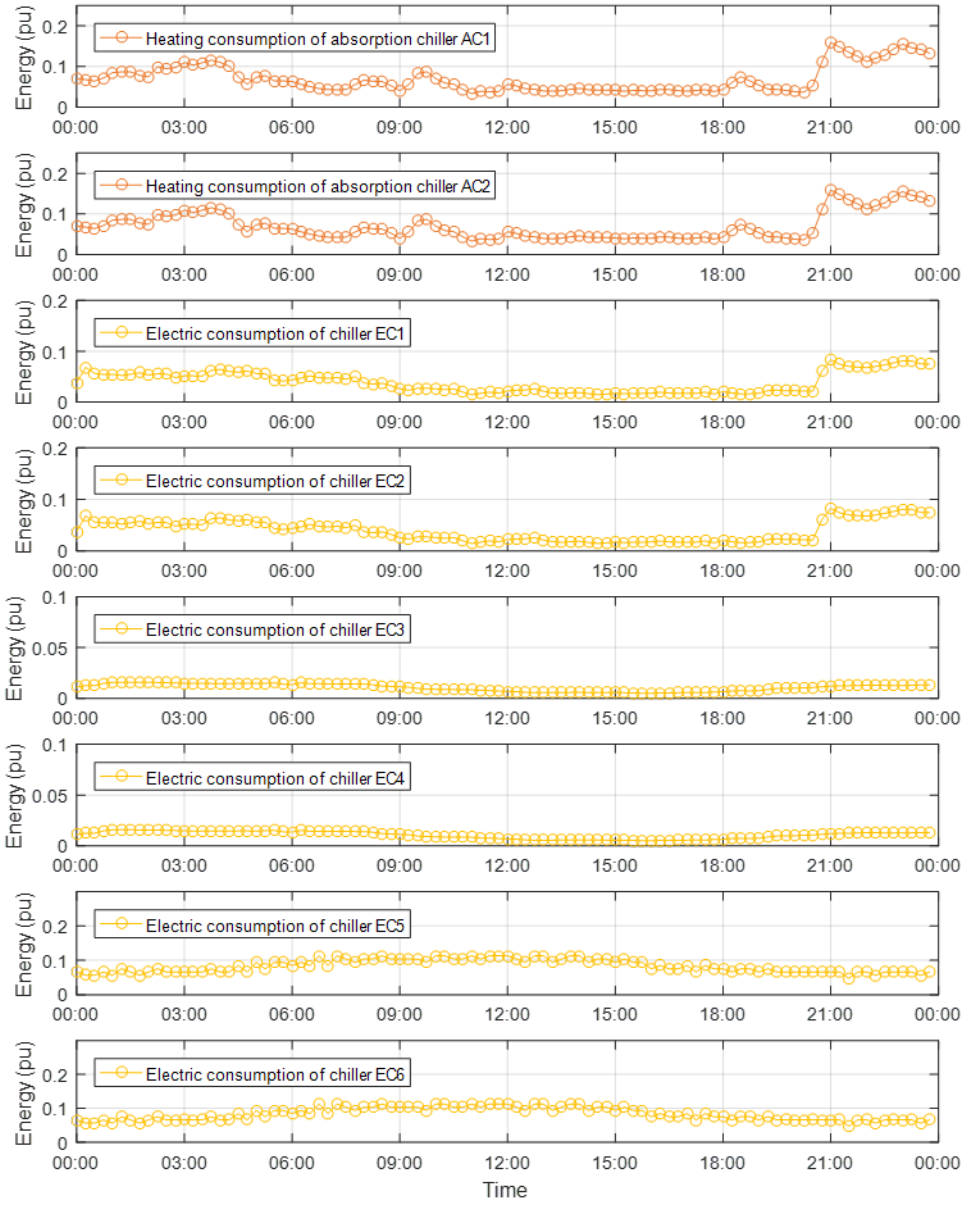

Figure 4.25: Heating and electric consumption of the chillers.

Figure 4.26 presents a comparison between the real operation of the chiller equipment and the optimized one, expressed in terms of total energy production. As it can be observed in the figure, the operation of the equipment in both cases is almost the same. This could explained due to the fact that all of the four chiller groups consist of 2 identical equipment of the same technical characteristics. Thus, any modification of the energy production proportions of the equipment would result to the same fitness values.

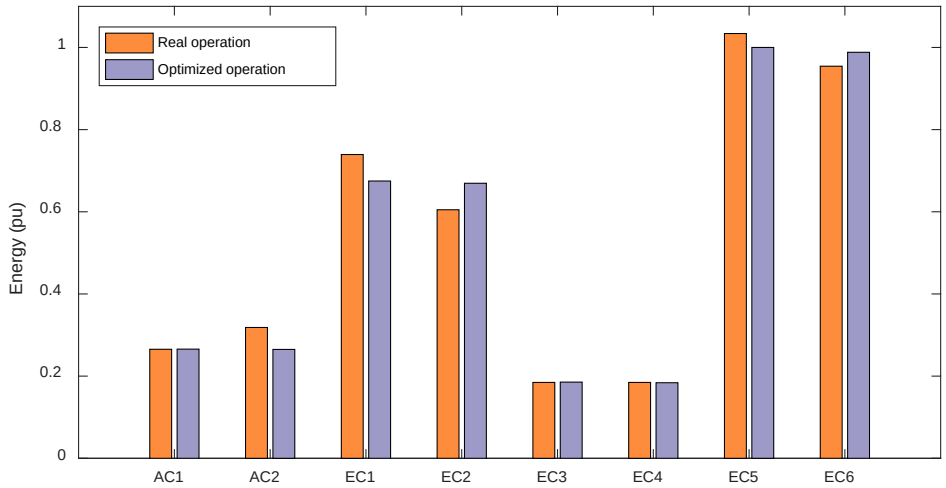

Figure 4.26: Total energy production of chiller equipment. Comparison between real and optimized operation.

Finally, Figure 4.27 presents the total amount of electric and heating energy that is required for the cooling production. The values are depicted in per-units and are referred to the range of the actual electric and heating demand profiles.

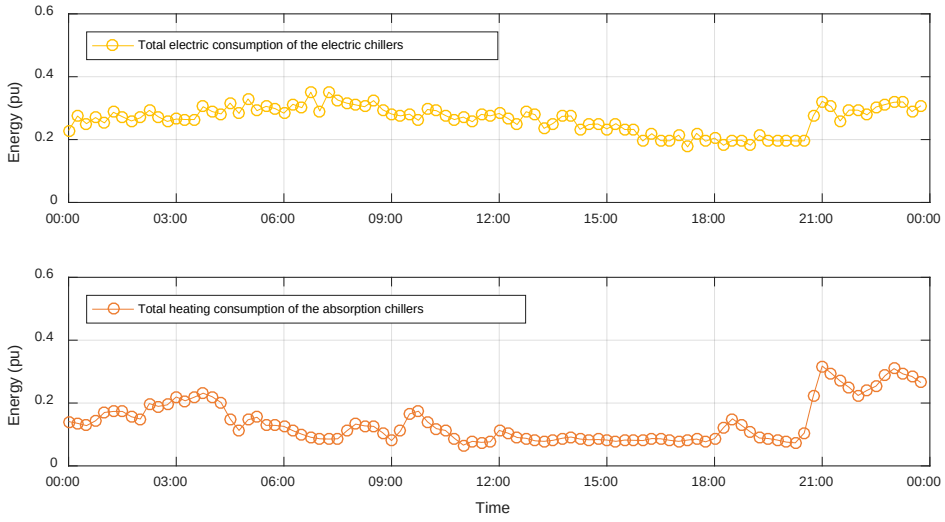

Figure 4.27: Total energy consumption of the chillers.

Based on the calculated energy requirements for the cooling production, the new demand vectors of heat and electricity are updated, including the necessary energy for the operation of the chillers. The new demand vectors are depicted in Figure 4.28, which are compared with the initial demand profiles, presented in Figure 4.15.

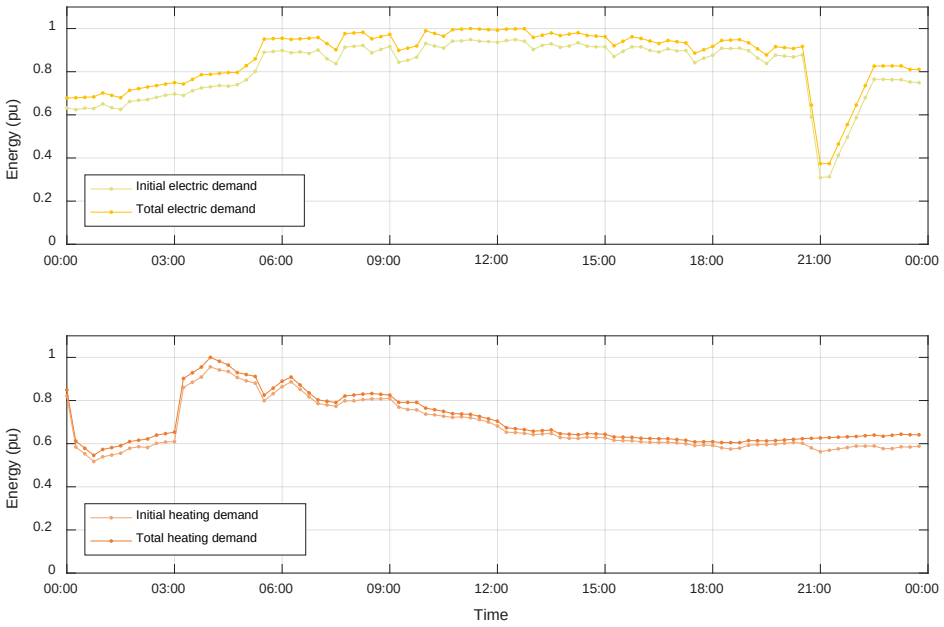

Figure 4.28: Comparison between the initial demand profiles and the updated ones, for the case of electricity and heat.

Then, the optimization process is executed for the electricity and heating production stage of the system (Figure 4.16), evaluating every time instant in descending order, based on the peaks of the heating vector (Figure 4.29).

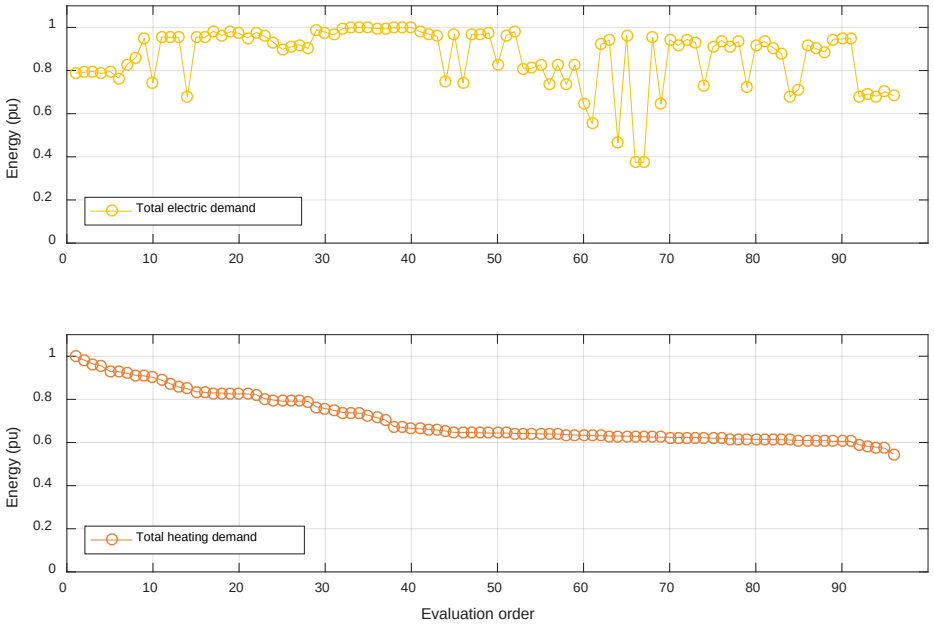

Figure 4.29: Evaluation order of the electric and heating demands.

As the operation of the boilers is scalar (due to the existing control system that is implemented in the plant), the GA uses a discrete codified variable *d* to define their operation status. This variable, as shown in (4.31), takes integer values between 0 and 4, which corresponds to an available produced output of the equipment (i.e. 0%, 25%, 50%, 75% and 100% respectively). Of course, more accuracy can be obtained by a finer discretization, but calculation burden is incremented. Equations (4.29)-(4.30) express the mathematical formulation of the available energy carriers (equality constraints) for the production of electricity and heat.

$$L_{elec} = P_{grid}^{in,elec} + P_{CHP}^{in,gas} \cdot \eta_{CHP}^{g2e} \tag{4.29}$$

$$L_{heat} = P_{CHP}^{in,gas} \cdot C_{CHP}^{heat} + P_{Boiler1}^{in,gas} \cdot C_{Boiler1}^{heat}(d_1) + P_{Boiler2}^{in,gas} \cdot C_{Boiler2}^{heat}(d_2) + P_{Boiler3}^{in,gas} \cdot C_{Boiler3}^{heat}(d_3) \tag{4.30}$$

where

$$d_j \in N \text{ I } [0,4] \tag{4.31}$$

Figure 4.30 presents the fitness results that were obtained by evaluating different combination of the criteria, applying similar weights.

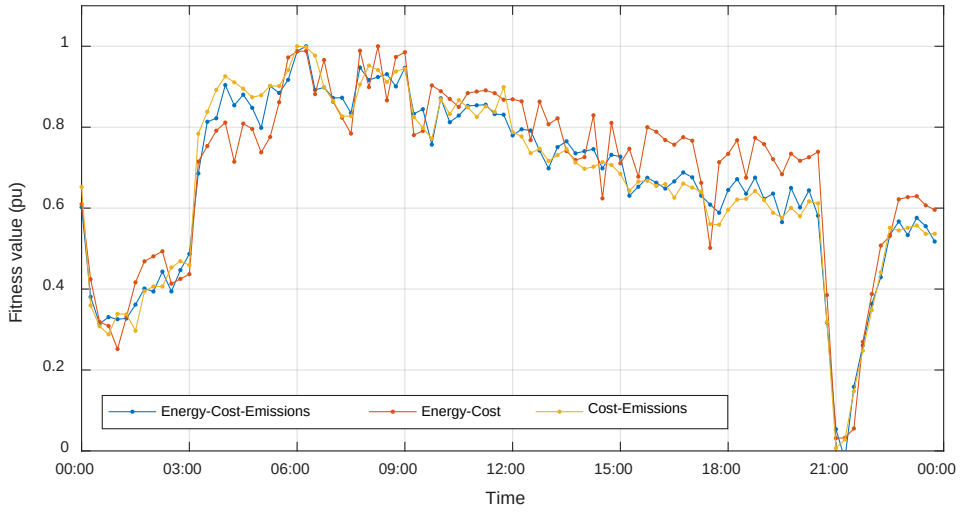

Figure 4.30: Fitness values of the optimization, applying different criteria combinations.

Figure 4.31 presents the operation profiles of the real operation strategy of the system, as well as the optimized one, that was calculated by the algorithm, for the whole optimization horizon of 24 hours by considering all of the criteria.

Furthermore, a comparison between the optimal operation of the plant and the conventional one is shown in Figure 4.32, indicating the energy amounts of electricity and gas, as well as the total energy production per equipment for the evaluated period of 24 hours.

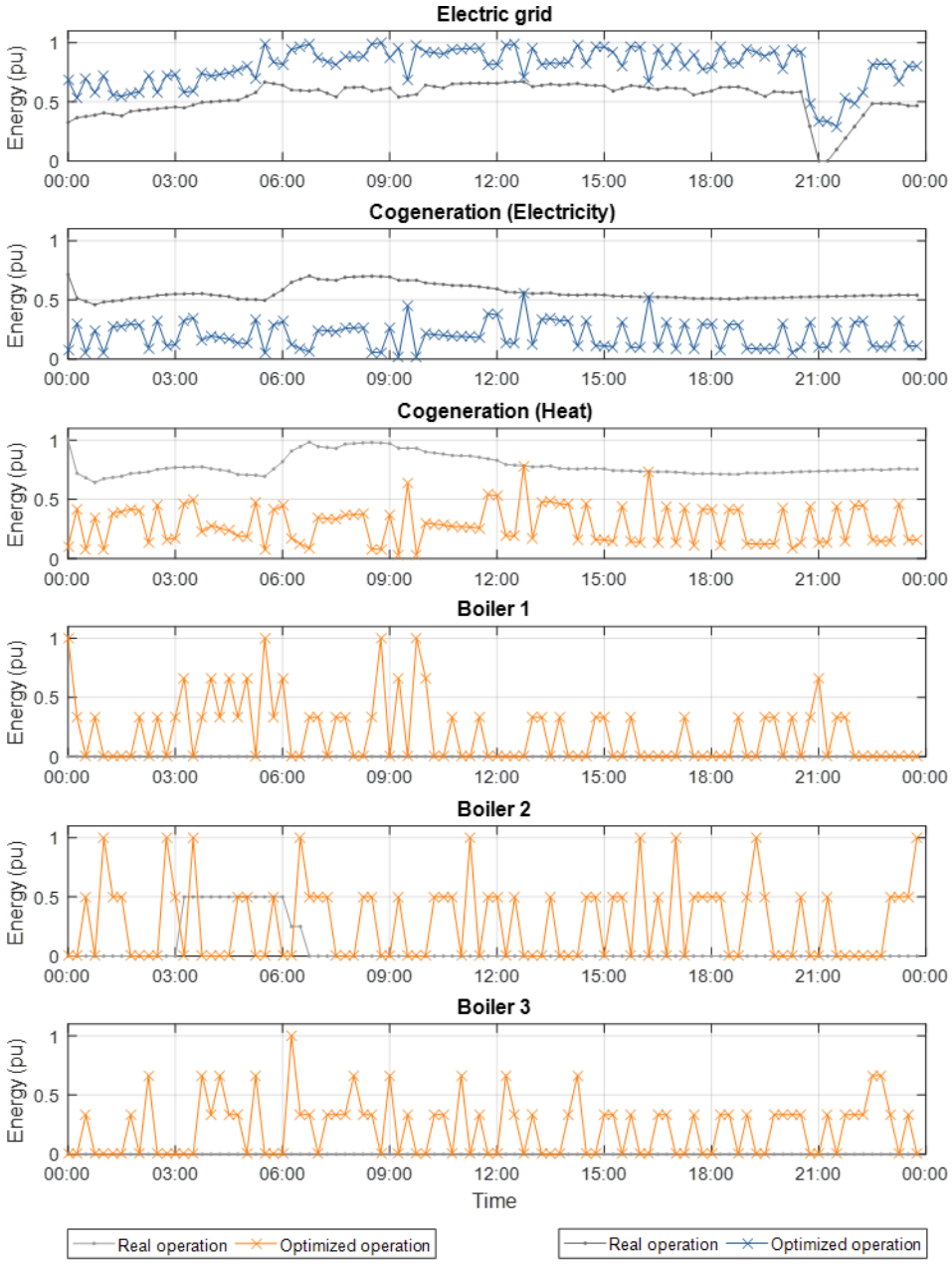

Figure 4.31: Energy production per equipment.

It can be observed that the conventional operation strategy of the multi-carrier plant gives operation priority to the cogeneration equipment for the satisfaction of the heating demand (and partially the electric one), minimizing the use of the boilers and the grid´s electric supply. However, the algorithm's solution presents a homogeneous distribution of effort between the equipment, reducing the consumption of natural gas. This occurs because of the higher performance value of the boilers in comparison to the cogeneration, which results in reduced

amount of primary energy use for the fulfillment of the heating demand. Nevertheless, the consequence is the increment of the electric supply by the grid in order to satisfy the electric demand as well. This operation strategy may vary by considering different weight of the optimization criteria, or in cases in which the system has different price rates for the energy through the day.

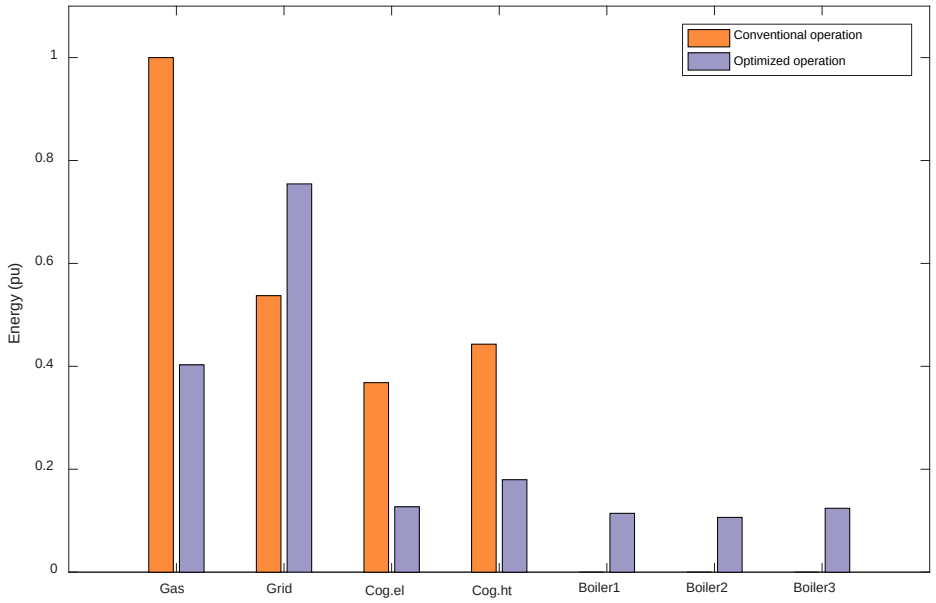

Figure 4.32: Comparison of total energy use and production between conventional and optimized operation.

Finally, Figure 4.33 shows a comparison of the optimized results between the two operations. It can be observed that the optimized operation of the system presents a minimization of the energy use by 33%, a 22.7% of operating cost savings, and a 60.2% of CO2 emissions reduction.

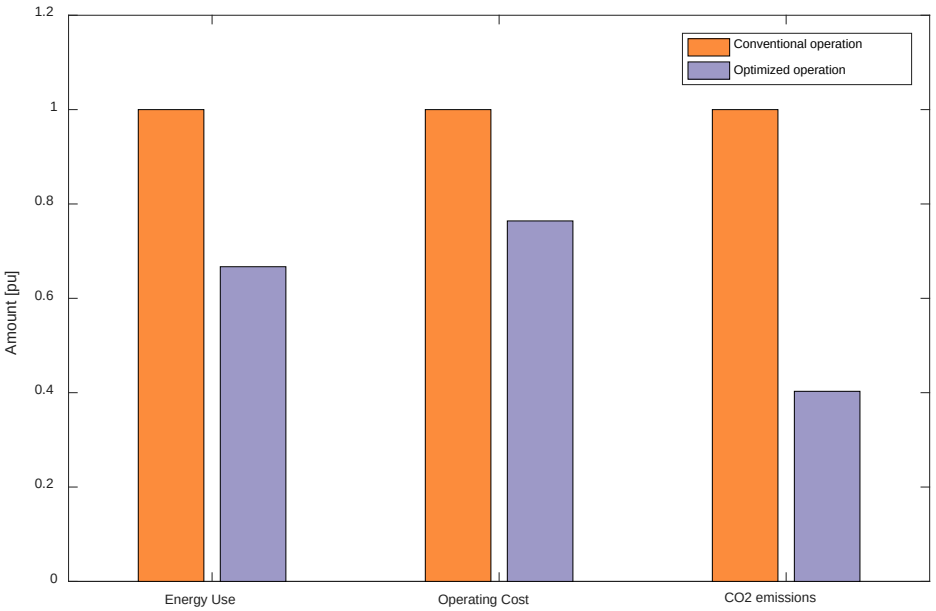

Figure 4.33: Comparison of total energy use and production between conventional and optimized operation.

It is worth to mention the presented comparisons have been done by using as a reference a well hand-optimized plant, which is operated by maintenance experts with years of experience in energy optimization. Therefore, these improved values can be considered as excellent results for the demonstration of the advantages of the proposed methodology.

The following subsections present the results of the long term validation analysis of the proposed methodology for the three 3 months period, as described in Table XI.

4.5.3 Validation period – January 2015

Figure 4.34 presents the energy demand profiles of electricity and heat for all the validation period of January 2015. The consumption data reach a total of several tens of GWh/month for both the cases of electric and heating demand. Due to their confidentiality, their energy values, as well as their costs and emissions are represented in per-unit values, **referenced to the total heating demand value of the month**.

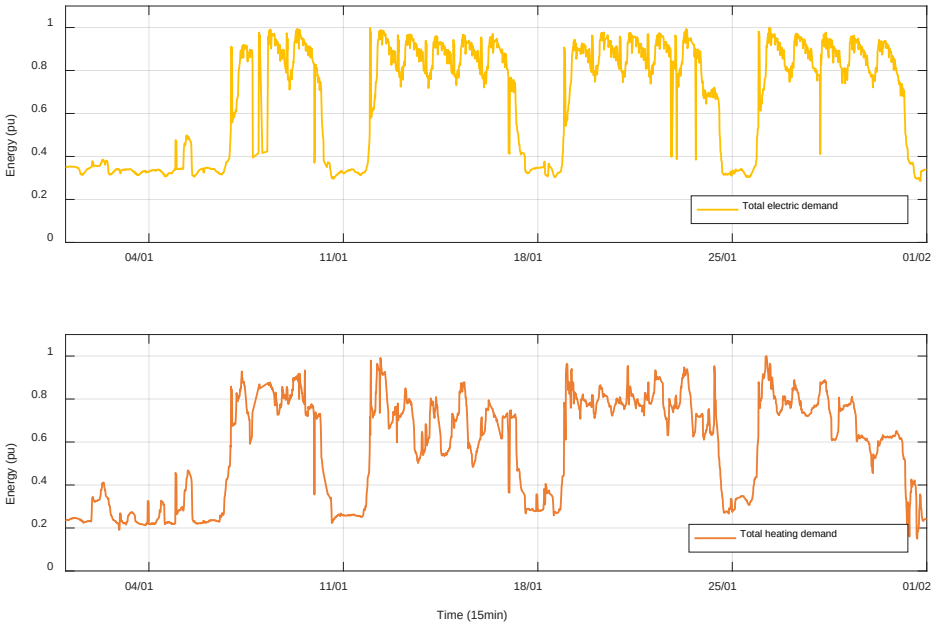

Figure 4.34: Energy demand profiles of the validation plant: 01 – 31 Jan. 2015.

Table XII. Total energy demands of the plant: 01 – 31 Jan. 2015.

DEMAND	ENERGY (PU)
Total electric demand	*0.9698*
Total heating demand	*1*

The following sections present the obtained results by operating the optimization algorithm with different criteria. A comparison between the real operation and the optimized one is presented, indicating the differences in term of costs, primary energy sources and CO2 emissions.

4.5.3.1 Minimization of the primary energy use and the CO_2 emissions

This section presents the results of the optimization algorithm, focused only on the minimization of the primary energy use and the minimization of the generation of CO2 emissions. The primary energy sources of the plant are: electricity supplied by the grid and natural gas supplied by the network.

The following figure presents a comparison between the real operation of the plant and the optimized strategy that was obtained by the optimization algorithm.

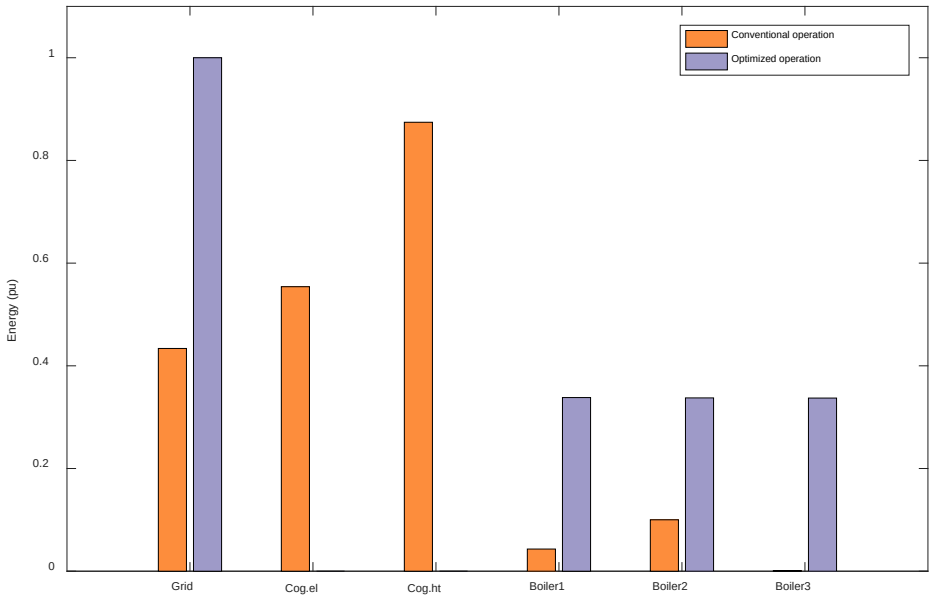

Figure 4.35: Total energy production: Jan. 2015 – Minimization of PES and CO_2.

The following table presents the numeric values of the energy production equipment, as well as the use of electricity from the grid, which are depicted in Figure 4.32.

Table XIII. Total energy production: Jan. 2015 - Minimization of PES use and CO_2.

Operation	Electricity (pu)		Heat (pu)			
	Grid	Cog.el	Cog.ht	Boiler 1	Boiler 2	Boiler 3
Real	*0.4259*	*0.5439*	*0.8584*	*0.0424*	*0.0983*	*0.0009*
Optimized	*0.9698*	*0*	*0*	*0.3340*	*0.3332*	*0.3328*

The following table presents the amount of primary energy sources that was used for the operation of the energy production equipment. Furthermore, the table contains the approximate resulting costs of the energy sources, as well as the difference of the energy use between the real operation of the plant and the optimized one.

Table XIV. Use of primary energies: Jan. 2015 - Minimization of pes use and co_2.

Operation	Energy Use (pu)		Total Costs (pu)		Energy Difference (pu)	
	Electricity	Gas	Electricity	Gas	Electricity	Gas
Real	*0.4259*	*2.3310*	*0.4842*	*0.2028*	*-0.5439*	*0.9120*
Optimized	*0.9698*	*1.4190*	*1.1027*	*0.1235*		

As it can be observed by the analysis of the data, by operating the plant with the recommendations of the optimization algorithm, it would result to an approximate energy savings of 0.3681 pu. This occurs due to the algorithm focuses on the operation of the boilers which present a higher COP than the cogeneration, satisfying the electric demand by using electricity supplied by the grid.

$$energy\ savings = -0.5439 + 0.9120 = 0.3681\ pu \tag{4.32}$$

Finally, the following figure present a comparison of the primary energy use, the total energy costs and the total CO2 emissions between the real operation and the optimized one, presented in Table XV. Due to the difference on the parameters' units, all the values have been normalized for their better representation.

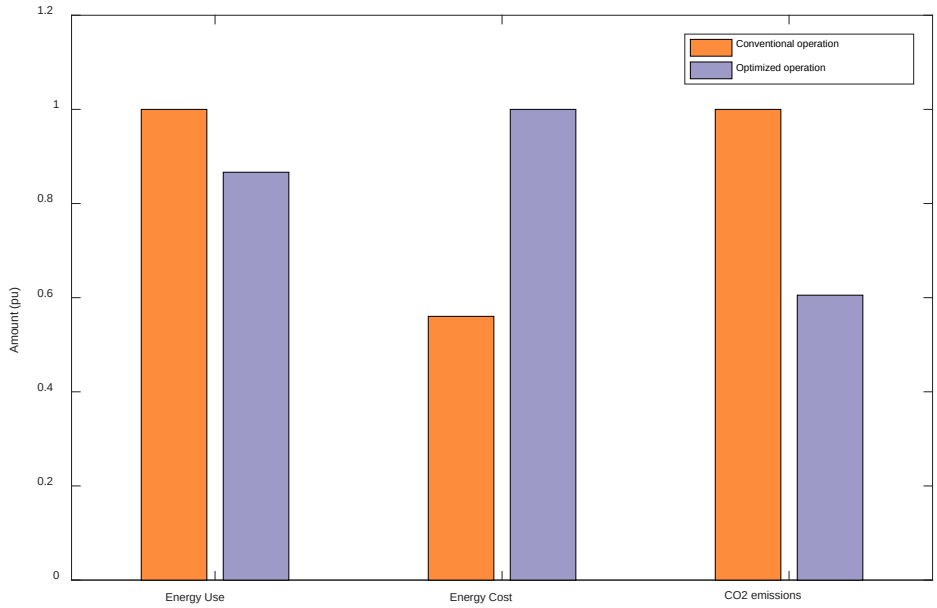

Figure 4.36: Optimization criteria: Jan. 2015 – Minimization of PES and CO_2.

Table XV. Optimization criteria: Jan. 2015 – Minimization of PES and CO_2.

Operation	Energy (pu)	Energy Cost (pu)	Emissions (pu)
Conventional operat.	*2.7569*	*0.6870*	*0.5874*
Optimized operation	*2.3888*	*1.2261*	*0.3576*

Based on the results, the savings of CO_2 emissions would be approximately 0.2298 pu.

$$CO_2\ savings = \ 0.5874 - 0.3576 = 0.2298\ pu \tag{4.33}$$

The total energy savings percentage of the algorithm would result to:

$$energy\ savings\ \% = \left(\frac{0.3681}{2.7569}\right) * 100 = 13{,}35\% \tag{4.34}$$

4.5.3.2 Minimization of the primary energy use, costs and CO_2 emissions

This section presents the results of the optimization algorithm, focused on the minimization of the primary energy use, the cost of the primary energies and the minimization of the CO2 emissions, referred in the following tables and figures as “minimization of 3 objectives”. The following figure presents a comparison between the real operation of the plant and the optimized strategy that was obtained by the optimization algorithm.

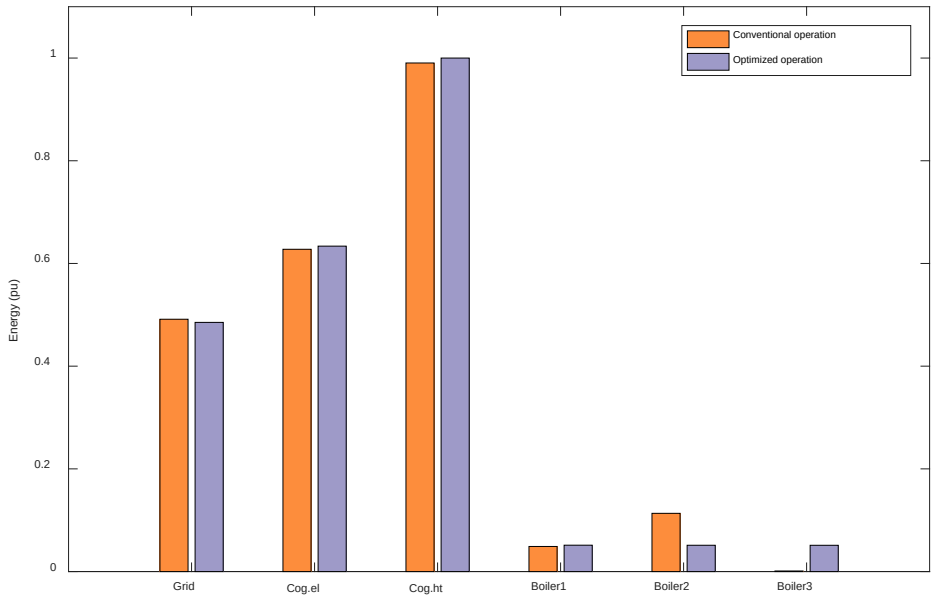

Figure 4.37: Total energy production: Jan. 2015 – Minimization of 3 objectives.

The following table presents the numeric values of the energy production equipment, as well as the use of electricity from the grid, which are depicted in Figure 4.37.

Table XVI. Total energy production: Jan. 2015 - Minimization of 3 objectives.

Operation	Electricity (pu)		Heat (pu)			
	Grid	Cog.el	Cog.ht	Boiler 1	Boiler 2	Boiler 3
Real	*0.4259*	*0.5439*	*0.8584*	*0.0424*	*0.0983*	*0.0009*
Optimized	*0.4206*	*0.5493*	*0.8667*	*0.0445*	*0.0444*	*0.0444*

The following table presents the amount of primary energy sources that was used for the operation of the energy production equipment, or used directly for the fulfillment of the energy demands (case of electricity). Furthermore, the table contains the approximate resulting costs of the energy sources, as well as the difference between the real operation of the plant and the optimized one.

Table XVII. Use of primary energies: Jan. 2015 - Minimization of 3 objectives.

Operation	Energy Use (pu)		Total Costs (pu)		Energy Difference (pu)	
	Electricity	Gas	Electricity	Gas	Electricity	Gas
Real	*0.4259*	*2.3310*	*0.4842*	*0.2028*	*0.0060*	*-0.0022*
Optimized	*0.4206*	*2.3559*	*0.4782*	*0.2050*		

As it can be observed by the analysis of the data, by operating the plant with the recommendations of the optimization algorithm, it would result to an approximate cost savings of 0.0039 pu. This occurs due to the algorithm takes into consideration also the prices of the primary energy sources. Therefore, it focuses on the operation of the cogeneration to its maximum point, due to the lower price of the natural gas. Furthermore, the operation priority is focused on the cogeneration because of its parallel generation of heat and electricity, which offers an additional energy and monetary saving, by reducing the grid's electric energy as well as its equivalent cost.

Finally, the following figure present a comparison of the primary energy use, the total energy costs and the total CO2 emissions between the real operation and the optimized one, presented in Table XXXV. Due to the difference on the parameters' units, all the values have been normalized for their better representation.

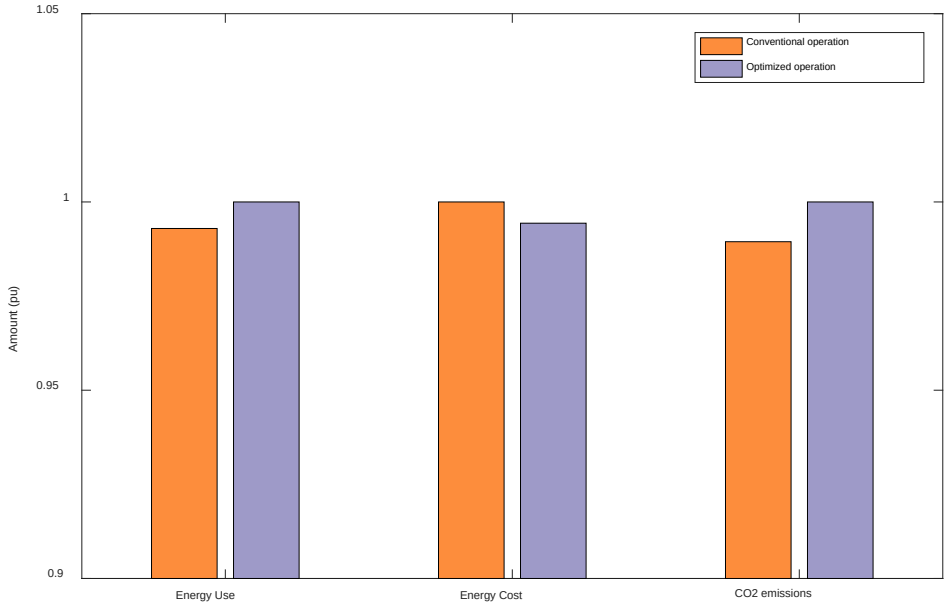

Figure 4.38: Optimization criteria: Jan. 2015 – Minimization of 3 objectives.

Table XVIII. Optimization criteria: Jan. 2015 – Minimization of 3 objectives.

Operation	Energy (pu)	Energy Cost (pu)	Emissions (pu)
Conventional operat.	*2.7569*	*0.6870*	*0.5874*
Optimized operation	*2.7764*	*0.6831*	*0.5937*

It has to be mentioned that by modifying the weighted factors of the optimization criteria by giving more importance to the desired ones, the obtained results will change.

4.5.4 Validation period – February 2015

Figure 4.44 presents the energy demand profiles of the electricity and heat for all the period of February 2015. All the below values are represented in per-units, **referenced to the total heating demand value of the month**.

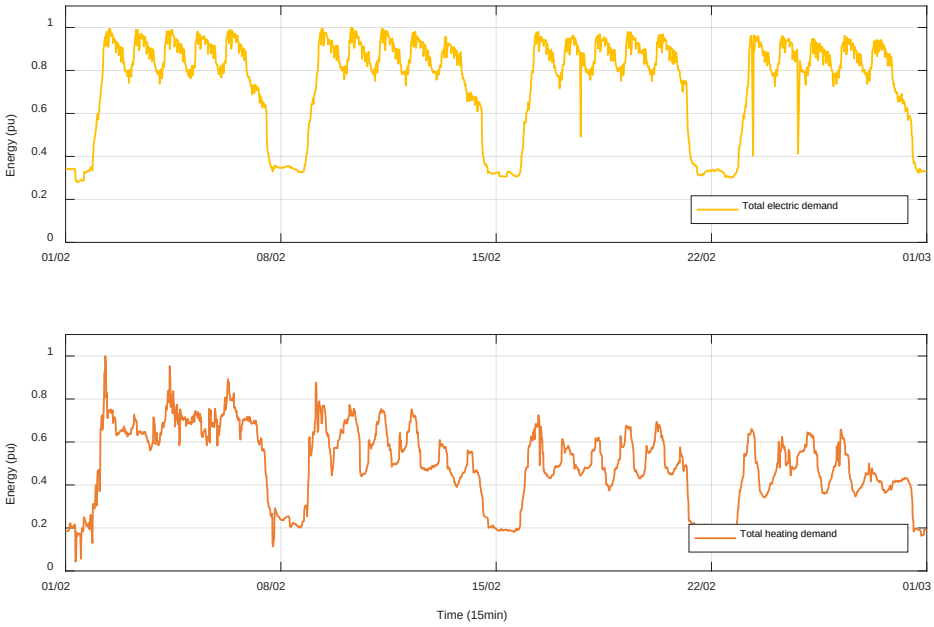

Figure 4.39: Energy demand profiles of the validation plant: 01 – 28 Feb. 2015.

Table XIX. Total energy demands of the plant: 01 – 31 Jan. 2015.

DEMAND	ENERGY (PU)
Total electric demand	*0.9873*
Total heating demand	*1*

The following sections present the obtained results by operating the optimization algorithm with different criteria. A comparison between the real operation and the optimized one is presented, indicating the differences in term of costs, primary energy sources and CO2 emissions.

4.5.4.1 Minimization of the primary energy use and the CO_2 emissions

This section presents the results of the optimization algorithm, focused only on the minimization of the primary energy use and the minimization of the generation of CO2 emissions. The following figure presents a comparison between the real operation of the plant and the optimized strategy that was obtained by the optimization algorithm.

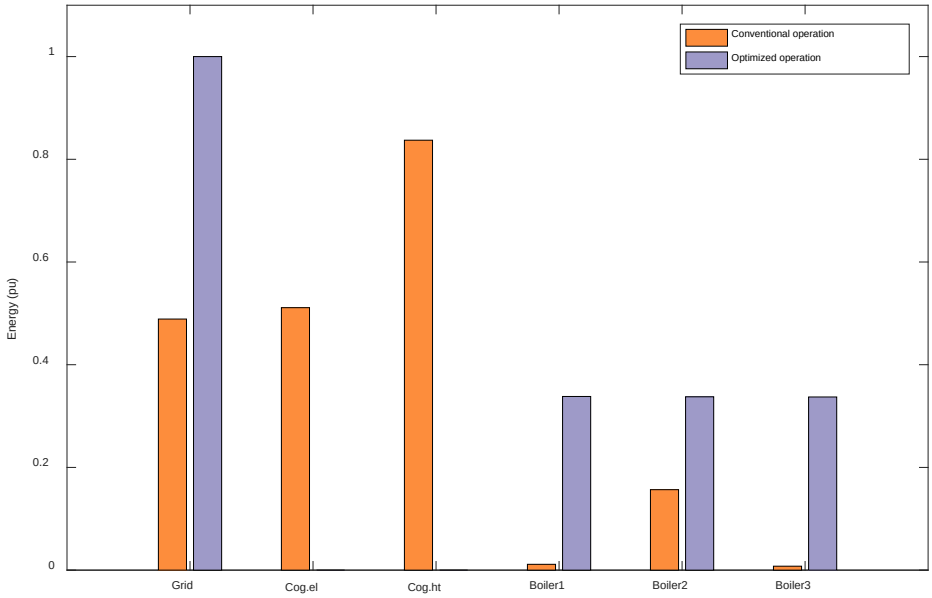

Figure 4.40: Total energy production: Feb. 2015 – Minimization of PES and CO_2.

The following table presents the numeric values of the energy production equipment, as well as the use of electricity from the grid, which are depicted in Figure 4.40.

Table XX. Total energy production: Feb. 2015 - Minimization of PES use and CO_2.

Operation	Electricity (pu)		Heat (pu)			
	Grid	Cog.el	Cog.ht	Boiler 1	Boiler 2	Boiler 3
Real	*0.4827*	*0.5046*	*0.8265*	*0.0112*	*0.1547*	*0.0076*
Optimized	*0.9873*	*0*	*0*	*0.3339*	*0.3332*	*0.3329*

The following table presents the amount of primary energy sources that was used for the operation of the energy production equipment. Furthermore, the table contains the approximate resulting costs of the energy sources, as well as the difference of the energy use between the real operation of the plant and the optimized one.

Table XXI. Use of primary energies: Feb. 2015 - Minimization of pes use and co_2.

Operation	Energy Use (pu)		Total Costs (pu)		Energy Difference (pu)	
	Electricity	Gas	Electricity	Gas	Electricity	Gas

Real	*0.4827*	*2.3379*	*0.5488*	*0.2034*	*-0.5046*	*0.9189*
Optimized	*0.9873*	*1.4190*	*1.1225*	*0.1235*		

As it can be observed by the analysis of the data, by operating the plant with the recommendations of the optimization algorithm, it would result to an approximate energy savings of 0.4143 pu.

$$energy\ savings = -0.5046 + 0.9189 = 0.4143\ pu \tag{4.35}$$

The following figure present a comparison of the primary energy use, the total energy costs and the total CO2 emissions between the real operation and the optimized one.

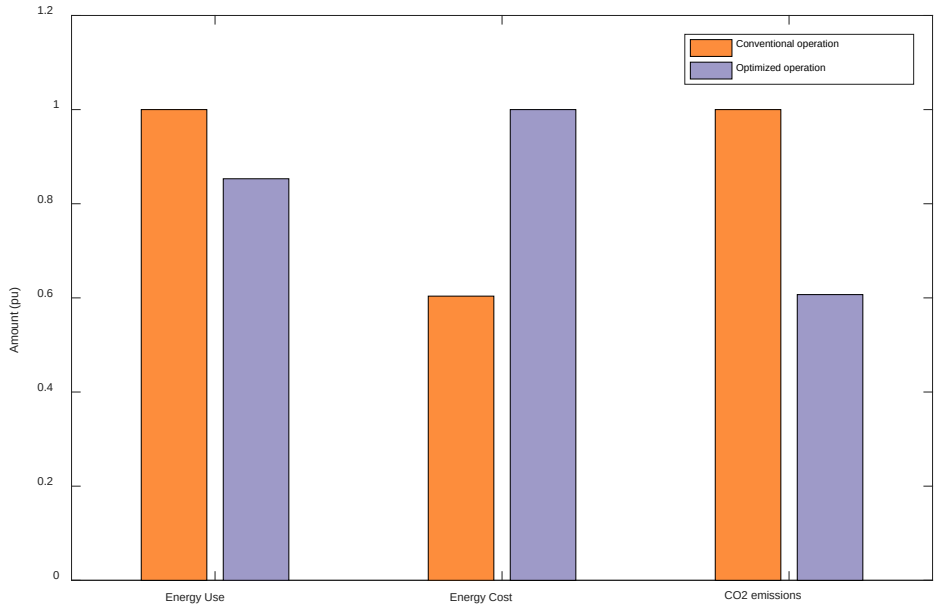

Figure 4.41: Optimization criteria: Feb. 2015 – Minimization of PES and CO_2.

Table XXII. Optimization criteria: Feb. 2015 – Minimization of PES and CO_2.

OPERATION	ENERGY (PU)	ENERGY COST (PU)	EMISSIONS (PU)
Conventional operat.	*2.8206*	*0.7522*	*0.5891*
Optimized operation	*2.4063*	*1.2460*	*0.3576*

Based on the results, the savings of CO_2 emissions would be approximately 0.2316 pu.

$$CO_2\ savings = 0.5907 - 0.3576 = 0.2331\ pu \tag{4.36}$$

The total energy savings percentage of the algorithm would result to:

$$energy\ savings\ \% = \left(\frac{0.4143}{2.8206}\right) * 100 = 14{,}69\% \tag{4.37}$$

4.5.4.2 Minimization of the primary energy use, costs and CO_2 emissions

This section presents the results of the optimization algorithm, focused on the minimization of the primary energy use, the cost of the primary energies and the minimization of the CO2 emissions. The following figure presents a comparison between the real operation of the plant and the optimized strategy that was obtained by the optimization algorithm.

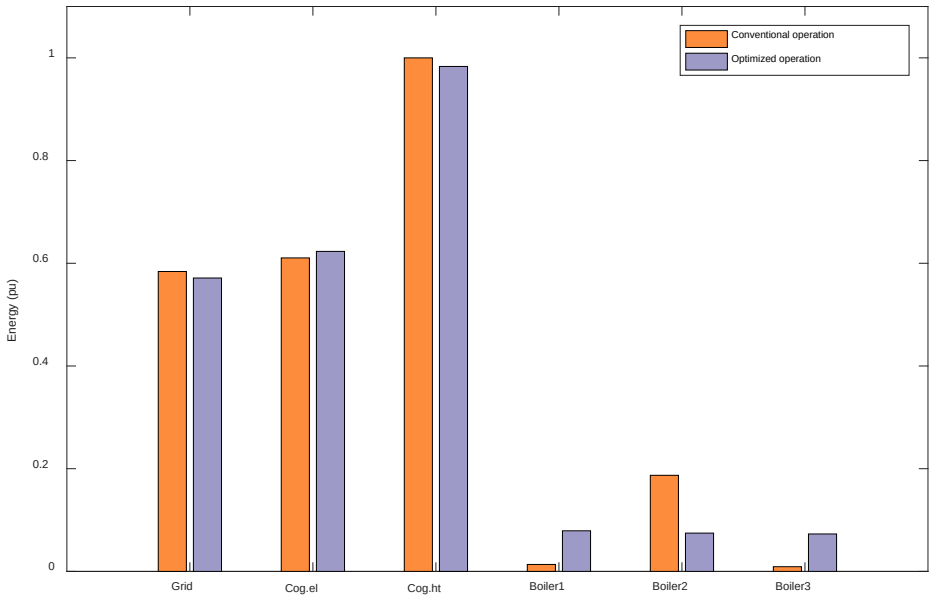

Figure 4.42: Total energy production: Feb. 2015 – Minimization of 3 objectives.

The following table presents the numeric values of the energy production equipment, as well as the use of electricity from the grid, which are depicted in Figure 4.42.

Table XXIII. Total energy production: Feb. 2015 - Minimization of 3 objectives.

Operation	Electricity (pu)		Heat (pu)			
	Grid	Cog.el	Cog.ht	Boiler 1	Boiler 2	Boiler 3
Real	*0.4827*	*0.5046*	*0.8265*	*0.0112*	*0.1547*	*0.0076*
Optimized	*0.4722*	*0.5151*	*0.8127*	*0.0654*	*0.0616*	*0.0603*

The following table presents the amount of primary energy sources that was used for the operation of the energy production equipment, or used directly for the fulfillment of the energy demands (case of electricity). Furthermore, the table contains the approximate resulting costs of the energy sources, as well as the difference between the real operation of the plant and the optimized one.

Table XXIV. Use of primary energies: Feb. 2015 - Minimization of 3 objectives.

Operation	Energy Use (pu)		Total Costs (pu)		Energy Difference (pu)	
	Electricity	Gas	Electricity	Gas	Electricity	Gas
Real	*0.4827*	*2.3379*	*0.5488*	*0.2034*	*0.0119*	*0.0035*
Optimized	*0.4722*	*2.2975*	*0.5369*	*0.1999*		

As it can be observed by the analysis of the data, by operating the plant with the recommendations of the optimization algorithm, it would result to an approximate cost savings of 0.0154 pu. Finally, the following figure present a comparison of the primary energy use, the total energy costs and the total CO2 emissions between the real operation and the optimized one.

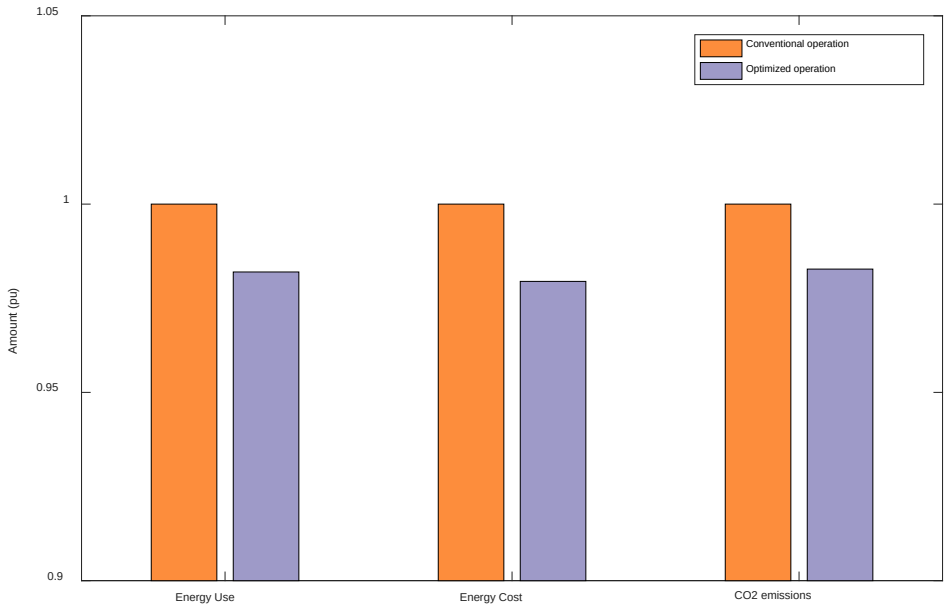

Figure 4.43: Optimization criteria: Feb. 2015 – Minimization of 3 objectives.

Table XXV. Optimization criteria: Feb. 2015 – Minimization of 3 objectives.

Operation	Energy (pu)	Energy Cost (pu)	Emissions (pu)
Conventional operat.	*2.8206*	*0.7522*	*0.5891*
Optimized operation	*2.7698*	*0.7368*	*0.5790*

4.5.5 Validation period – March 2015

Figure 4.44 presents the energy demand profiles of the electricity and heat for all the period of March 2015. All the below values are represented in per-units, **referenced to the total electric demand value of the month**.

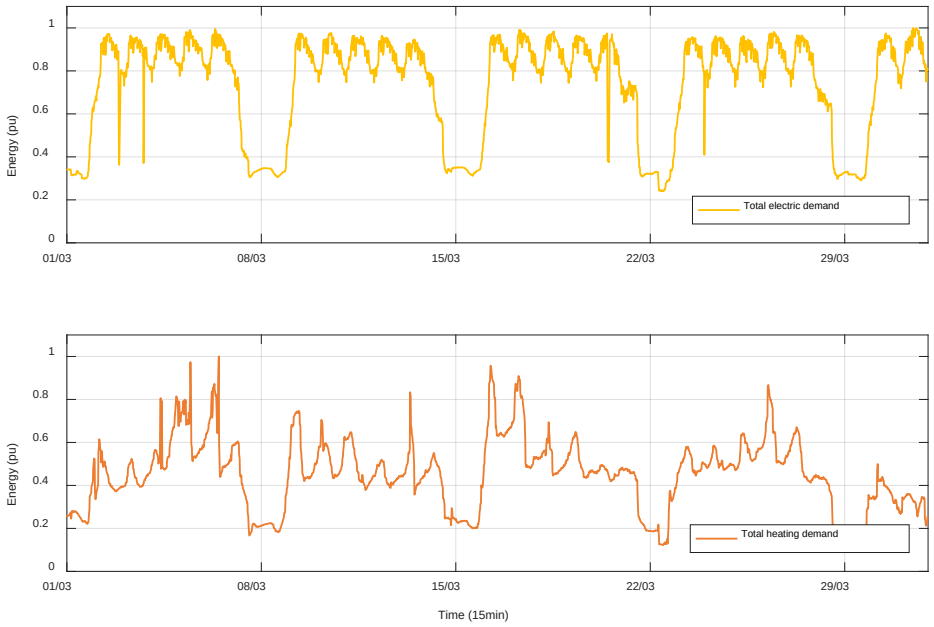

Figure 4.44: Energy demand profiles of the validation plant: 01 – 31 Mar. 2015.

Table XXVI. Total energy demands of the plant: 01 – 31 Mar. 2015.

DEMAND	ENERGY (PU)
Total electric demand	*1*
Total heating demand	*0.7036*

The following sections present the obtained results by operating the optimization algorithm with different criteria. A comparison between the real operation and the optimized one is presented, indicating the differences in term of costs, primary energy sources and CO2 emissions.

4.5.5.1 Minimization of the primary energy use and the CO_2 emissions

This section presents the results of the optimization algorithm, focused only on the minimization of the primary energy use and the minimization of the generation of CO2

emissions. The following figure presents a comparison between the real operation of the plant and the optimized strategy that was obtained by the optimization algorithm.

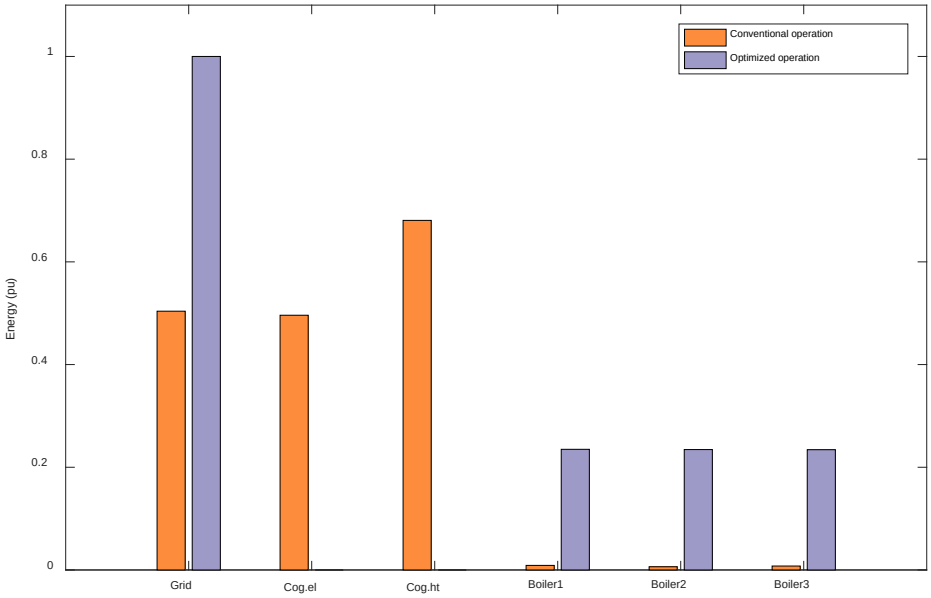

Figure 4.45: Total energy production: Mar. 2015 – Minimization of PES and CO_2.

The following table presents the numeric values of the energy production equipment, as well as the use of electricity from the grid, which are depicted in Figure 4.45.

Table XXVII. Total energy production: Feb. 2015 - Minimization of PES use and CO_2.

Operation	Electricity (pu)		Heat (pu)			
	Grid	Cog.el	Cog.ht	Boiler 1	Boiler 2	Boiler 3
Real	*0.5039*	*0.4961*	*0.6808*	*0.0089*	*0.0062*	*0.0077*
Optimized	*1*	*0*	*0*	*0.2350*	*0.2344*	*0.2342*

The following table presents the amount of primary energy sources that was used for the operation of the energy production equipment. Furthermore, the table contains the approximate resulting costs of the energy sources, as well as the difference of the energy use between the real operation of the plant and the optimized one.

Table XXVIII. Use of primary energies: Feb. 2015 - Minimization of pes use and co_2.

Operation	Energy Use (pu)		Total Costs (pu)		Energy Difference (pu)	
	Electricity	Gas	Electricity	Gas	Electricity	Gas
Real	*0.5039*	*2.0153*	*0.5730*	*0.1753*	*-0.4961*	*1.0169*
Optimized	*1*	*0.9984*	*1.1370*	*0.0869*		

As it can be observed by the analysis of the data, by operating the plant with the recommendations of the optimization algorithm, it would result to an approximate energy savings of 0.5208 pu.

$$energy\ savings = -0.4961 + 1.0169 = 0.5208\ pu \tag{4.38}$$

The following figure present a comparison of the primary energy use, the total energy costs and the total CO2 emissions between the real operation and the optimized one.

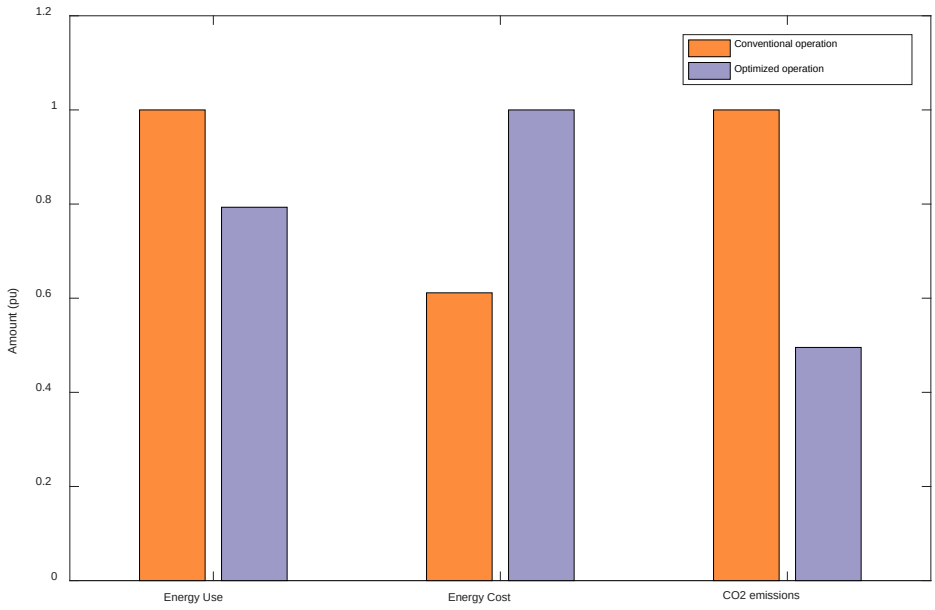

Figure 4.46: Optimization criteria: Mar. 2015 – Minimization of PES and CO_2.

Table XXIX. Optimization criteria: Mar. 2015 – Minimization of PES and CO_2.

OPERATION	ENERGY (PU)	ENERGY COST (PU)	EMISSIONS (PU)
Conventional operat.	*2.5192*	*0.7483*	*0.5079*
Optimized operation	*1.9984*	*1.2239*	*0.2516*

Based on the results, the savings of CO2 emissions would be approximately 0.2563 pu.

$$CO_2\ savings = 0.5079 - 0.2516 = 0.2563\ pu \tag{4.39}$$

The total energy savings percentage of the algorithm would result to:

$$energy\ savings\ \% = \left(\frac{0.5208}{2.5192}\right) * 100 = 20{,}68\% \tag{4.40}$$

4.5.5.2 Minimization of the primary energy use, costs and CO_2 emissions

This section presents the results of the optimization algorithm, focused on the minimization of the primary energy use, the cost of the primary energies and the minimization of the CO2 emissions. The following figure presents a comparison between the real operation of the plant and the optimized strategy that was obtained by the optimization algorithm.

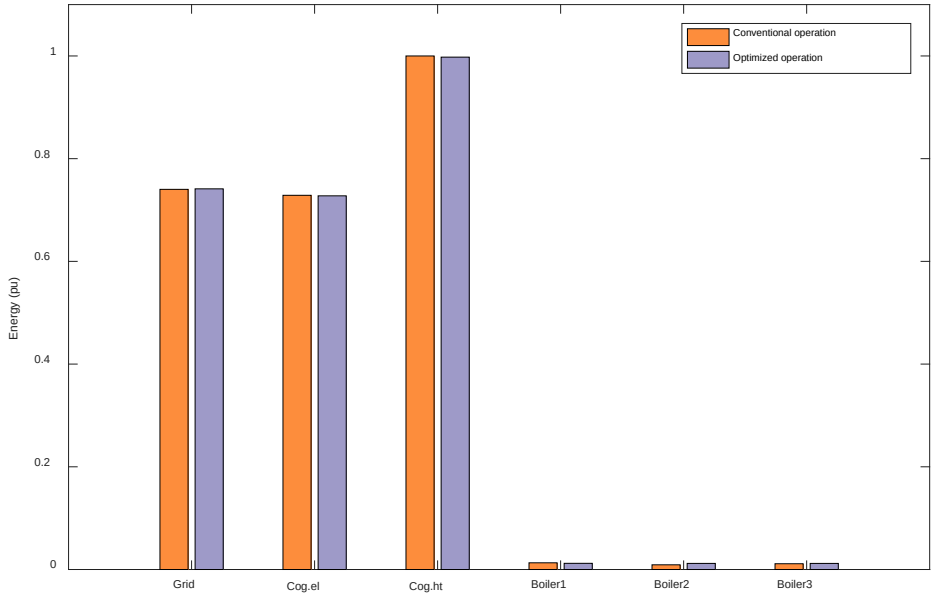

Figure 4.47: Total energy production: Mar. 2015 – Minimization of 3 objectives.

The following table presents the numeric values of the energy production equipment, as well as the use of electricity from the grid, which are depicted in Figure 4.47.

Table XXX. Total energy production: Mar. 2015 - Minimization of 3 objectives.

Operation	Electricity (pu)		Heat (pu)			
	Grid	Cog.el	Cog.ht	Boiler 1	Boiler 2	Boiler 3
Real	*0.5039*	*0.4961*	*0.6808*	*0.0089*	*0.0062*	*0.0077*
Optimized	*0.5046*	*0.4954*	*0.6792*	*0.0082*	*0.0081*	*0.0081*

The following table presents the amount of primary energy sources that was used for the operation of the energy production equipment, or used directly for the fulfillment of the energy demands (case of electricity). Furthermore, the table contains the approximate resulting costs of the energy sources, as well as the difference between the real operation of the plant and the optimized one.

Table XXXI. Use of primary energies: Mar. 2015 - Minimization of 3 objectives.

Operation	Energy Use (pu)	Total Costs (pu)	Energy Difference (pu)

	ELECTRICITY	GAS	ELECTRICITY	GAS	ELECTRICITY	GAS
Real	*0.5039*	*2.0153*	*0.5730*	*0.1753*	*-0.000787*	*0.0011*
Optimized	*0.5046*	*2.0024*	*0.5738*	*0.1742*		

As it can be observed by the analysis of the data, by operating the plant with the recommendations of the optimization algorithm, it would result to an approximate cost savings of 0.000337 pu. Finally, the following figure present a comparison of the primary energy use, the total energy costs and the total CO2 emissions between the real operation and the optimized one.

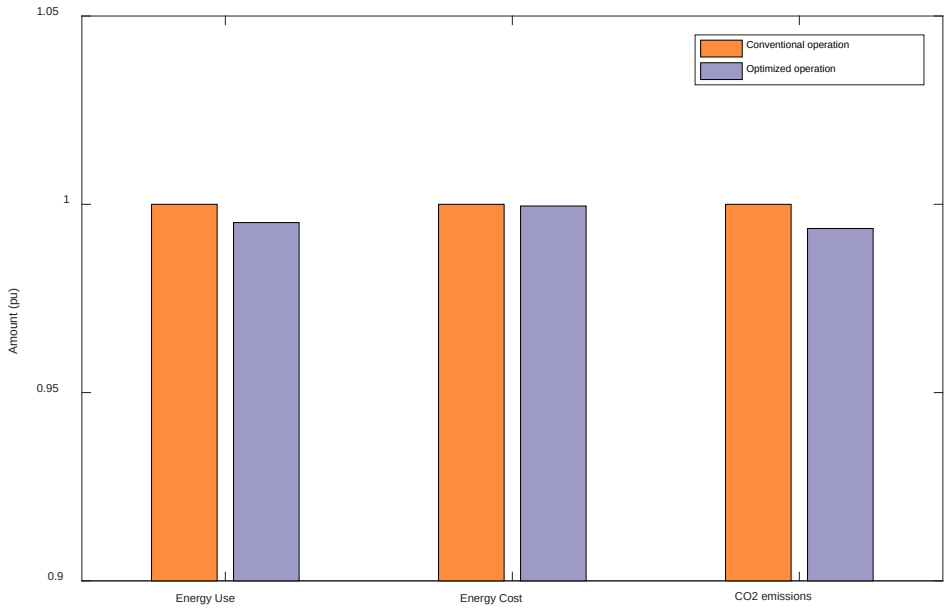

Figure 4.48: Optimization criteria: Mar. 2015 – Minimization of 3 objectives.

Table XXXII. Optimization criteria: Mar. 2015 – Minimization of 3 objectives.

OPERATION	ENERGY (PU)	ENERGY COST (PU)	EMISSIONS (PU)
Conventional operat.	*2.5192*	*0.7483*	*0.5079*
Optimized operation	*2.5070*	*0.7480*	*0.5046*

4.6 Conclusions

The main contribution of this chapter is the presentation of a methodology for the determination of the optimal operating strategy of a multi-carrier energy system, combining demand forecasting and nonlinear mixed-integer programming. This methodology uses multiple optimization objectives, focused on the fulfillment of the energy demands, the minimization of the total operation costs and energy, as well as on the minimization of the equivalent CO_2 emissions. Additionally, it has to be highlighted that other criteria could be considered, as the maintenance cost of the equipment, the investment and devaluation costs of the equipment, the human and material resources for their operation, among other, based on the user's preferences and the operating conditions of the system. Furthermore, the presented methodology takes into account the dynamic system response, expressed as thermal inertias of the energy production equipment, to calculate its effect to the equipment's operation bounds during the multi-time period optimization, with objective to guarantee that the system is working into the engineering boundaries, avoiding operation anomalies that can be caused by unsatisfied energy requirements or overload of the infrastructure. Additionally, the presented methodology permits to optimize the energy flow of the system for an entire prediction horizon, but resolving the problem's instants individually. By this way, the required computational effort and time are reduced, due to the problem is split in multiple single-instants problems. The methodology uses a multiobjective genetic algorithm for the optimization, which has been selected based on its following advantages:

- ✓ Its ability to optimize with both continuous and discrete variables, making it adequate for resolving problems of systems that contain equipment with both continuous operating ranges, as well as scalar operating modes.
- ✓ It does not require any derivative information, simplifying the complexity and the computational effort of the general system.
- ✓ It simultaneously searches from a wide sampling of the defined cost surface, permitting to avoid or bypass local minimums of the solution, making capable of optimizing variables with extremely complex cost surfaces.
- ✓ It is able to deal with a large number of variables, making ideal for solving problems of energy systems with multiple sources, energy carriers, equipment and demands. Thus, its use in an optimization system that is focused on the industrial environment is beneficiary based on its flexibility on adapting on different structures

(interconnections of the energy hub system of each plant) without complex configurations.

- ✓ It does not provide just a single optimum solution but multiple strategies, permitting to decide between possible alternatives for the operation of the plant.
- ✓ It uses encoding techniques to simplify the processing of the variables and thus accelerate the optimization process.

The validation process of the proposed methodology was performed in a car manufacturing plant, in the framework of the FP7 Euroenergest project. During the validation, the developed algorithm was executed continuously for a total period of 3 months, while its results were being registered in the database of the software, together with the conventional operation of the system. After that, comparisons between the results of the real operation and the optimized one were performed. The validation of this algorithm was applied in the energy production equipment related to the electric and heating generation, while the cooling production equipment were partially used due to the lack of cooling demand during the validation period (winter season). All the tests were made by applying two combinations of optimization criteria: minimization of the use of primary energy sources and CO_2 emissions, and minimization of primary energy sources, energy costs and CO_2 emissions.

Finally, by analyzing the registered results it was observed that in all of the cases the optimization algorithm was capable of satisfying the energy demand of the plant. In the presented examples, detailed information related to the primary energy use, primary energy costs and generated emissions, are included for both operation cases (real operation and optimized one).

Related to the optimization criteria, it was observed that by operating the system focused on the energy and environmental impact (first case), the energy savings could result to a value between 13.35 % and 20.68% of the total power. Nevertheless, even this operation presents an important amount of energy savings, it is more expensive than the actual one. On the other hand, by operating the system giving more priority to the minimization of the energy costs, it was observed that the outputs of the algorithm were very similar to the real situation of the plant (for all the validation period of 3 months). In such a case, the obtained results presented a cost savings between 0.2% and 0.56%. In summary, from the 3 months validation of the algorithm in real-site it was concluded an average potential savings of 16.24% of energy use, a 4.75% of energy cost decrement, and a 42.96% of generated emissions reduction.

Nevertheless, it has to be mentioned that the energy saving potential of the algorithm strictly depends on the implemented energy plant and its current operation mode. That means that the obtained energy savings from the validation reflects only the situation of the demonstration plant, based on its current operation strategy.

5. Conclusions

Finally this chapter presents the conclusions that were derived from this dissertation thesis. Some observations, comments and conclusions of the research are summarized, and publications in international conference proceedings and international journals are synthesized. The future research lines that can be derived from this research work are mentioned at the end of the chapter.

5.1 Key Contributions

In order to achieve the thesis objective and to validate the initial performed hypotheses, a methodological approach was used during the elaboration of this dissertation, as presented below.

As a starting point, a complete review was made, describing the state of the art of the energy hub concept, applied to multi-carrier energy systems, its potential benefits in terms of reliability and improvement of the system's overall performance, as well as its key elements for its mathematical representation. Additionally, a procedure for calculating the formulation of a given energy hub system was introduced, together with an application example that describes the experimental plant for the testing and validation of the hypotheses of this dissertation. This procedure, applied to multi-carrier energy systems, describes the physical

limitations of the energy equipment of a given system, their operating restrictions and bounds, their interconnection and their operating inertias.

On the other hand, the state of the art of the recent data-driven approaches for the load modeling and prediction was performed, describing the disadvantages and potential advantages of each one, as well as the fields of their application. In this line, a short-term load forecasting methodology, based on adaptive neuro-fuzzy inference systems and genetic algorithms was presented. This algorithm uses historical data from the consumptions' operation as well as other operation parameters that can influence on the demands' behavior, with aim to generate high accuracy customizable mathematical models for different consumptions in order to obtain short-term demand forecasts, able to be used in the energy hub optimization strategy. This methodology was implemented and validated under real operation conditions of the demonstration plant, applied to 14 cases of consumptions, which represent the most significant loads in terms of manufacturing processes, power and load profiles. Finally, a multi-model training approach was proposed, aiming at improving the training performance of the models. This approach develops multiple models for a single signal, based on a hierarchical clustering of similar load behaviors, being able to identify the necessary number of models to be trained, based on the operation conditions and the profile of the consumption.

As final point, the review of different applications and algorithms used to optimize multivariable problems was performed, covering both deterministic and stochastic methods. Additionally, the mathematical description of the optimization problems of the energy flow in multi-carrier energy systems was made, which depends on the structure of the system as well as the type of available technologies and equipment that it contains. Finally a new methodology for the dynamic optimization of multi-carrier energy systems, combining demand forecasting and nonlinear mixed-integer programming was presented, based on a multiobjective genetic algorithm. The methodology takes into account the dynamic system response, expressed as thermal inertias of the energy production equipment, to calculate its effect to the equipment's operation bounds during the multi-time period optimization. The validation process of the proposed methodology was performed using real operating data of the demonstration plant, permitting to compare and evaluate the potential benefit of the proposed optimization algorithm. During the validation, two optimization strategies were applied, consisting of different combinations of economic, energetic and environmental criteria.

Summarizing, the following main contributions can be stated for this thesis work, related to the mentioned activities:

1. A methodology was presented for the analysis of the energetic infrastructure of a multi-carrier energy system, as well as for its mathematical formulation as an energy hub in terms of system interconnections, energy restrictions, as well as operation bounds and energy availability. The energy hub model obtained by implementing this methodology, guarantee that the system is working into the engineering boundaries, avoiding operation anomalies that can be caused by unsatisfied energy requirements or overload of the infrastructure.

2. Another contributions is the presentation of a methodology for the modeling and energy forecasting using a combination of Genetic Algorithms and Adaptive Neuro-Fuzzy Inference Systems, with aim to generate high accuracy customizable mathematical models for different consumptions in order to obtain short-term demand forecasts that are used in the energy hub optimization strategy. In the proposed methodology, the ANFIS is used to train the mathematical model of the consumption and to provide a short-term load forecast while the GA is responsible for analyzing the database and the possible correlations between the demand and the input candidates and evaluate which are the optimal ones to be used as inputs in the training and the prediction process.

3. Also related to model forecasting is the presented multi-model training approach, which increases even more the modelling performance and the prediction accuracies, by clustering the database into separate datasets, based on the consumption patterns. Since the initially complex modeling problem is split into a set of smaller problems, it is easier for the algorithm to train each group, as its members present a similar behavior, and so it helps the training algorithm converge faster. Also, the proposed methodology accomplishes a forecast response that adapts better to the different dynamics of the load demand signal.

4. Finally, the last and main contribution of this thesis is the presentation of procedures and mathematical tools for the determination of the optimal operating strategy of a multi-carrier energy system, combining demand forecasting and nonlinear mixed-integer programming. This methodological solution uses multiple optimization

objectives, focused on the fulfillment of the energy demands, the minimization of the total operation costs and energy, as well as on the minimization of the equivalent CO2 emissions, taking also into account the dynamic system response to guarantee that the system will work under stable conditions.

Simulations and experimental result have been presented in order to validate the proposed methodology, energy flow analysis and optimization approach.

The flexibility and power of the presented solution allows its application to complex problems of energy optimization, which include multiple sources of energy and different forms of thermal and electrical demand. The energy hub solution allows the mathematical modeling of complex energy infrastructures, thus facilitating the application of advanced multivariable optimization solutions in real time.

5.2 Future Work

For future work related to these thesis developments, the following issues could be addressed.

1. The integration and analysis of energy storage systems in the mathematical formulation as well as in the optimization strategies of the multi-carrier energy system. It is possible to develop new strategies that improve the performance of the operation of the multi-carrier energy systems, by implementing energy storage systems. Nevertheless, due to these elements can behave both as energy suppliers, as well as, as energy consumptions, it is challenging to determine their optimal operation in a long term (prediction horizon), taking simultaneously into account the energy availability and flow that depends on the entire operating strategy of the system. Thus, this topic could be considered as a new field of research, with an immediate potential of application in both industrial as well as tertiary sector. Also, local renewable power sources can be included as energy producers, thus allowing considering not only an additional freedom for energy optimization but also bidirectional energy flows in energy infrastructures.

2. The adaptation and implementation of the optimization methodology at the stage of the design of the energetic infrastructure, rather than only at its operation. Facing the scenario shift in the building sector, promoted by the EU towards a Zero Energy Building paradigm (directive 2010/31/EU), the society has been significantly focused on the development of more efficient systems. Thus, a potential use of the proposed methodology would be applying it with objective to determine the optimal energetic infrastructure of a given system. The challenge of this task is the simultaneously evaluation of multiple combinations of competing systems, for both the energy sources (including grid connection and renewable sources), the conversion systems (energy equipment) as well as consumptions (HVAC terminals). This optimization problem, also formulated as a multi-objective mixed-integer problem, could be analyzed and resolved by adapting the proposed methodology. Nevertheless, further study on both the mathematical formulation as well as on the optimization strategies should be made, applying necessary adaptations and improvements.

5.3 Publications

5.3.1 Journal Publications

- K. Kampouropoulos, F. Andrade, E. Sala, A. Garcia Espinosa and J. L. Romeral, "Multiobjective Optimization of Multi-Carrier Energy System using a Combination of ANFIS and Genetic Algorithms", in *IEEE Transactions on Smart Grid*, vol. PP, no. 99, pp. 1-1, 2016. doi: 10.1109/TSG.2016.2609740

- K. Kampouropoulos, F. Andrade, E. Sala, A. Garcia and L. Romeral, "A Combined Methodology of Adaptive Neuro-Fuzzy Inference System and Genetic Algorithm for Short-term Energy Forecasting", *AECE - Advanced in Electrical and Computer Engineering Journal*, vol. 14, no. 1, pp. 9-14, 2014. doi:10.4316/AECE.2014.01002

5.3.2 Conference Publications

- K. Kampouropoulos, E. Crespo Sánchez, J. Macià i Cid, L. Cases Fàbregas and M. Castellà, "A novel methodology for the optimisation of the retrofitting actions in building of the tertiary sector", *22th International Passive House Conference*, Munich, Germany, 2018, accepted.

- K. Kampouropoulos and E. Crespo Sánchez, "IESD – Herramienta de optimización en rehabilitaciones energéticas de edificios no residenciales", *IV Congreso Edificios Energía Casi Nula 2017*, vol., pp., Madrid, Spain, 2017.

- K. Kampouropoulos, F. Andrade, E. Sala, A. G. Espinosa and L. Romeral, "Multi-carrier optimal power flow of energy hubs by means of ANFIS and SQP", *IECON 2016 - 42nd Annual Conference of the IEEE Industrial Electronics Society*, Florence, Italy, 2016, pp. 3990-3995. doi: 10.1109/IECON.2016.7793570

- K. Kampouropoulos and F. Andrade, "Energy hub optimization applied on car manufacturing plants," *2016 IEEE ANDESCON*, Arequipa, Peru, 2016, pp. 1-4. doi: 10.1109/ANDESCON.2016.7836236

- K. Kampouropoulos, F. Andrade, E. Sala and L. Romeral, "Optimal control of energy hub systems by use of SQP algorithm and energy prediction", *IECON 2014 - 40th Annual Conference of the IEEE Industrial Electronics Society*, Dallas, TX, 2014, pp. 221-227. doi: 10.1109/IECON.2014.7048503

- K. Kampouropoulos, J. J. Cárdenas, F. Giacometto and L. Romeral, "An energy prediction method using Adaptive Neuro-Fuzzy Inference System and Genetic Algorithms," *ISIE 2013 - IEEE International Symposium on Industrial Electronics*, Taipei, Taiwan, 2013, pp. 1-6. doi: 10.1109/ISIE.2013.6563627

- K. Kampouropoulos, F. Andrade, J.J. Cárdenas and L. Romeral, "A Methodology for Energy Prediction and Optimization of a System based on the Energy Hub Concept using Particle Swarms", *SAAEI 2012 - The Annual Seminar on Automation, Industrial Electronics and Instrumentation*, Guimaraes, Portugal, 2012.

5.3.3 Collaborative Work

- J. Marcià i Cid, M. Heredero de Pablos, K. Kampouropoulos and L. Romeral, "A novel methodology for the optimal selection of multisource renewable energy systems for tertiary and residential buildings", *Alternative Energy Sources, Materials & Technologies (AESMT'18)*, 2018, under review.

- E. Sala, L. Romeral, K. Kampouropoulos and M. Delgado, "Activity-Aware HVAC Power Demand Forecasting", *Energy and Buildings*, 2017, under review.

- E. Sala, D. Zurita, K. Kampouropoulos, M. Delgado and L. Romeral, "Occupancy forecasting for the reduction of HVAC energy consumption in smart buildings", *IECON 2016 - 42nd Annual Conference of the IEEE Industrial Electronics Society*, Florence, 2016, pp. 4002-4007. doi: 10.1109/IECON.2016.7793491

- E. Sala, K. Kampouropoulos, M. D. Prieto and L. Romeral, "Intelligent monitoring of HVAC equipment by means of aggregated power analysis", *IECON 2016 - 42nd*

Annual Conference of the IEEE Industrial Electronics Society, Florence, 2016, pp. 3978-3983. doi: 10.1109/IECON.2016.7794112

- E. Sala, K. Kampouropoulos, M. D. Prieto and L. Romeral, "Disaggregation of HVAC load profiles for the monitoring of individual equipment", *ETFA 2016 - IEEE 21st International Conference on Emerging Technologies and Factory Automation*, Berlin, 2016, pp. 1-6. doi: 10.1109/ETFA.2016.7733568

- F. Giacometto, E. Sala, K. Kampouropoulos and L. Romeral, "Short-term load forecasting using Cartesian Genetic Programming: An efficient evolutive strategy: Case: Australian electricity market", *IECON 2015 - 41st Annual Conference of the IEEE Industrial Electronics Society*, Yokohama, 2015, pp. 5087-5094. doi: 10.1109/IECON.2015.7392898

- E. Sala, D. Zurita, K. Kampouropoulos, M. Delgado-Prieto and L. Romeral, "Enhanced load forecasting methodology by means of probabilistic prediction intervals estimation," *ICIT 2015 - IEEE International Conference on Industrial Technology*, Seville, 2015, pp. 1299-1304. doi: 10.1109/ICIT.2015.7125277

- F. Andrade, K. Kampouropoulos, L. Romeral, J. C. Vasquez and J. M. Guerrero, "Study of large-signal stability of an inverter-based generator using a Lyapunov function", *IECON 2014 - 40th Annual Conference of the IEEE Industrial Electronics Society*, Dallas, TX, 2014, pp. 1840-1846. doi: 10.1109/IECON.2014.7048752

- E. Sala, K. Kampouropoulos, F. Giacometto and L. Romeral, "Smart multi-model approach based on adaptive Neuro-Fuzzy Inference Systems and Genetic Algorithms", *IECON 2014 - 40th Annual Conference of the IEEE Industrial Electronics Society*, Dallas, TX, 2014, pp. 288-294. doi: 10.1109/IECON.2014.7048513

- F. Andrade, L. Romeral, K. Kampouropoulos and J. Cusido, "New mathematical model of an inverter-based generator for stability studies of microgrid systems", *POWERENG 2013 - 4th International Conference on Power Engineering, Energy and Electrical Drives*, Istanbul, 2013, pp. 944-949. doi: 10.1109/PowerEng.2013.6635738

- F. Andrade, K. Kampouropoulos, J. Cusido and L. Romeral, "Stability Analysis of a Microgrid System based on Inverter-Interfaced Distributed Generators", *AECE - Advances in Electrical and Computer Engineering*, vol. 13, no. 3, pp. 17-22, 2013. doi:10.4316/AECE.2013.03003

- F. Giacometto, J. J. Cárdenas, K. Kampouropoulos and J. L. Romeral, "Load forecasting in the user side using wavelet-ANFIS," *IECON 2012 - 38th Annual Conference on IEEE Industrial Electronics Society*, Montreal, QC, 2012, pp. 1049-1054. doi: 10.1109/IECON.2012.6388575

- F. Andrade, K. Kampouropoulos, L. Romeral and J. Cusido, "Modeling and Studying of the Power flow in a Micro-grid based in Solar and Wind Energies with Plug-in Vehicles", *Smart City Expo World Congress*, Barcelona, Spain, 2011.

- F. Andrade, K Kampouropoulos, J Cusido, L. Martínez, "Estudio de Microgrids con interfaces de convertidores de DC/AC", *SAAEI 2011 - Seminario Anual de Automática*, *Electrónica Industrial e Instrumentación*, Badajoz, España, 2011.

- J. J. Cárdenas, A. García, J. L. Romeral and K. Kampouropoulos, "Evolutive ANFIS training for energy load profile forecast for an IEMS in an automated factory", *ETFA2011 – 16th Conference on Emerging Technologies & Factory Automation*, Toulouse, 2011, pp. 1-8. doi: 10.1109/ETFA.2011.6059079

References

[1] N. Anglani and G. Muliere, "Energy conversion technologies benefiting from local policy actions: The role of distributed generation", *2010 IEEE International Energy Conference*, pp. 345-350, 2010. doi: 10.1109/ENERGYCON.2010.5771702

[2] M. Gomez and F. Jurado, "Feasibility of fuel cell systems using forest residues", *2007 IEEE Power Engineering Society General Meeting*, 2007, pp. 1-7. doi: 10.1109/PES.2007.385671

[3] M. Geidl and G. Andersson, "Optimal Power Flow of Multiple Energy Carriers", in *IEEE Transactions on Power Systems*, vol. 22, no. 1, pp. 145-155, 2007. doi: 10.1109/TPWRS.2006.888988

[4] M. Geidl, G. Koeppel, P. Favre-Perrod, B. Klockl, G. Andersson and K. Frohlich, "The Energy Hub – A Power Concept for Future Energy Systems", *Third Annual Carnegie Mellon Conference on the Electricity Industry*, 2007.

[5] G. Andersson, K. Fröhlich and T. Krause, "Vision of Future Energy Networks (VoFEN)", *Eidgenössisches Departement für Umwelt, Verkehr, Energie und Kommunikation UVEK,* 2011.

[6] T. Krause, G. Andersson, K. Frohlich and A. Vaccaro, "Multiple-Energy Carriers: Modeling of Production, Delivery, and Consumption", in *Proceedings of the IEEE*, vol. 99, no. 1, pp. 15-27, 2011. doi: 10.1109/JPROC.2010.2083610

[7] R. Frik and P. Favre-Perrod, "Proposal for a multifunctional energy bus and its interlink with generation and consumption", diploma thesis, *Power Systems and High Voltage Laboratories*, ETH, Zurich, Switzerland, 2004.

[8] M. Geidl, P. Favre-Perrod, B. Klöckl and G. Koeppel, "A greenfield approach for future power systems", in *Proc. of Cigre General Session 41*, 2006.

[9] H. M. Groscurth, T. Bruckner and R. Kümmel, "Modeling of energy-services supply systems", *Energy*, vol. 20, no. 9, pp. 941-958, 1995, ISSN 0360-5442. doi: 10.1016/0360-5442(95)00067

[10] I. Bouwmans and K. Hemmes, "Optimising energy systems—Hydrogen and distributed generation", in *Proc. 2nd Int. Symp. Distributed Generation: Power System Market Aspects*, 2002.

[11] R. H. Lasseter and P. Paigi, "Microgrid: a conceptual solution", *2004 IEEE 35th Annual Power Electronics Specialists Conference (IEEE Cat. No.04CH37551)*, vol. 6, pp. 4285-4290, 2004. doi: 10.1109/PESC.2004.1354758

[12] M. Moeini-Aghtaie, P. Dehghanian, M. Fotuhi-Firuzabad and A. Abbaspour, "Multiagent Genetic Algorithm: An Online Probabilistic View on Economic Dispatch of Energy Hubs Constrained by Wind Availability", in *IEEE Transactions on Sustainable Energy*, vol. 5, no. 2, pp. 699-708, 2014. doi: 10.1109/TSTE.2013.2271517

[13] M. Geidl and G. Andersson, "Optimal power dispatch and conversion in systems with multiple energy carriers", in *Proc. 15th Power Systems Computation Conference (PSCC)*, 2005.

[14] A. Hajimiragha, C. Canizares, M. Fowler, M. Geidl and G. Andersson, "Optimal Energy Flow of integrated energy systems with hydrogen economy considerations", *2007 iREP Symposium - Bulk Power System Dynamics and Control - VII. Revitalizing Operational Reliability*, pp. 1-11, 2007. doi: 10.1109/IREP.2007.4410517

[15] M. Moeini-Aghtaie, A. Abbaspour, M. Fotuhi-Firuzabad and E. Hajipour, "A Decomposed Solution to Multiple-Energy Carriers Optimal Power Flow", in *IEEE Transactions on Power Systems*, vol. 29, no. 2, pp. 707-716, 2014. doi: 10.1109/TPWRS.2013.2283259

[16] L. Ramirez-Elizondo, V. Velez and G. C. Paap, "A technique for unit commitment in multiple energy carrier systems with storage", *2010 9th International Conference on Environment and Electrical Engineering*, pp. 106-109, 2010. doi: 10.1109/EEEIC.2010.5489999

[17] L. M. Ramirez-Elizondo and G. C. Paap, "Unit commitment in multiple energy carrier systems", *41st North American Power Symposium*, pp. 1-6, 2009. doi: 10.1109/NAPS.2009.5484065

[18] M. Geidl and G. Andersson, "Operational and topological optimization of multi-carrier energy systems", *2005 International Conference on Future Power Systems*, Amsterdam, pp. 6, 2005. doi: 10.1109/FPS.2005.204199

[19] M. Geidl and G. Andersson, "Operational and structural optimization of multi-carrier energy systems", *Euro. Trans. Electr. Power*, vol. 16, no. 5, pp. 463–477, 2006. doi: 10.1002/etep.112

[20] F. Kienzle, P. Ahcin and G. Andersson, "Valuing Investments in Multi-Energy Conversion, Storage, and Demand-Side Management Systems Under Uncertainty", in *IEEE Transactions on Sustainable Energy*, vol. 2, no. 2, pp. 194-202, 2011. doi: 10.1109/TSTE.2011.2106228

[21] F. Adamek, M. Arnold and G. Andersson, "On Decisive Storage Parameters for Minimizing Energy Supply Costs in Multicarrier Energy Systems", in *IEEE Transactions on Sustainable Energy*, vol. 5, no. 1, pp. 102-109, 2014. doi: 10.1109/TSTE.2013.2267235

[22] M. Geidl and G. Andersson, "Optimal Coupling of Energy Infrastructures", *2007 IEEE Lausanne Power Tech*, pp. 1398-1403, 2007. doi: 10.1109/PCT.2007.4538520

[23] M. Schulze and P. Crespo Del Granado, "Optimization modeling in energy storage applied to a multi-carrier system", *IEEE PES General Meeting*, pp. 1-7, 2010. doi: 10.1109/PES.2010.5589763

[24] M. Rayati, A. Sheikhi and AM. Ranjbar, "Optimizing operational cost of a smart energy hub, the reinforcement learning approach", International Journal of Parallel, Emergent and Distributed Systems, vol. 30, pp. 325-341, 2015. doi: 10.1080/17445760.2014.974600

[25] A. Sheikhi, M. Rayati, S. Bahrami, AM. Ranjbar, and S. Sattari, "A cloud computing framework on demand side management game in smart energy hubs", *International Journal of Electrical Power & Energy Systems*, vol. 64, pp. 1007-1016, Jan 2015. doi: 10.1016/j.ijepes.2014.08.020.

[26] A. Sheikhi, M. Rayati, S. Bahrami and AM. Ranjbar, "Integrated Demand Side Management Game in Smart Energy Hubs", in *IEEE Transactions on Smart Grid*, vol. 6, no. 2, pp. 675-683, 2015. doi: 10.1109/TSG.2014.2377020

[27] S. Bahrami and A. Sheikhi, "From Demand Response in Smart Grid Toward Integrated Demand Response in Smart Energy Hub", in *IEEE Transactions on Smart Grid*, vol. 7, no. 2, pp. 650-658,. 2016. doi: 10.1109/TSG.2015.2464374

[28] A. Sheikhi, S. Bahrami and AM. Ranjbar, "An autonomous demand response program for electricity and natural gas networks in smart energy hubs", *Energy*, vol. 89, pp. 490-499, 2015. doi: 10.1016/j.energy.2015.05.109

[29] M. Alipour, K. Zare and M. Abapour, "MINLP Probabilistic Scheduling Model for Demand Response Programs Integrated Energy Hubs", *in IEEE Transactions on Industrial Informatics*, vol. 14, no. 1, pp. 79-88, 2018. doi: 10.1109/TII.2017.2730440

[30] W. Zhang et al., "Optimal operation of wind-solar-hydrogen storage system based on energy hub", *2017 IEEE Conference on Energy Internet and Energy System Integration (EI2)*, pp. 1-5, , 2017. doi: 10.1109/EI2.2017.8245493

[31] A. Dolatabadi, M. Jadidbonab and B. Mohammadi-ivatloo, "Short-term Scheduling Strategy for Wind-based Energy Hub: A Hybrid Stochastic/IGDT Approach", *in IEEE Transactions on Sustainable Energy*, vol. PP, no. 99, pp. 1-1. doi: 10.1109/TSTE.2017.2788086

[32] A. Maroufmashat, A. Elkamel, M. Fowler, S. Sattari, R. Roshandel, A. Hajimiragha, S. Walker and E. Entchev, "Modeling and optimization of a network of energy hubs to improve economic and emission considerations", *Energy*, vol. 93, pp 2546-2558, 2015. doi: 10.1016/j.energy.2015.10.079

[33] M. Geidl, "Integrated Modeling and Optimization of Multi-Carrier Energy Systems", *Ph.D. dissertation*, D-ITET, ETH Zurich, Zurich, Switzerland, 2007.

[34] A. Tisot, "Industrial energy management: Doing more with less", *Pulp & Paper-Canada*, vol. 105, pp. 21-23, 2004.

[35] P. J. Santos, A. G. Martins and A. J. Pires, "Designing the input vector to ANN-based models for short-term load forecast in electricity distribution systems", *International Journal of Electrical Power & Energy Systems*, vol. 29, 2007. doi: 10.1016/j.ijepes.2006.09.002

[36] Z. Xiao, S. J. Ye, B. Zhong and C. X. Sun, "BP neural network with rough set for short term load forecasting", *Expert Systems with Applications*, vol. 36, pp. 273–279, 2009. doi: 10.1016/j.eswa.2007.09.031

[37] S. Kouhi and F. Keynia, "A new cascade NN based method to short-term load forecast in deregulated electricity market", *Energy Conversion and Management*, vol. 71, pp. 76-83, 2013. doi: 10.1016/j.enconman.2013.03.014.

[38] A. Badri, Z. Ameli, and A. M. Birjandi, "Application of artificial neural networks and fuzzy logic methods for short term load forecasting", *2nd International Conference on Advances in Energy Engineering*, vol. 14, pp. 1883-1888, 2012. doi: 10.1016/j.egypro.2011.12.1183

[39] F. R. Fulginei, A. Laudani, A. Salvini and M. Parodi, "Automatic and parallel optimized learning for neural networks performing MIMO applications", *Advances in Electrical and Computer Engineering*, vol. 13, no. 1, pp. 3-12, 2013. doi: 10.4316/AECE.2013.01001

[40] F. Zhang, C. Deb, S. E. Lee, J. Yang and K. W. Shah, "Time series forecasting for building energy consumption using weighted Support Vector Regression with differential evolution optimization technique", *Energy and Buildings*, vol. 126, pp. 94-103, 2016. doi: 10.1016/j.enbuild.2016.05.028

[41] L. C. Ying and M. C. Pan, "Using adaptive network based fuzzy inference system to forecast regional electricity loads", *Energy Conversion and Management*, vol. 49, no. 2, pp. 205-211, 2008. doi: 10.1016/j.enconman.2007.06.015

[42] O. Brudaru, D. Popovici and C. Copaceanu, "Cellular genetic algorithm with communicating grids for assembly line balancing problems", *Advances in Electrical and Computer Engineering*, vol. 10, no. 2, pp. 87-93, 2010. doi:10.4316/AECE.2010.02015

[43] M. Z. Ali, K. Alkhatib and Y. Tashtoush, "Cultural algorithms: Emerging social structures for the solution of complex optimization problems", *International Journal of Artificial Intelligence*, vol. 11, no. 13, pp. 20-42, 2013.

[44] J. S. R. Jang, "ANFIS - Adaptive-network-based fuzzy inference system", in *IEEE Transactions on Systems Man and Cybernetics*, vol. 23, no. 3, pp. 665-685, 1993. doi: 10.1109/21.256541

[45] D. Wieland, F. Wotawa and G. Wotawa, "From neural networks to qualitative models in environmental engineering", *Computer-Aided Civil and Infrastructure Engineering*, vol. 17, pp. 104-118, 2002. doi: 10.1111/1467-8667.00259

[46] A. Mellit, S. Saglam and S. A. Kalogirou, "Artificial neural network-based model for estimating the produced power of a photovoltaic module", *Renewable Energy*, vol. 60, pp. 71-78, 2013. doi: 10.1016/j.renene.2013.04.011

[47] A. Khotanzad, E. Zhou and H. Elragal, "A neuro-fuzzy approach to short-term load forecasting in a price-sensitive environment", in *IEEE Transactions on Power Systems*, vol. 17, no. 4, pp.1273-1282, 2002. doi: 10.1109/TPWRS.2002.804999

[48] J. J. Cardenas, A. Garcia, J. L. Romeral and K. Kampouropoulos, "Evolutive ANFIS training for energy load profile forecast for an IEMS in an automated factory", ETFA2011, 2011, pp. 1-8. doi: 10.1109/ETFA.2011.6059079

[49] T. Takagi and M. Sugeno, "Fuzzy identification of systems and its applications to modeling and control", in *IEEE Transactions on Systems Man and Cybernetics*, vol. 15, no. 1, pp. 116-132, 1985. doi: 10.1109/TSMC.1985.6313399

[50] L. B. Fazlic, Z. Avdagic and I. Besic, "GA-ANFIS expert system prototype for detection of tar content in the manufacturing process", *38th International Convention on Information and Communication Technology, Electronics and Microelectronics (MIPRO)*, pp. 1194-1199, 2015. doi: 10.1109/MIPRO.2015.7160457

[51] D. Kalpanadevi and M. Mayilvaganan, "Computational Results of Hybrid Learning in Adaptive Neuro Fuzzy Inference System for Optimal Prediction", *International Journal of Applied Engineering Research*, vol 12, no. 16, pp. 5810-5818, 2017.

[52] R. Poli, W. B. Langdon, N. F. McPhee and J. R. Koza, "Genetic Programming An Introductory Tutorial and a Survey of Techniques and Applications", CES-475, 2007. ISSN: 1744-8050

[53] C. Yang, Q. Qian, F. Wang and M. Sun, "An improved adaptive genetic algorithm for function optimization", *2016 IEEE International Conference on Information and Automation (ICIA)*, pp. 675-680, 2016. doi: 10.1109/ICInfA.2016.7831905

[54] G. Renner and A. Ekart, "Genetic algorithms in computer aided design", *Computer-Aided Design*, vol. 35, 2003. doi: 10.1016/S0010-4485(03)00003-4

[55] D. E. Goldberg, "Genetic Algorithms in Search, Optimization, and Machine Learning", pp. 60-76, Addison-Wesley Longman, 1989. ISBN: 0201157675

[56] E. C. Brown and R. T. Sumichrast, "Evaluating performance advantages of grouping genetic algorithms", *Engineering Applications of Artificial Intelligence*, vol. 18, no. 1, pp. 1-12, 2005. doi: 10.1016/j.engappai.2004.08.024

[57] K. Sungil, and K. Heeyoung, “A new metric of absolute percentage error for intermittent demand forecasts,” International Journal of Forecasting, vol. 32, pp.669-679, 2016.

[58] I. P. Panapakidis, M. C. Alexiadis and G. K. Papagiannis, "Three-stage clustering procedure for deriving the typical load curves of the electricity consumers", *2013 IEEE Grenoble Conference, Grenoble*, pp. 1-6, 2013. doi: 10.1109/PTC.2013.6652370

[59] C. Kao, "Performance of several nonlinear programming software packages on microcomputers", *Computers & Operations Research*, vol. 25, no. 10, pp. 807-816, 1998. doi: 10.1016/S0305-0548(98)00013-6

[60] O. Yeniay, "A comparative study on optimization methods for the constrained nonlinear programming problems", *Mathematical Problems in Engineering*, vol. 2005, no. 2, pp. 165-173, 2005. doi: 10.1155/MPE.2005.165

[61] T. Wakui and R. Yokoyama, "Optimal sizing of residential gas engine cogeneration system for power interchange operation from energy-saving viewpoint", *Energy*, vol. 36, no. 6, pp. 3816-3824, 2011. doi: 10.1016/j.energy.2010.09.025

[62] T. Wakui, R. Yokoyama, I. Tamura and A. Kegasa, "Effect of power interchange operation of multiple household gas engine cogeneration systems on energy saving", *Energy*, vol. 34, no. 12, pp. 2092-2100, 2009. doi: 10.1016/j.energy.2008.08.019.

[63] M. T. Tsay, W. M. Lin and J. L. Lee, "Interactive best-compromise approach for operation dispatch of cogeneration systems", in *IEE Proceedings - Generation, Transmission and Distribution*, vol. 148, no. 4, pp. 326-332, Jul 2001. doi: 10.1049/ip-gtd:20010163

[64] L. Wang and C. Singh, "Stochastic combined heat and power dispatch based on multi-objective particle swarm optimization", *International Journal of Electrical Power & Energy Systems*, vol. 30, no 3, pp. 226-234, 2008. doi: 10.1016/j.ijepes.2007.08.002.

[65] S. Sanaye, M. Ziabasharhagh and M. Ghazinejad, "Optimal design of gas turbine CHP plant with pre heater and HRSG", *International Journal of Energy Research*, vol. 33, no. 8, pp. 766-777, 2009. doi: 10.1002/er.1509

[66] A. Rong, R. Lahdelma and P. B. Luh, "Lagrangian relaxation based algorithm for tri-generation planning with storages", *European Journal of Operational Research*, vol. 188, no. 1, pp. 240-257, 2008. doi: 10.1016/j.ejor.2007.04.008

[67] H. H. Chang, "Genetic algorithms and non-intrusive energy management system based economic dispatch for cogeneration units", *Energy*, vol. 36, no. 1, pp. 181-190, 2011. doi: 10.1016/j.energy.2010.10.054.

[68] C. Chang and W. Fu, "Stochastic multiobjective generation dispatch of combined heat and power systems", in *IEE Proceedings - Generation, Transmission and Distribution*, vol. 145, no. 5, pp. 583-591, 1998. doi: 10.1049/ip-gtd:19981997

[69] S. Salinas, M. Li and P. Li, "Multi-objective optimal energy consumption scheduling in smart grids", in *IEEE Transactions on Smart Grid*, vol. 4, no. 1, pp. 341–348, Mar. 2013. doi: 10.1109/TSG.2012.2214068

[70] S. Conti, R. Nicolosi, S. Rizzo and H. Zeineldin, "Optimal dispatching of distributed generators and storage systems for MV islanded Microgrids", in *IEEE Transactions on Power Delivery*, vol. 27, no. 3, pp. 1243-1251, July 2012. doi: 10.1109/TPWRD.2012.2194514

[71] H. Mostafa, R. El-Shatshat and M. Salama, "Multi-objective optimization for the operation of an electric distribution system with a large number of single phase solar generators", in *IEEE Transactions on Smart Grid*, vol. 4, no. 2, pp. 1038-1047, June 2013. doi: 10.1109/TSG.2013.2239669

[72] S. X. Chen and H. B. Gooi, "Jump and Shift Method for Multi-Objective Optimization", in *IEEE Transactions on Industrial Electronics*, vol. 58, no. 10, pp. 4538-4548, 2011. doi: 10.1109/TIE.2011.2116756

[73] J. Tant, F. Geth, D. Six, P. Tant and J. Driesen, "Multiobjective Battery Storage to Improve PV Integration in Residential Distribution Grids", in *IEEE Transactions on Sustainable Energy*, vol. 4, no. 1, pp. 182-191, Jan. 2013. doi: 10.1109/TSTE.2012.2211387

[74] C. M. Colson, M. H. Nehrir, R. K. Sharma and B. Asghari, "Improving Sustainability of Hybrid Energy Systems Part II: Managing Multiple Objectives With a Multiagent System", in *IEEE Transactions on Sustainable Energy*, vol. 5, no. 1, pp. 46-54, Jan. 2014. doi: 10.1109/TSTE.2013.2269319

[75] P. M. Pardalos and M. G. C. Resende, "Handbook of Applied Optimization", *Oxford University Press*, Oxford, 2002. ISBN 0-19-512594-0

[76] R. Fletcher, "Practical Methods of Optimization", 2nd edition, Wiley, Chichester, 1987. ISBN 0-471-91547-5

[77] H. W. Kuhn and A.W. Tucker, "Nonlinear programming", in *Proceedings of the Second Berkeley Symposium on Mathematical Statistics and Probability*, pp. 481-492, 1951.

[78] R. T. Marler and J. S. Arora, "Survey of multi-objective optimization methods for engineering", *Structural and Multidisciplinary Optimization*, vol. 26, pp. 369-395, 2004. doi: 10.1007/s00158-003-0368-6

[79] Apros.fi, "Apros – Dynamic process simulation software for nuclear and thermal power plant applications," *Internet*: www.apros.fi, Jan 2016.

[80] J. Savolainen, J. Lappalainen, A. Aikala and P. Ruuska, "Enhancing energy management of a car manufacturing plant through modelling and dynamic simulation", *29th European Conference on Modelling and Simulation (ECMS)*, pp. 259-265, May 2015.

A.Appendix

A.1 Forecasting Validation Cases

This section presents the validation cases of the energy modelling and prediction methodology, which is presented in Section 3.2, based on real data of the automotive manufacturing plant. The presented cases consists of 1 electric and 1 thermal energy load for each car manufacturing process, evaluated in 3 time periods (i.e. February 11th, March 11th and April 15th, respectively). The test of the prediction was made in different periods of time to validate the correct operation of the proposed methodology, having different weather and production conditions as inputs in the models. Table XXXIII presents the external temperature and the total production units of the three indicated dates.

Table XXXIII. Temperature and production data of the validation periods.

Date Range	Temperature (°C)			Production (pu)		
	Avg.	Min	Max	Body shop	Paint	Assemb.
11 – 12 Feb. 2015	*7,86*	*1,4*	*16,7*	*2141*	*1754*	*2162*
11 – 12 Mar. 2015	*15,43*	*9*	*26,8*	*2213*	*1672*	*2088*
15 – 16 Apr. 2015	*16,6*	*9,1*	*23,9*	*2152*	*1658*	*2178*

Table XXXIV lists the selected consumption cases, indicating their energy type and the production area in which they belong.

Table XXXIV. Validation cases of the modelling and prediction methodology.

Title	Energy Type	Manufacturing Process
Total electric demand of the plant	*Electric energy*	*Global*
Total heating demand of the plant	*Thermal energy*	*Global*
Total electric demand of workshop 1	*Electric energy*	*Body shop*
Total heating demand of workshop 1	*Thermal energy*	*Body shop*
Total electric demand of workshop 4	*Electric energy*	*Painting*
Total heating demand of workshop 4	*Thermal energy*	*Painting*
Total electric demand of workshop 9	*Electric energy*	*Assembling*
Total heating demand of workshop 10	*Thermal energy*	*Assembling*

Total electric demand of the plant

Table XXXV. Characteristics of the model: Total electric demand of the plant.

MODELS CHARACTERISTICS	
Training inputs	*Day of week* *Time of day* *External temperature* *Scheduled production* *Signal reference of 1 day ago* *Signal reference of 1 week ago*
MAPE index (pu)	*0,085*
SMAPE index (pu)	*0,033*
RMSE index (%)	*6,22%*

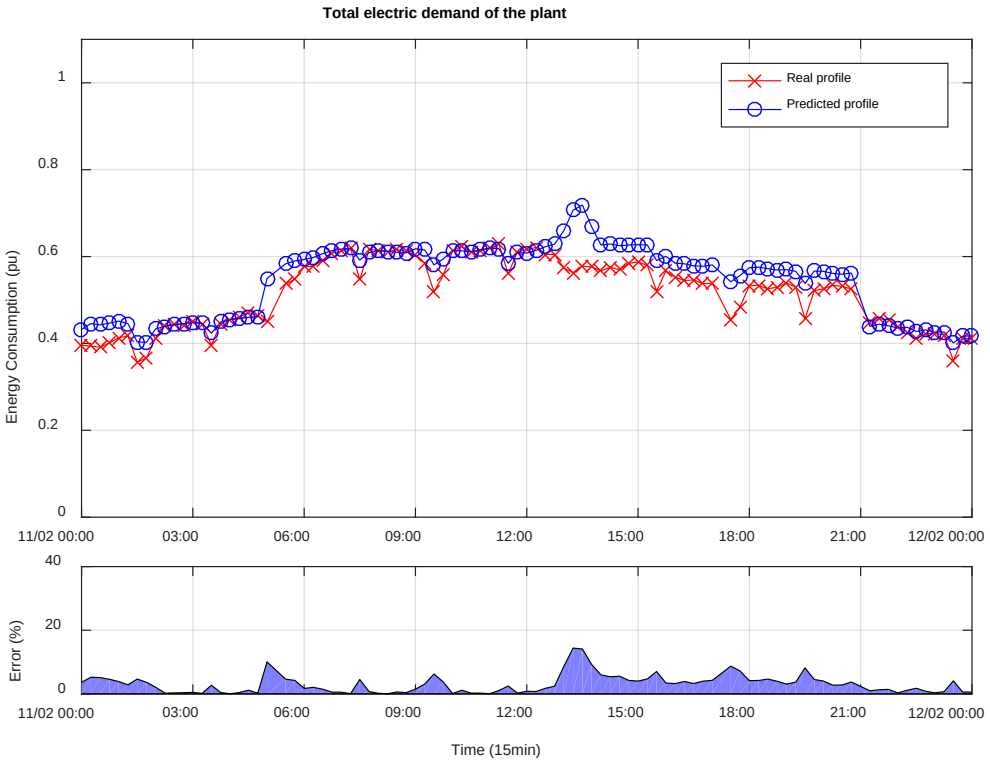

Figure A.1: Prediction result of the total electric demand of the plant: 11th February 2015.

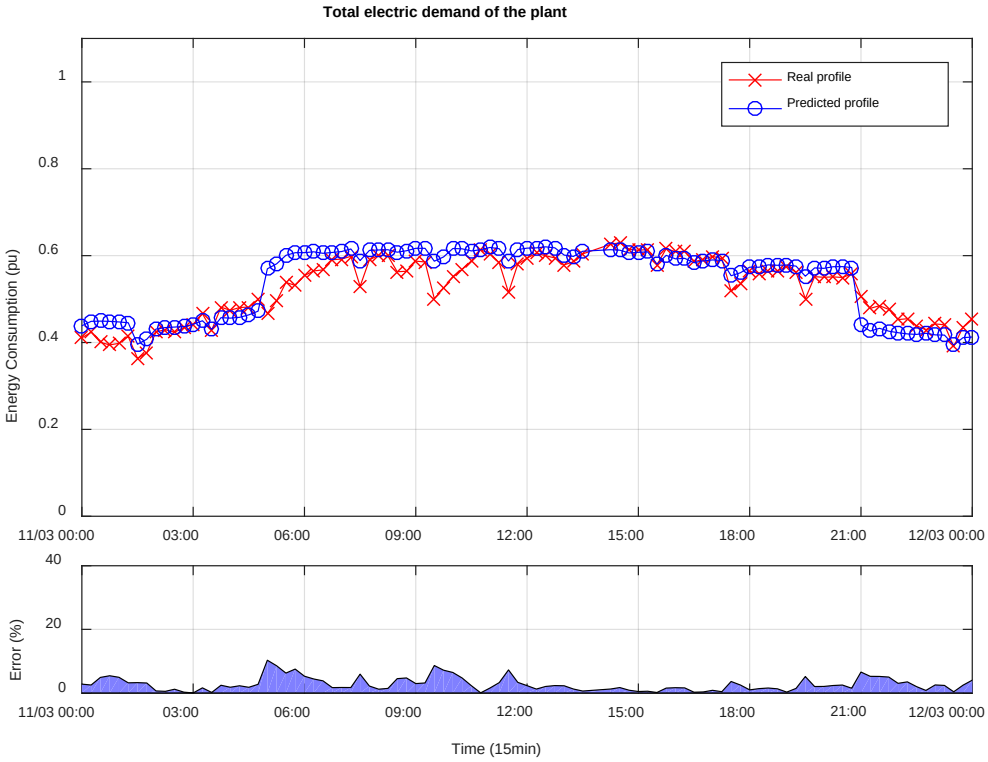

Figure A.2: Prediction result of the total electric demand of the plant: 11th March 2015.

Figure A.3: Prediction result of the total electric demand of the plant: 15th Abril 2015.

Total heating demand of the plant

Table XXXVI. Characteristics of the model: Total heating demand of the plant.

MODELS CHARACTERISTICS	
Training inputs	*Day of week* *Time of day* *External temperature* *Scheduled production* *Signal reference of 1 day ago* *Signal reference of 1 week ago*
MAPE index (pu)	*12,00*
SMAPE index (pu)	*5,37*
RMSE index (%)	*7,49%*

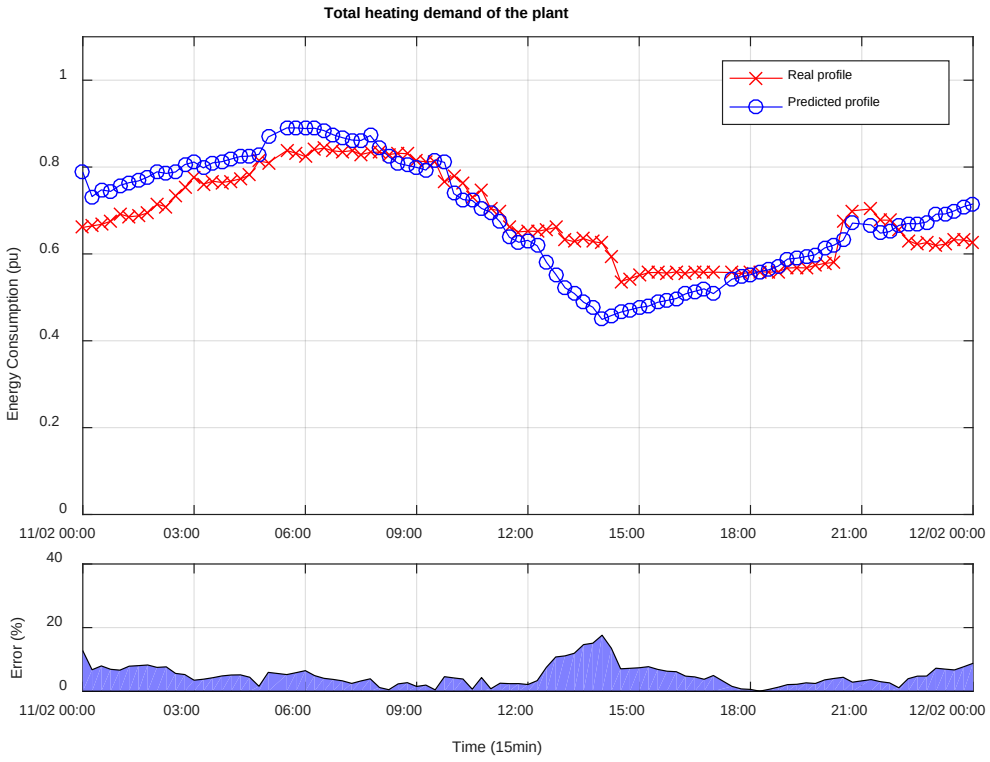

Figure A.4: Prediction result of the total heating demand of the plant: 11th February 2015.

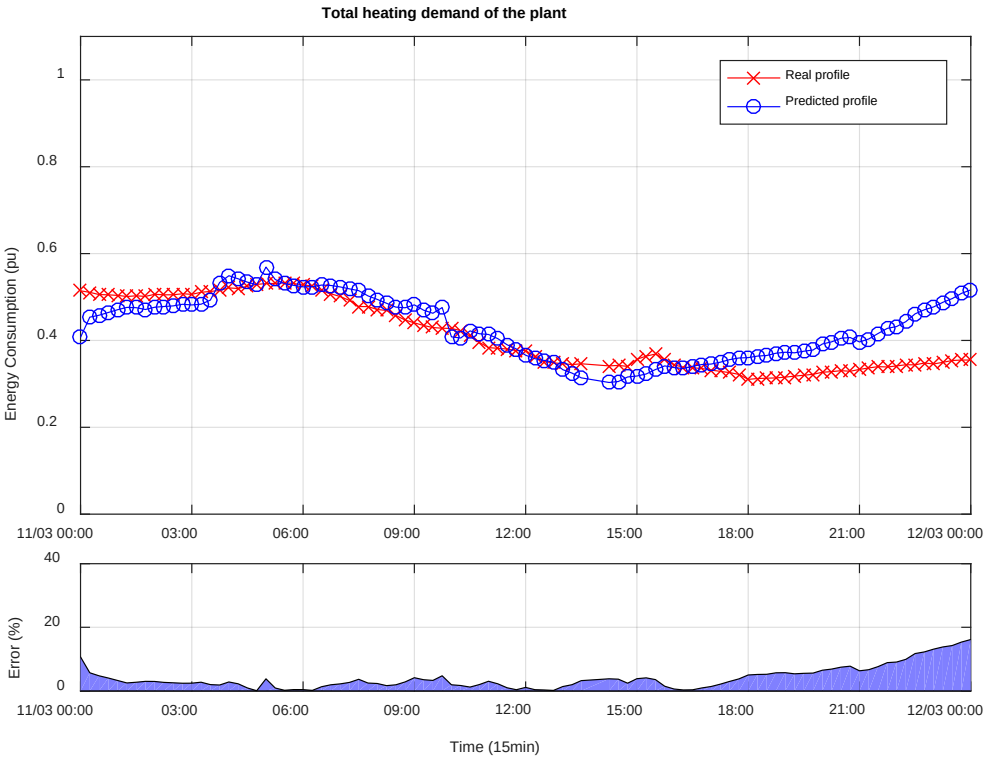

Figure A.5: Prediction result of the total heating demand of the plant: 11th March 2015.

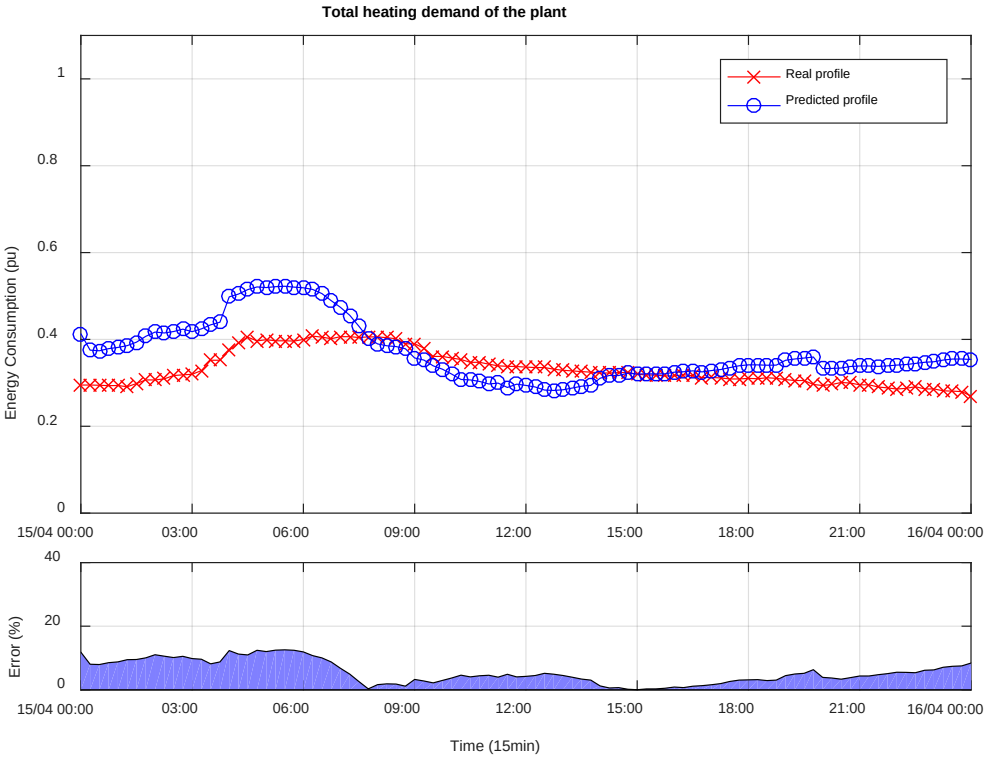

Figure A.6: Prediction result of the total heating demand of the plant: 15th Abril 2015.

Total electric demand of workshop 1

Table XXXVII. Characteristics of the model: Total electric demand of workshop 1.

MODELS CHARACTERISTICS	
Training inputs	*Day of week* *Time of day* *External temperature* *Scheduled production* *Signal reference of 1 day ago* *Signal reference of 1 week ago*
MAPE index (pu)	*16,89*
SMAPE index (pu)	*6,89*
RMSE index (%)	*6,33%*

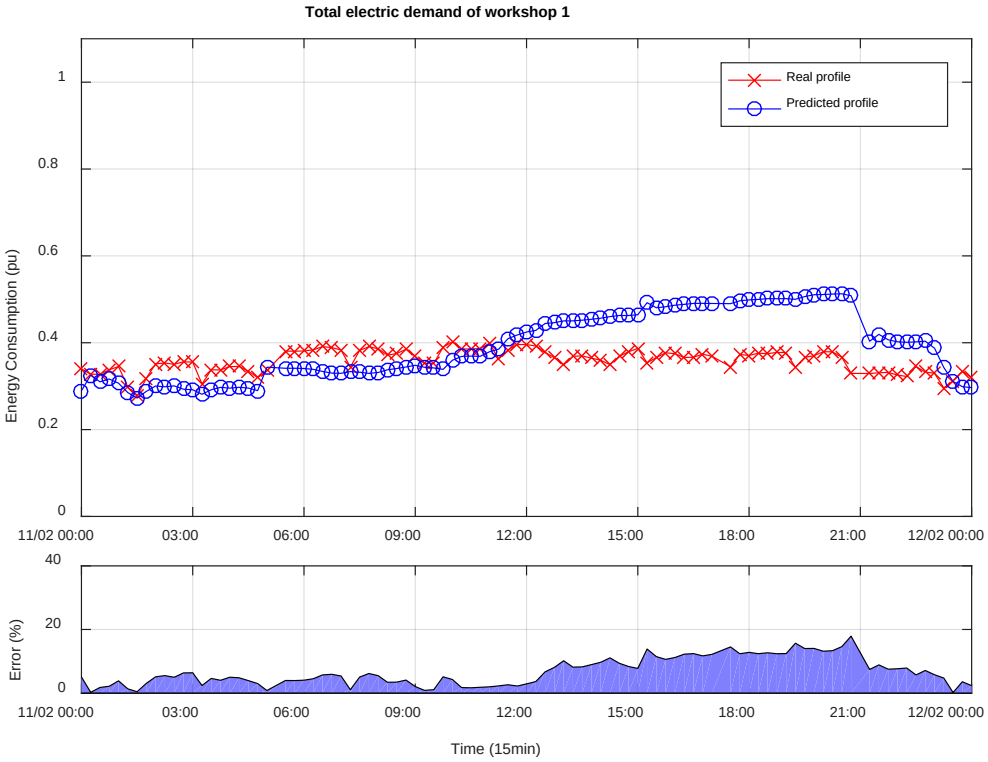

Figure A.7: Prediction result of the total electric demand of workshop 1: 11th February 2015.

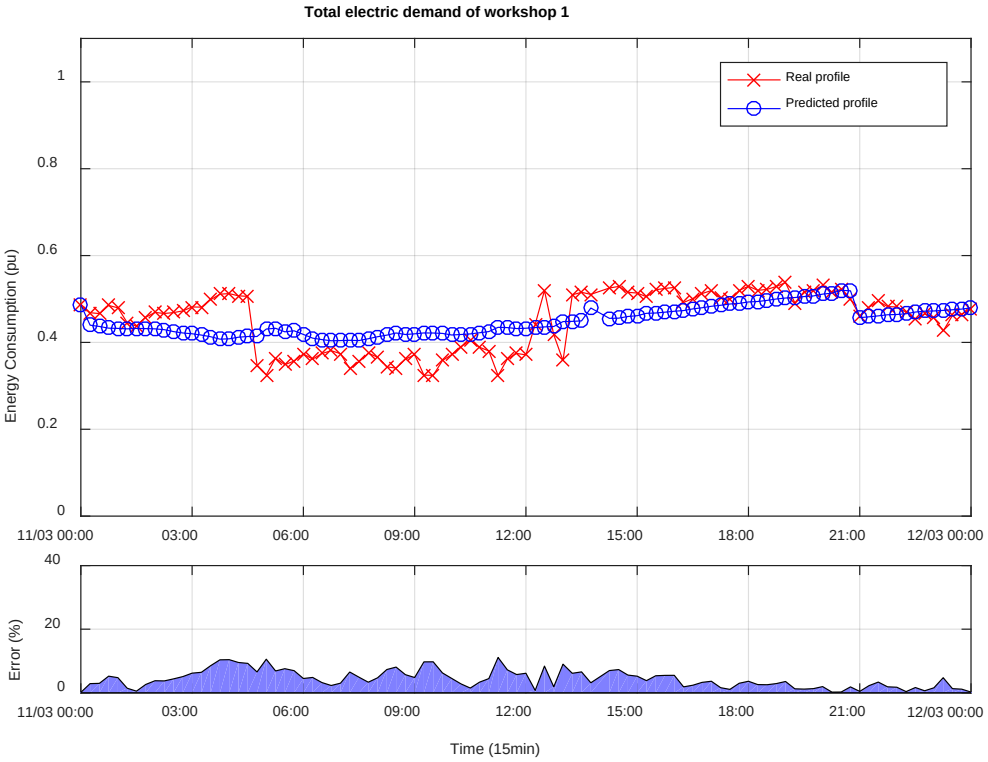

Figure A.8: Prediction result of the total electric demand of workshop 1: 11th March 2015.

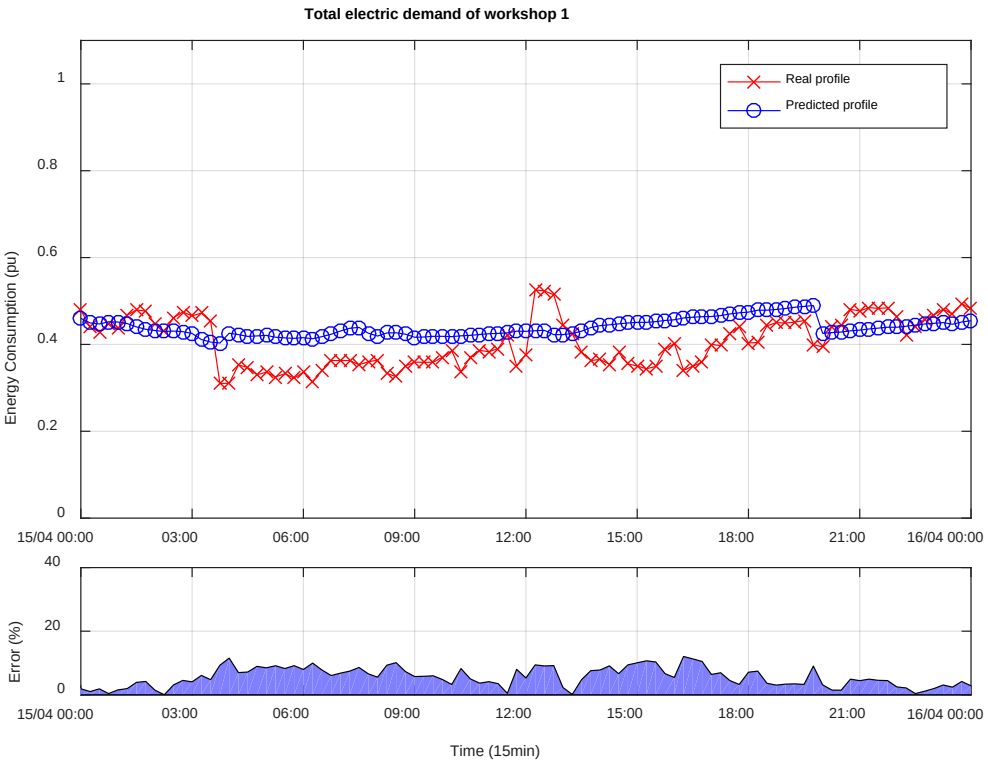

Figure A.9: Prediction result of the total electric demand of workshop 1: 15th Abril 2015.

Total heating demand of workshop 1

Table XXXVIII. Characteristics of the model: Total heating demand of workshop 1.

MODELS CHARACTERISTICS	
Training inputs	*Day of week* *Time of day* *External temperature* *Scheduled production* *Signal reference of 1 day ago* *Signal reference of 1 week ago*
MAPE index (pu)	*32,99*
SMAPE index (pu)	*16,35*
RMSE index (%)	*10,70%*

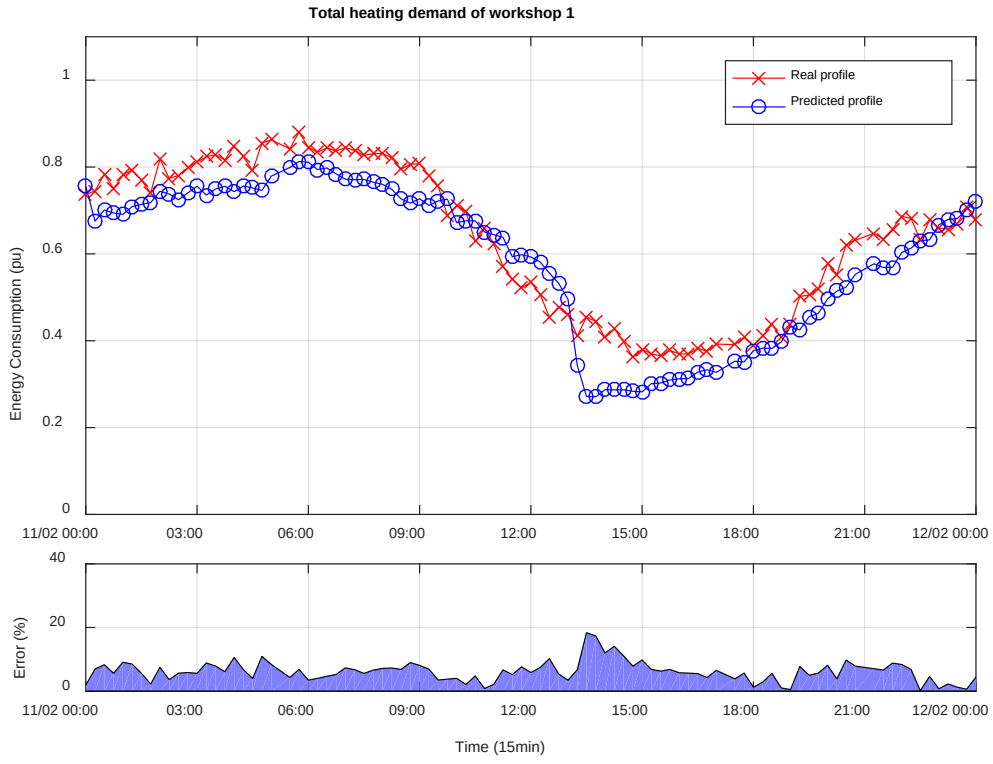

Figure A.10: Prediction result of the total heating demand of workshop 1: 11th February 2015.

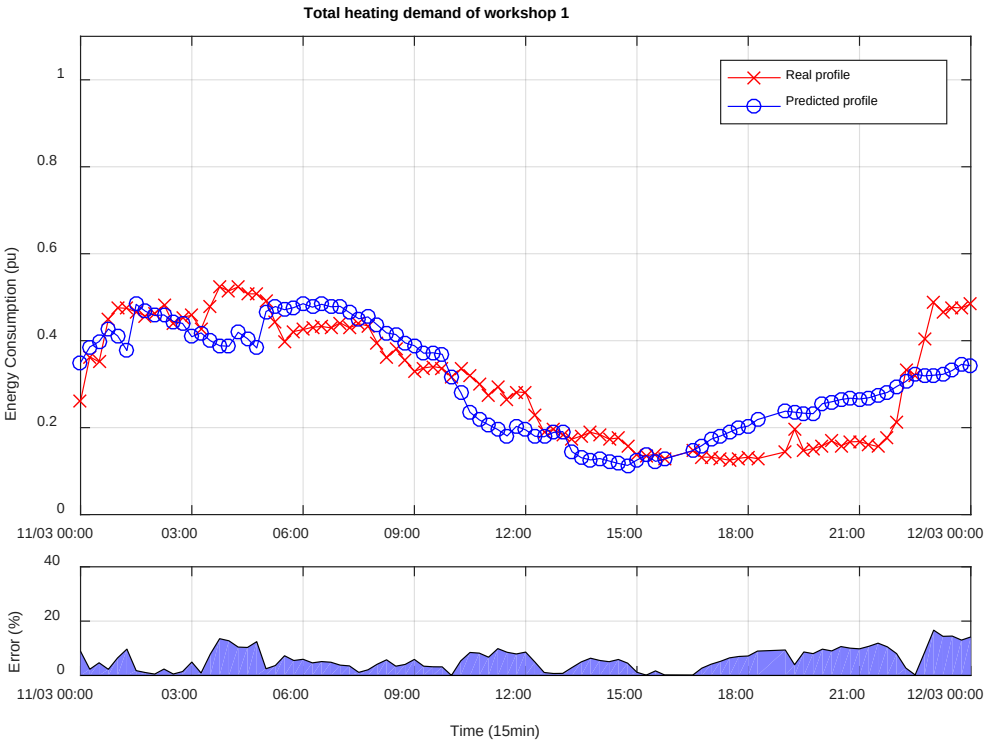

Figure A.11: Prediction result of the total heating demand of workshop 1: 11th March 2015.

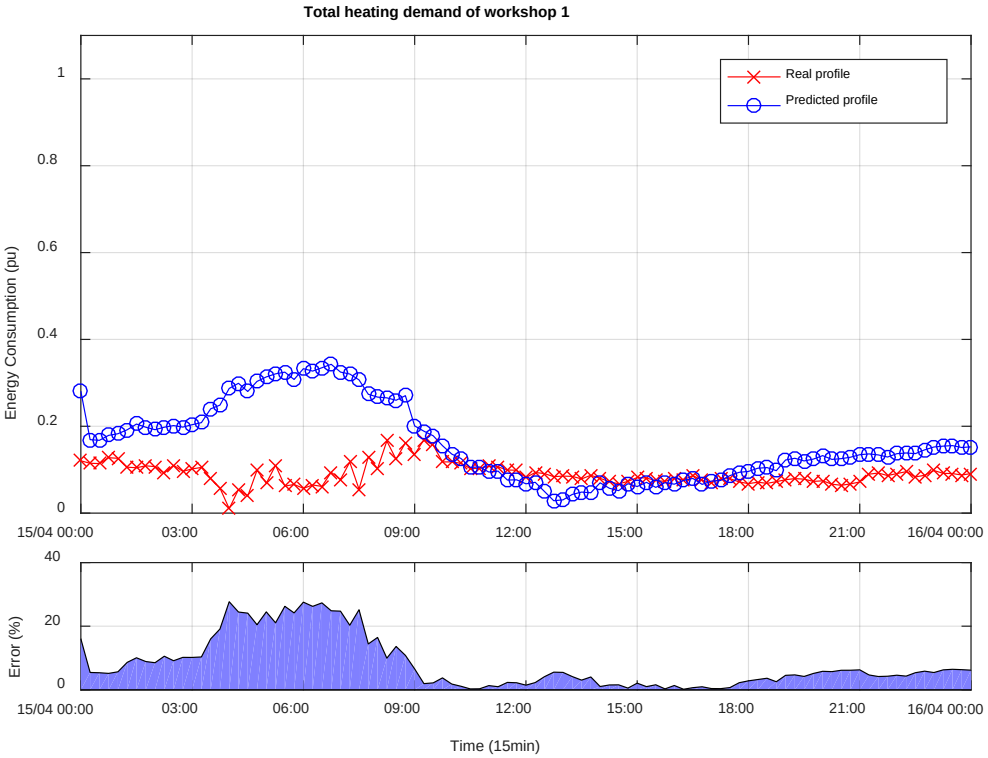

Figure A.12: Prediction result of the total heating demand of workshop 1: 15th Abril 2015.

Total electric demand of workshop 4

Table XXXIX. Characteristics of the model: Total electric demand of workshop 4.

MODELS CHARACTERISTICS	
Training inputs	*Day of week* *Time of day* *External temperature* *Scheduled production* *Signal reference of 1 day ago* *Signal reference of 1 week ago*
MAPE index (pu)	*6,34*
SMAPE index (pu)	*2,46*
RMSE index (%)	*5,56%*

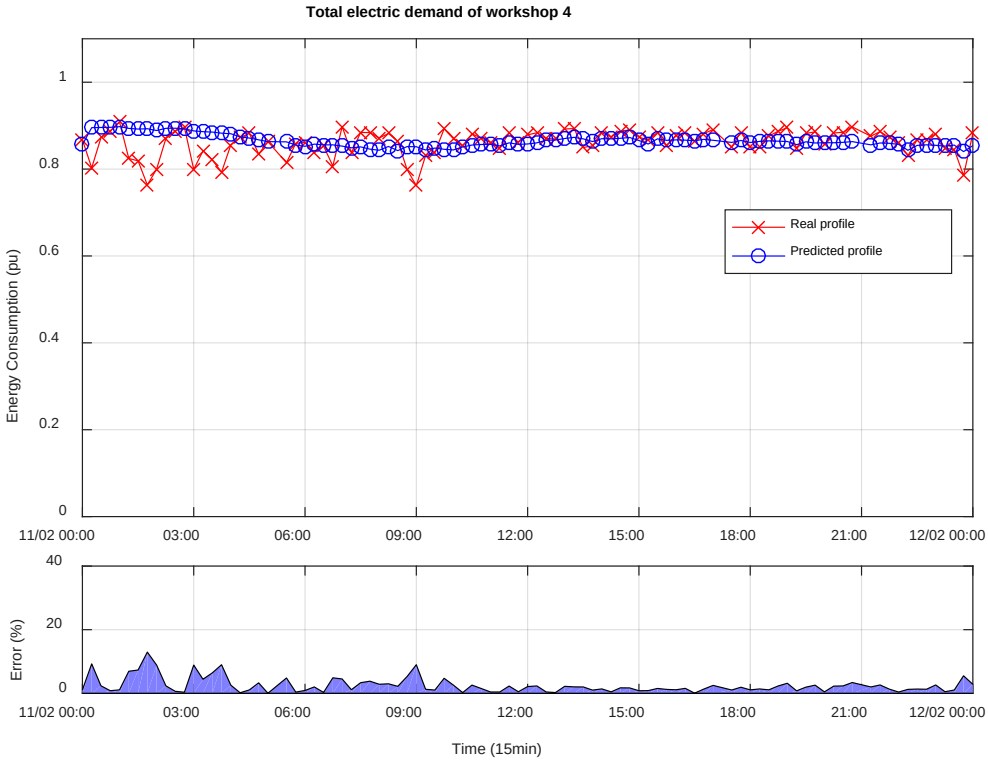

Figure A.13: Prediction result of the total electric demand of workshop 4: 11th February 2015.

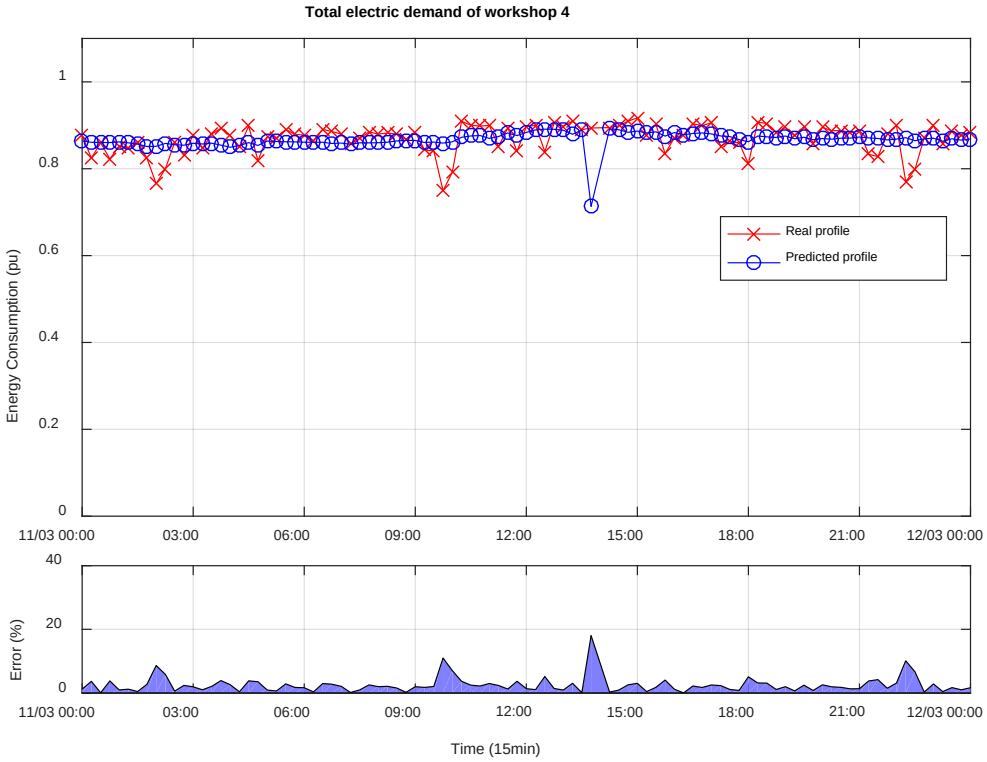

Figure A.14: Prediction result of the total electric demand of workshop 4: 11th March 2015.

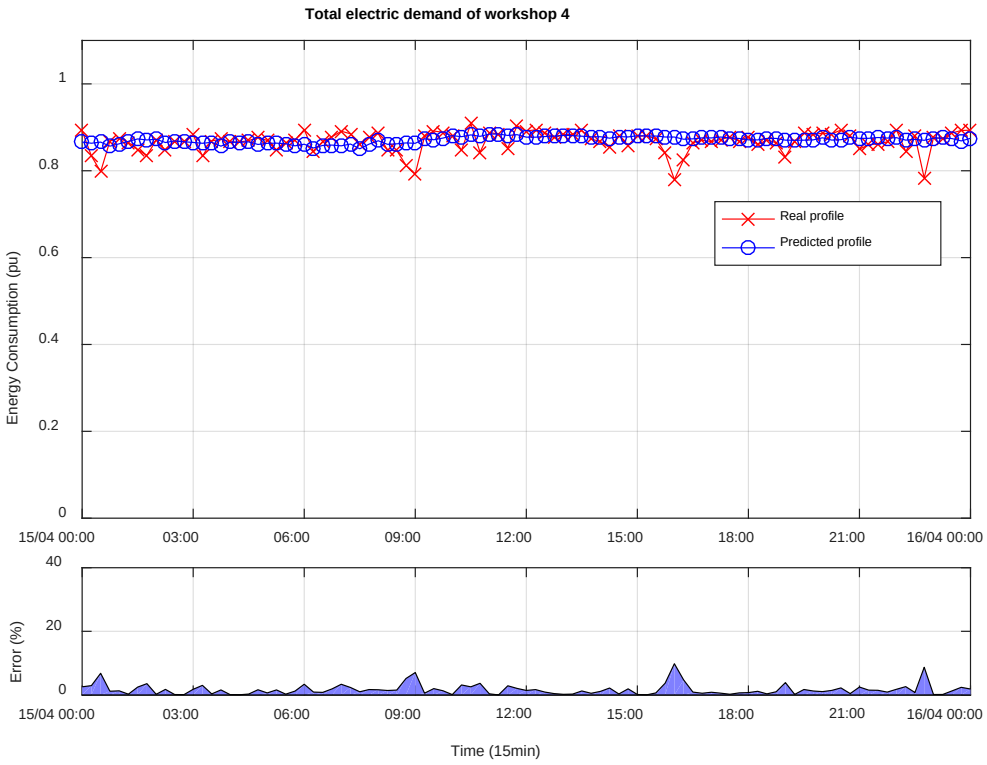

Figure A.15: Prediction result of the total electric demand of workshop 4: 15th Abril 2015.

Total heating demand of workshop 4

Table XL. Characteristics of the model: Total heating demand of workshop 4.

MODELS CHARACTERISTICS	
Training inputs	*Day of week* *Time of day* *External temperature* *Scheduled production* *Signal reference of 1 day ago* *Signal reference of 1 week ago*
MAPE index (pu)	*30,17*
SMAPE index (pu)	*15,26*
RMSE index (%)	*11,52%*

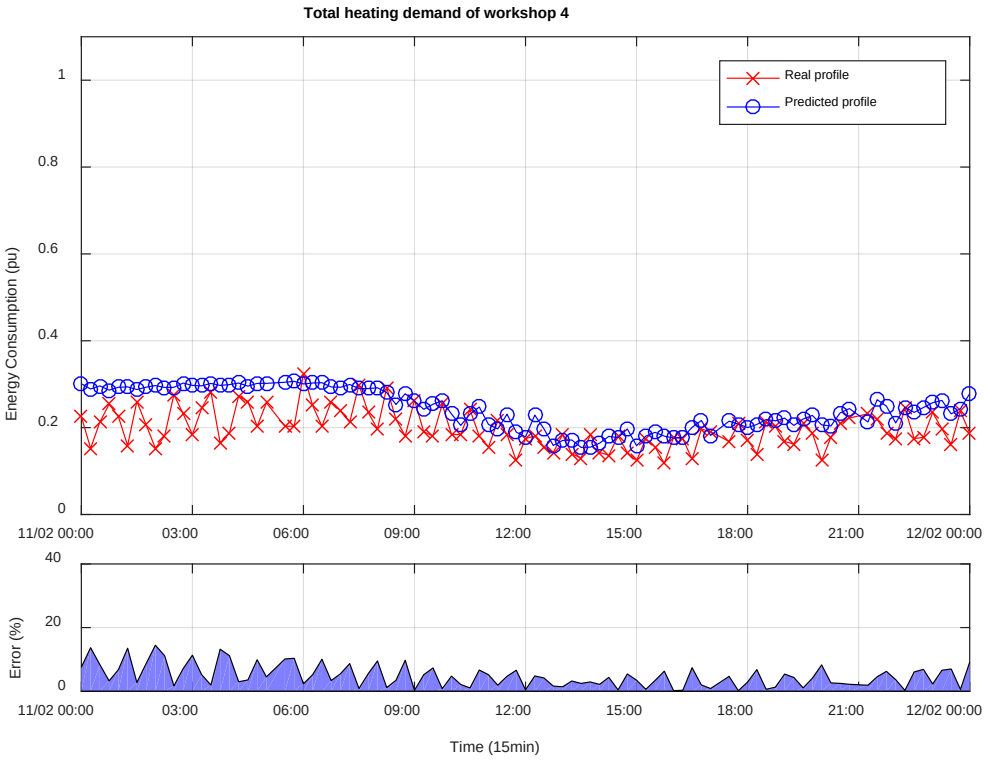

Figure A.16: Prediction result of the total heating demand of workshop 4: 11th February 2015.

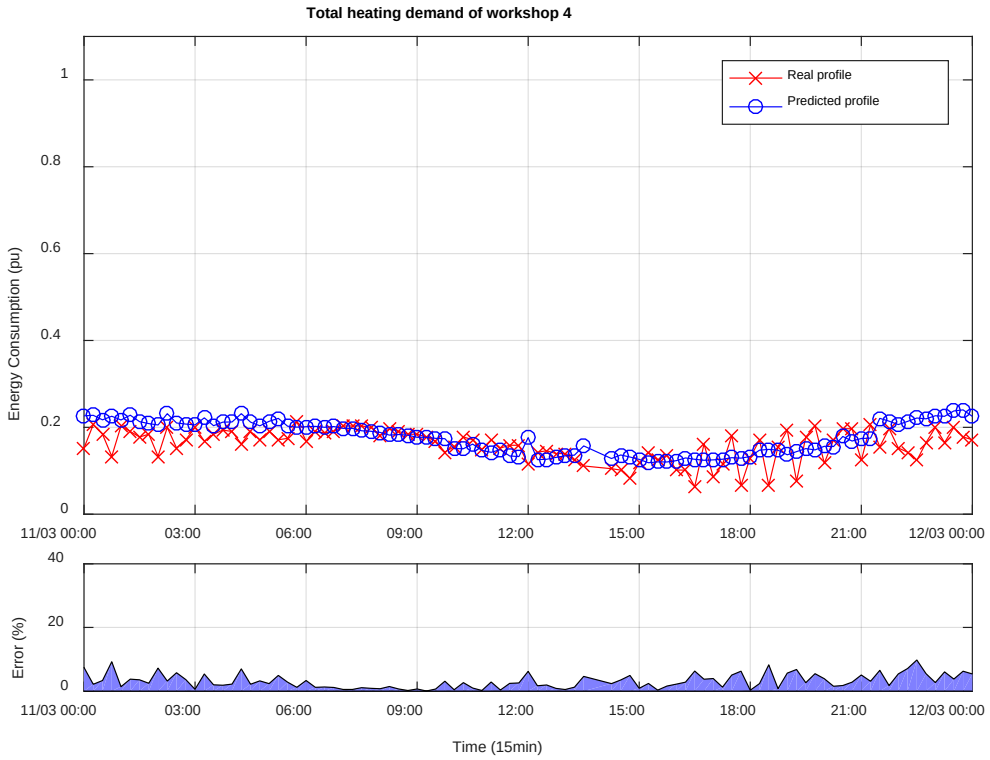

Figure A.17: Prediction result of the total heating demand of workshop 4: 11th March 2015.

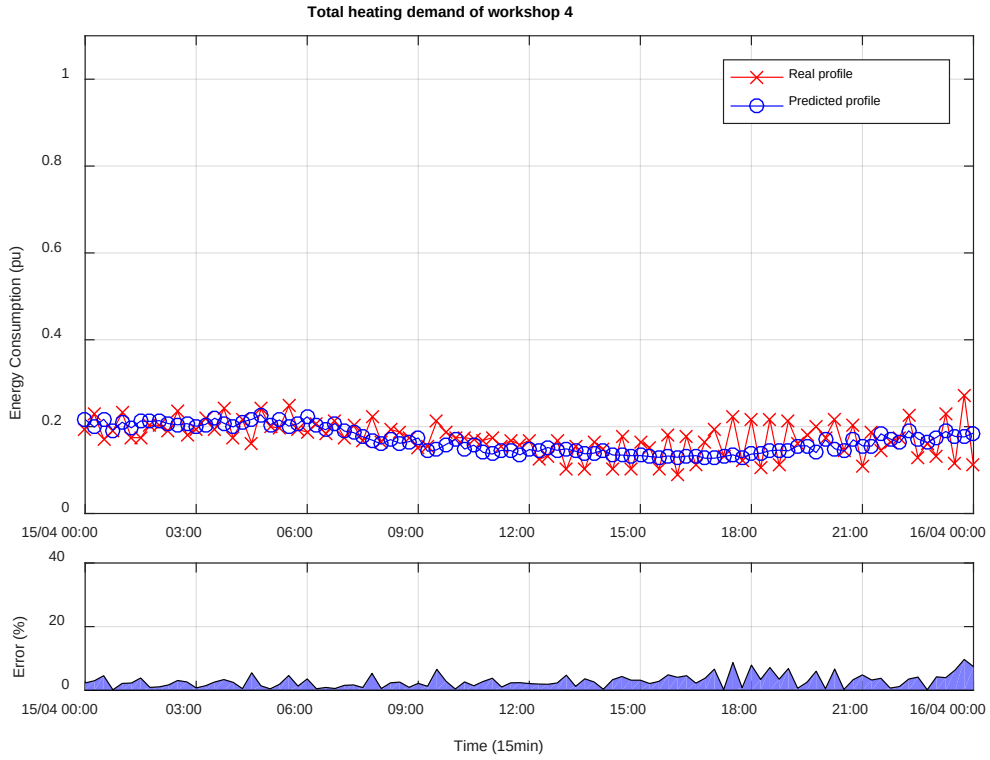

Figure A.18: Prediction result of the total heating demand of workshop 4: 15th Abril 2015.

Total electric demand of workshop 9

Table XLI. Characteristics of the model: Total electric demand of workshop 9.

MODELS CHARACTERISTICS	
Training inputs	*Day of week* *Time of day* *External temperature* *Scheduled production* *Signal reference of 1 day ago* *Signal reference of 1 week ago*
MAPE index (pu)	*7,11*
SMAPE index (pu)	*2,45*
RMSE index (%)	*5,76%*

Figure A.19: Prediction result of the total electric demand of workshop 9: 11th February 2015.

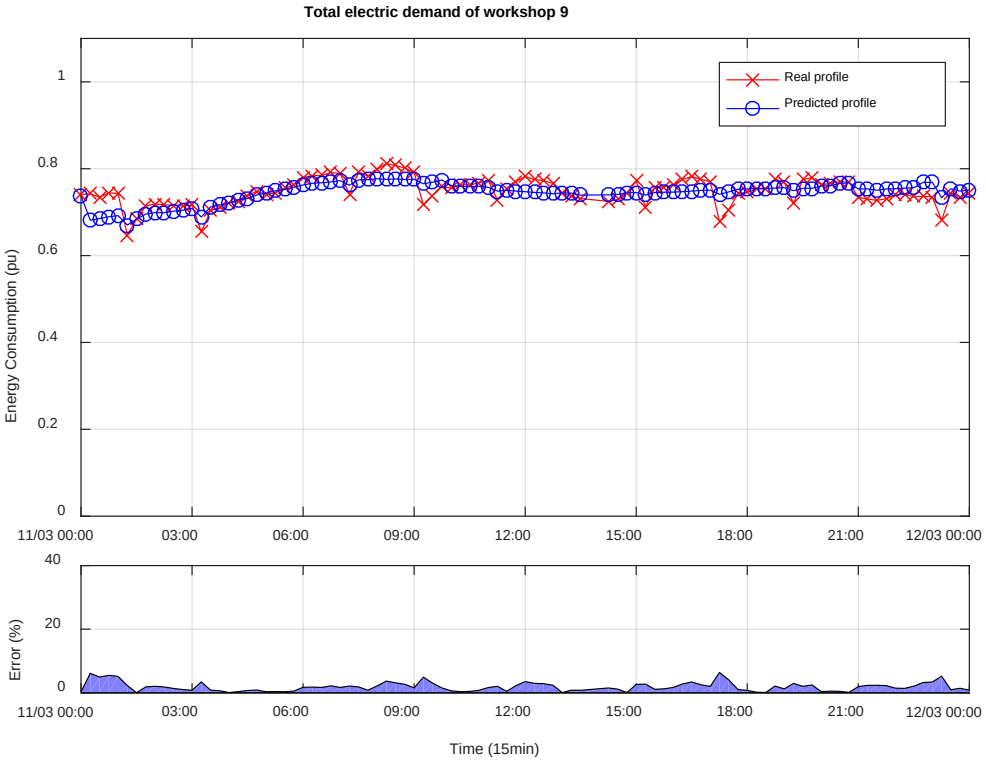

Figure A.20: Prediction result of the total electric demand of workshop 9: 11th March 2015.

Figure A.21: Prediction result of the total electric demand of workshop 9: 15th Abril 2015.

Total heating demand of workshop 10

Table XLII. Characteristics of the model: Total heating demand of workshop 10.

MODELS CHARACTERISTICS	
Training inputs	*Day of week* *Time of day* *External temperature* *Scheduled production* *Signal reference of 1 day ago* *Signal reference of 1 week ago*
MAPE index (pu)	*25,55*
SMAPE index (pu)	*11,23*
RMSE index (%)	*11,08%*

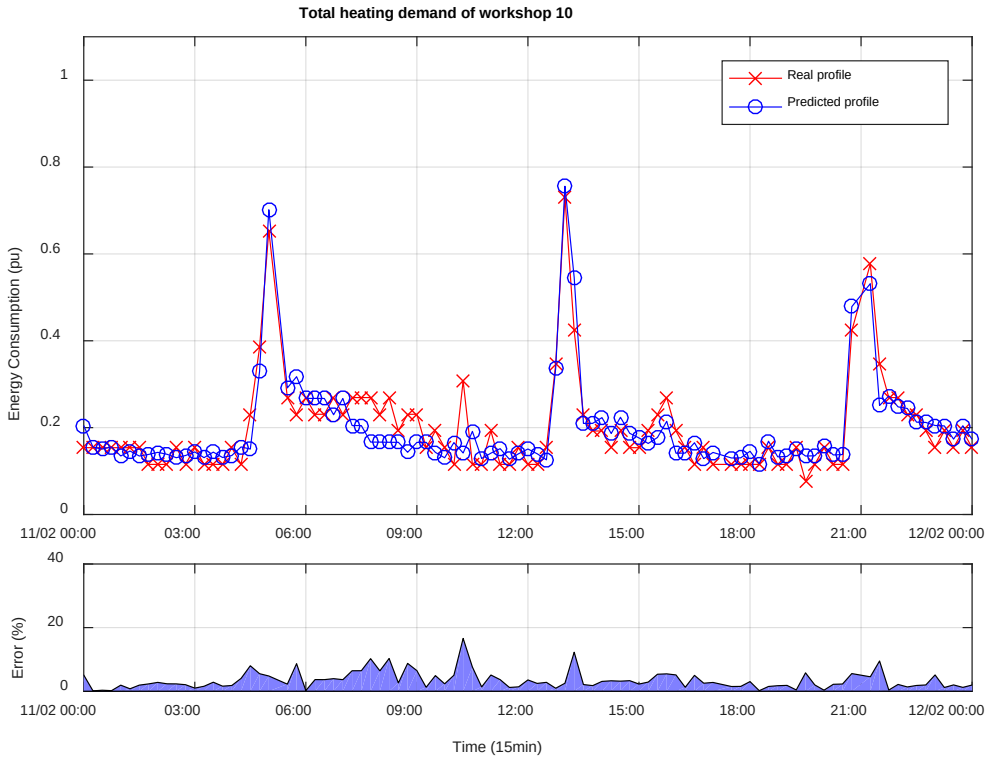

Figure A.22: Prediction result of the total heating demand of workshop 10: 11th February 2015.

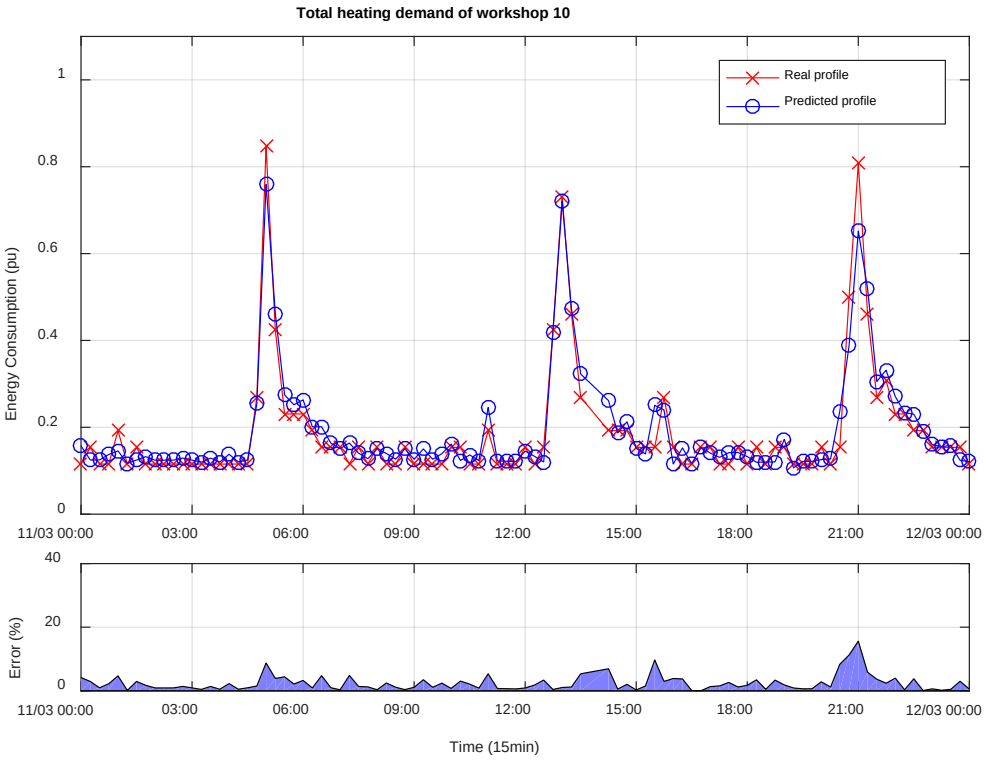

Figure A.23: Prediction result of the total heating demand of workshop 10: 11th March 2015.

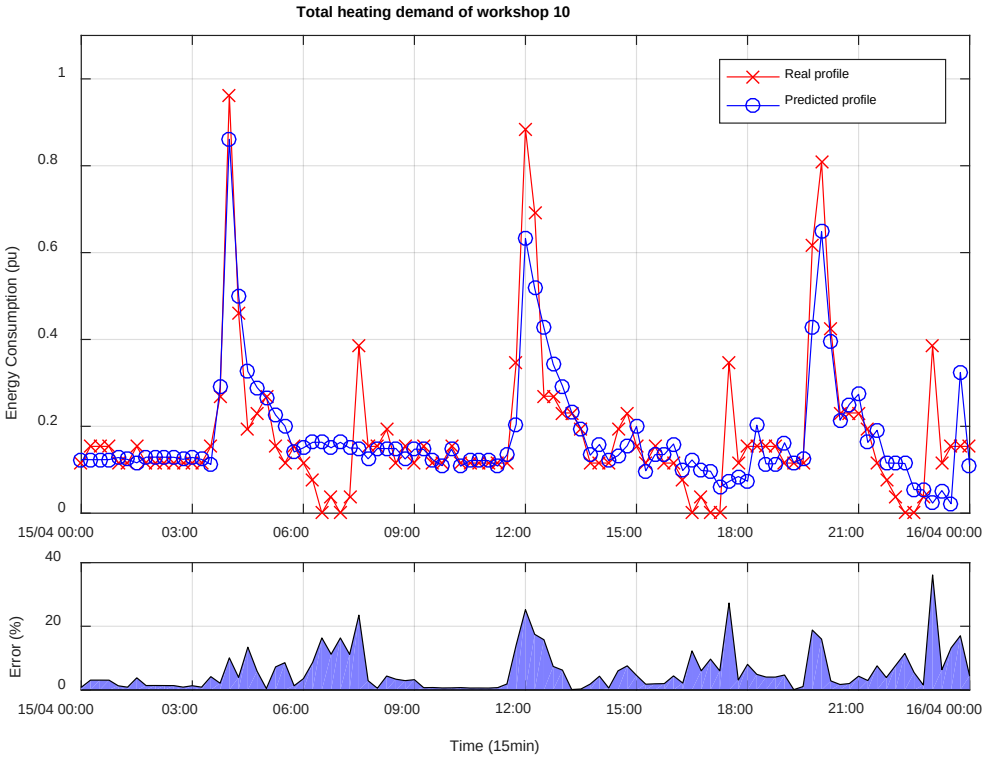

Figure A.24: Prediction result of the total heating demand of workshop 10: 15th Abril 2015.